SCUOLA DI DOTTORATO
UNIVERSITÀ DEGLI STUDI DI MILANO-BICOCCA

Dipartimento di / Department of
Scienze dell'Ambiente e della Terra

Dottorato di Ricerca in / PhD program: **Scienze Chimiche, Geologiche e Ambientali**
Ciclo / Cycle **XXXII**

Curriculum in (se presente / if it is) **Scienze dell'Ambiente Terrestre e Marino**

Remote sensing across multiple platforms and spatial scales: monitoring and assessment of eco-geomorphological changes on climatically sensitive coastal areas

Cognome / Surname **FALLATI** Nome / Name **LUCA**

Matricola / Registration number **750079**3

Tutore / Tutor: *Dr. Alessandra Savini*

Cotutore / Co-tutor: *Prof. Paolo Galli*
(se presente / if there is one)

Coordinatore / Coordinator: *Prof.ssa Maria Luce Frezzotti*

ANNO ACCADEMICO / ACADEMIC YEAR 2018/2019

Abstract

The Earth system, with the entering in the new Anthropocene Epoch, is facing increasing impacts from multi-sources. Among all the environments, coastal regions are the most vulnerable, dynamic and rapidly evolving systems on the planet. Moreover, for their position at the interface between sea and emerging lands, these ecosystems are characterised by substantial spatial and temporal variability and are exposed to the impacts of both terrestrial and marine origin. Threats from climate change and direct human disturbances can affect at a regional or global scale causing habitat loss and increases of the level of fragmentation. These disturbances can lead to severe transformations, and communities shift that can be linked to the reduction of the potential of natural ecosystems to recover from multiple stressors.

Under the described scenarios valid and repeatable monitoring and mapping techniques are essential to identify and quantify anthropogenic or climatic stress and their effects on coastal environments. The use of remote sensing platforms can represent a valid solution to obtain synoptic spatiotemporal data of threatened environments. According to this necessity, the primal aims of this doctoral project have been to propose monitoring protocols for collecting and analysing remote sensing data in coastal regions around the world, integrating innovative platforms and processing techniques.

This research provides new insights into remote data collection and elaboration on critical coastal environments through different spatial and temporal scales. Above and underwater sensing platforms like Satellite, Unmanned Aerial Vehicles (UAVs), underwater photogrammetry and multibeam echosounder (MBES) were used to collect data, and the retrieved information was processed applying recently developed algorithms such as Structure from Motion, Object Base Image Analysis and Machine Learning. The publications realised during the PhD project confirmed the high potential of the integration of different platforms and processing methodologies. The produced protocols describe innovative practices for collecting and analysing data in coastal regions in order to asses pressing anthropogenic and climatic impacts. Besides, the outputs generated from the analyses allow to highlight the occurrence of communities shift and tracking subsequent recovery or decline; they will be useful to monitor the response of the environments and address future protection strategies.

Table of Contents

"**But more wonderful than the lore of old men and the lore of books is the secret lore of ocean**. **Blue, green, grey, white, or black; smooth, ruffled, or mountainous; that ocean is not silent**. All my days have I watched it and listened to it, and I know it well. At first it told to me only the plain little tales of calm beaches and near ports, but with the years it grew more friendly and spoke of other things; of things more strange and more distant in space and in time. Sometimes at twilight the grey vapours of the horizon have parted to grant me glimpses of the ways beyond; and sometimes at night the deep waters of the sea have grown clear and phosphorescent, to grant me glimpses of the ways beneath. And these glimpses have been as often of the ways that were and the ways that might be, as of the ways that are; **for ocean is more ancient than the mountains, and freighted with the memories and the dreams of Time**"

H.P. Lovecraft

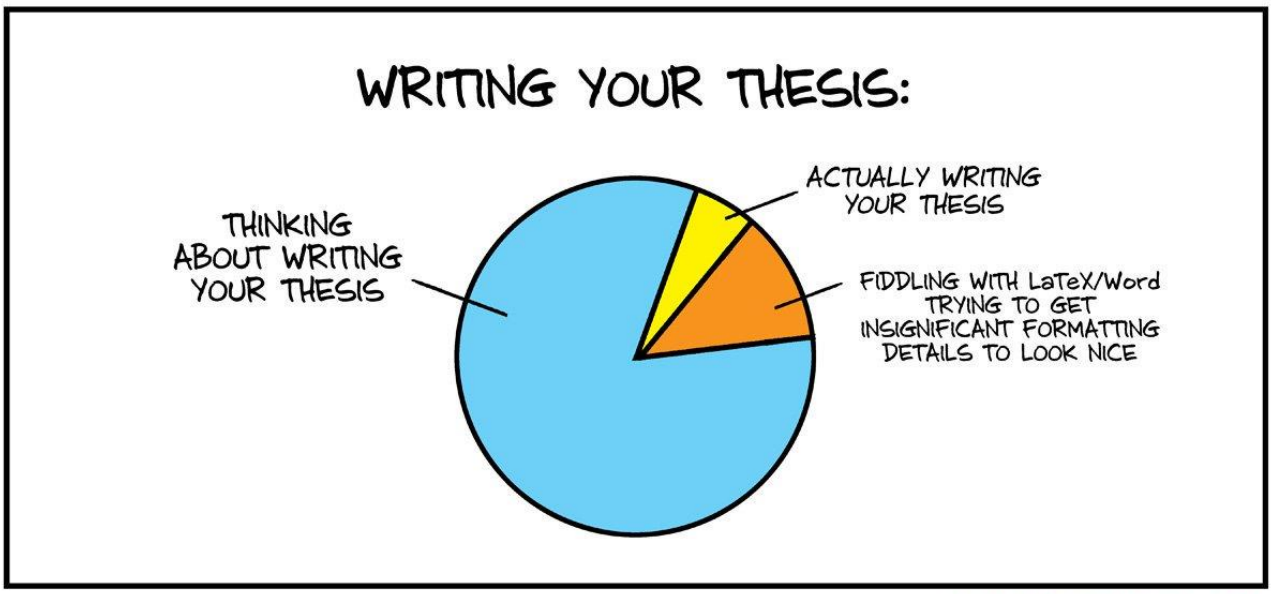

General Introduction

Anthropocene threats to the coastal environments

The Earth system, with the entering in the new Anthropocene Epoch, is facing increasing and multi-sources impacts (Lewis & Maslin, 2015; Zalasiewicz at al., 2011). Climate change, driven by anthropogenic emission, is a certainty and the intensification of extreme phenomena is modifying the Earth and its environments (National Academies et al., 2001; Oreskes, 2004). According to the last IPCC report (IPCC, 2019), in 2017 the global average temperature reached warming of 1°C above pre-industrial levels, increasing at 0.2°C per decade. Under actual greenhouse gas emissions scenarios, global warming is expected to surpass 1.5°C above pre-industrial levels within 2030. This increase places significant risks for natural and human systems altering the incidence, spatial scale and strength of severe weather events, such as heatwaves, droughts floods and fires (AghaKouchak et al., 2018; Hughes et al., 2018). On all environments, coastal regions are among the most dynamic and rapidly evolving systems on the planet (Davidson-Arnott, 2009). Amongst the coastal habitats coral reefs, mangroves, seagrasses, kelps and brown seaweeds forest are unique ecosystems that play an essential role in coastal primary production (Worm et al., 2006), disturbance control, nutrient cycling and promote the creation of complex three-dimensional structures that facilitated plentiful organisms (Guannel et al., 2016; Jackson & Sala, 2001). Therefore these habitats can be considered as underwater "hotspots" for biodiversity, and they provide high-value ecosystems services for communities that lived in close relationship with them (Boström et al., 2011; Foley, 2005; Hicks, 2017; Vassallo et al., 2013).

For their position at the interface between sea and emerging lands, these environments are characterized by substantial spatial and temporal variability and are exposed to impacts of both terrestrial and marine origin (Armynot du Châtelet et al., 2016). The coasts are naturally affected and shaped by tides, currents, wave regime and sea-level fluctuations (Siddall et al., 2003). Furthermore, during the last decades, worldwide coastal ecosystems are widely threatened by climate change and anthropic activities (Foley, 2005; Shalaby & Tateishi, 2007). Human disturbances such as the direct degradation and overexploitation of the resources, pollution and eutrophication, coastal land-use change and increase in sedimentation rates are direct triggers to habitat loss and increases of the level of fragmentation (Fahrig, 2003; Tanner, 2005). Threats from global climate change such as intensifications in intensity and frequency of storms (typhoon and hurricane), Sea Surface Temperature (SST) anomalies, ocean

acidification and sea-level rise can affect habitats at a regional or global scale. These disturbances can lead to severe transformations, and communities shift that can be linked to the reduction of the potential of natural ecosystems to recover from multiple stressors (Baker et al., 2008; Dolan & Walker, 2006; Fine et al., 2019; Hughes et al., 2019a; Pergent et al., 2014).

In tropical regions, coral reefs have had significant effects on the atmosphere, ocean chemistry, diversity and biogeographic distribution of life, and they provide hundreds of billions of dollars in value per year in goods and services to tens of millions of humans (Moberg & Folke, 1999; Moberg & Rönnbäck, 2003). During the actual interglacial period, coral reefs have been exceptionally favourite for thousands of years (Birkeland, 2015) until the recent three decades, in which the living coral cover has abruptly declined all over the world (Normile, 2016; Bellwood et al., 2004). Anthropogenic stress and natural disturbance, ever more frequent due to climate change, are reducing the resilience of natural communities and have slowed down the recovery rates (Hughes et al., 2003; Hughes et al., 2007; Hughes et al., 2019a; Perry & Alvarez-Filip, 2019). Since the 1980s, mass bleaching events triggered by SST anomalies increase in frequency and intensity, reaching unsustainable levels for the recovery of coral environments (Hughes et al., 2018). Bleaching occurs when the density of zooxanthellae (*Symbiodinium* sp.), algal symbionts that live as host in the tissues of corals, drastically decreases as a result of environmental stresses (Brown, 1997). Bleached corals are compromised, and prolonged bleaching events can lead to mass coral mortality (Baird & Marshall, 2002; Spalding & Brown, 2015). The last two most extreme bleaching events in 1998 and 2016 strongly altered the coral reefs around the world with mortality rates that in the Indian Ocean reach up to 90% (Hughes et al., 2019; Perry & Morgan, 2017; Pisapia et al., 2019; Pisapia et al., 2016). The direct consequences of these events are the transformation of the coral reef communities with a collapse in their three-dimensional structure, the loss of its growth potential and the reduction of ecosystem services provided by healthy environments (Alvarez-Filip et al., 2013; Kennedy et al., 2013; Perry et al., 2013).

In temperate coastal seas, similar situations are found. Seagrass meadows and forests of brown algae that provide biogenic structure, food and shelter for many organisms (Bermejo et al., 2018; Gianni, 2013; Jordà et al., 2012), are threatened by the immediate impacts of coastal development and growing human populations as well by climate change. Seagrass loss rates are comparable to those reported for coral reefs and indicate a severe deterioration of coastal environments around the world (’Waycott et al., 2009; Pergent et al., 2014). The canopy-forming fucoid *Cystoseira* spp. are some of the most critical marine ecosystem-engineers,

forming extended canopies, similar to land forests (Gianni, 2013), from the subtidal fringe down to the lower limit of the euphotic zone (Blanfune et al., 2016). These environments that form a complex tridimensional structure essential for shelter and food for many juveniles fish (Cheminée et al., 2013) are facing severe regression if not local extinction in all the Mediterranean area (Bulleri et al., 2018).

Alongside to the described threats, direct environmental contamination are pressing problem on coastal habitats, and Anthropogenic Marine-Debris (AMD) represents one of the most ubiquitous and long-lasting environmental change of our planet (Laist, 1987; Ryan, 2015). Once introduced into the marine environment from multiple sources (both sea- and land-based), buoyant plastic can be transported by surface currents and winds (Kako et al., 2010), recaptured by shorelines(Kako et al., 2014) or degraded into microplastic (Barnes et al., 2009; Cinner et al., 2018). Distribution and accumulation of plastic into the marine environment are indeed controlled by circulation patterns and prevailing winds, coastal and seafloor geomorphology (Barnes et al., 2009; Galgani et al., 2000; Savini et al., 2014) and anthropogenic activities (Ramirez-Llodra et al., 2013). Well known hotspots of accumulation include the sea surface, where aggregations of a large amount of persistent and light plastic take place at ocean gyres, creating giant "garbage-patches" (Francois Galgani et al., 2014; Law et al., 2014, 2010) and the shores, particularly beaches (Corcoran et al., 2009). Plastic accumulation on beaches may represent the terminal phase of oceanic transport or a transient stage with a successive washed to the sea following storms or tides movements. Knowing the accumulation rate on beaches and associated spatiotemporal oscillations would be a crucial information to refine global estimation on the dispersal mechanisms of plastic in the marine environment and its amount in each compartment.

Remote Sensing monitoring techniques and data processing

Under the described scenarios valid and repeatable monitoring and mapping techniques are essential to identify and quantify anthropogenic or climatic stresses and their effects on coastal environments, highlighting the occurrence of community shift and tracking subsequent recovery or decline. In this regard, the use of remote sensing platforms can represent a valid solution to obtain synoptic spatiotemporal data of threatened environments (Green et al., 1996; Mishra & Gould, 2016; Mumby et al., 1999; Hossain et al., 2014; Traganos & Reinartz, 2017). The processing and comparison of these data can be advantageous to outline impacts and describe both small and large scale processes in a money, and time-saving approach compares to direct monitoring techniques (Mumby et al., 1999).

Since the ‘70s, satellite platforms have become a keystone technology for the assessment of spatial and temporal patterns of large Earths environments (Boyd & Danson, 2005; Green et al., 1996). Nowadays, Earth and Sea monitoring satellites that orbit around the globe are numerous and equipped with sensors that can collect multi and hyperspectral data with a broad range of spatial and temporal resolutions (Ban et al., 2015; Belward & Skøien, 2015; Roy et al., 2014). Government programs like USGS/NASA Landsat and Copernicus Sentinel (ESA) allowed accessing to a vast quantity of multispectral data with good sensing quality for free: Sentinel 2 sensor acquired images from 23 June 2015 with a 5-day temporal resolution and with 10m/pix in visible bands (https://sentinel.esa.int/web/sentinel/user-guides/sentinel-2-msi/overview). Therefore these satellites are widely used for broad coastal environments monitoring programs as for seagrasses (Kovacs et al., 2018; Traganos et al., 2018; Traganos & Reinartz, 2017) and coral reef (Green et al., 1996; J. D. Hedley et al., 2018, 2016; Mumby et al., 1999). Anyway, despite the rapid increase in satellites temporal and spatial resolution, free data from governments program are not enough to detect and monitor rapid impacts or environmental process at a community scale. Data from the commercial satellites (DigitalGlobe, Ikonos, WorldView) can reach a higher resolution (<2 m/pix) but the cost of images acquisition with short revisit time can become an important limiting factor (Manfreda et al., 2018).

Recently advantages in Unmanned Aerial Vehicles (UAVs) have created an affordable alternative sensing platform to collect spatial, spectral and temporal data across a range of applications (Nowak et al., 2019). With UAV, data can be collected directly by individual researchers that can define the time of the surveys and the spatial coverage. Flying at a lower altitude than traditional remote sensing methods allows capturing images below cloud cover at a finer spatial resolution (centimetric) and a precisely temporal scale (Murfitt et al., 2017). This flexibility and the level of detail achieved placed the monitoring activities of coastal environments with the UAVs on a scale that lies between a satellite and a snorkelling/diving survey (Casella et al., 2016; Ventura et al., 2018).

Satellite and drone allowed to map and monitor shallow waters environments in optimal condition to a maximum of 30 meters (J. D. Hedley et al., 2018; Traganos et al., 2018) but to go deeper are necessary different sensing techniques that required submerged platforms (Micallef et al., 2017; Goodman et al., 2013). Recent advances in underwater photogrammetry enable 3D reconstructions from images of small habitat patches to entire seascapes (Ferrari et al., 2016). The models create during snorkelling or diving activities can effectively be used to

monitor environments over time without disturbing or manipulating them, and measuring their external structural changes with higher precision than direct methodologies (Ferrari et al., 2017; Figueira et al., 2015). However, if the water is too deep or turbid for optical techniques, acoustic remote sensing are ideal tools for seafloor and habitat mapping. Instruments like Multibeam echosounder transformed our ability to resolve seabed geomorphology and locally define its substrate from a deep from 2 to 11000m (Gardner & Armstrong, 2011; Micallef et al., 2017).

Thesis Objectives

The overall objectives of this thesis are the implementations of new techniques and protocols to monitor coastal regions with a focus on shores and nearshore environments. The main goal of the project is the integration of a set of remote sensing data, collected at multiple spatial scales from different aerial and underwater platforms (Satellite, UAVs, Underwater Cameras), and applying recent processing algorithms and techniques for their analysis. Structure from Motion (SfM), Object-Based Image Analysis (OBIA) and Machine Learning are used to process remote sensing data in order to estimate the impacts better, monitoring the response of the environments and address future protection strategies. In particular, Unmanned Aerial Vehicles (UAVs) has been used to monitor, through time and at multi-resolution scale, selected key areas where climate and anthropogenic impacts are strongly affecting natural environments.

The opportunity to investigate different environments for their geographic position, typologies and severity of the impacts, allowed proposing efficient, innovative and reliable protocols for collecting and analysing data in coastal regions all around the world.

References

’Waycott, M., Duarte, C. M., Carruthers, T. J. B., Orth, R. J., Dennison, W. C., Olyarnik, S., … Williams, S. L. (2009). Accelerating loss of seagrasses across the globe threatens coastal ecosystems. *Proceedings of the National Academy of Sciences of the United States of America*, *106*(30), 12377–12381. https://doi.org/10.1073/pnas.0905620106

AghaKouchak, A., Huning, L. S., Mazdiyasni, O., Mallakpour, I., Chiang, F., Sadegh, M., … Moftakhari, H. (2018). How do natural hazards cascade to cause disasters? *Nature*. https://doi.org/10.1038/d41586-018-06783-6

Alvarez-Filip, L., Carricart-Ganivet, J. P., Horta-Puga, G., & Iglesias-Prieto, R. (2013). Shifts in coral-assemblage composition do not ensure persistence of reef functionality. *Scientific Reports*, *3*(1), 3486. https://doi.org/10.1038/srep03486

Armynot du Châtelet, E., Bout-Roumazeilles, V., Coccioni, R., Frontalini, F., Francescangeli, F., Margaritelli, G., … Tribovillard, N. (2016). Environmental control on a land–sea transitional setting: integrated sedimentological, geochemical and faunal approaches. *Environmental Earth Sciences*, *75*(2), 1–18. https://doi.org/10.1007/s12665-015-4957-7

Baird, A. H., & Marshall, P. A. (2002). Mortality, growth and reproduction in scleractinian corals following bleaching on the Great Barrier Reef. *Marine Ecology Progress Series*. https://doi.org/10.3354/meps237133

Baker, A. C., Glynn, P. W., & Riegl, B. (2008). Climate change and coral reef bleaching: An ecological assessment of long-term impacts, recovery trends and future outlook. *Estuarine, Coastal and Shelf Science*. https://doi.org/10.1016/j.ecss.2008.09.003

Ban, Y., Gong, P., & Giri, C. (2015). Global land cover mapping using Earth observation satellite data: Recent progresses and challenges. *ISPRS Journal of Photogrammetry and Remote Sensing*. https://doi.org/10.1016/j.isprsjprs.2015.01.001

Barnes, D. K. A., Galgani, F., Thompson, R. C., & Barlaz, M. (2009). Accumulation and fragmentation of plastic debris in global environments. *Philosophical Transactions of the Royal Society B: Biological Sciences*, *364*(1526), 1985–1998. https://doi.org/10.1098/rstb.2008.0205

Bellwood, D. R., Hughes, T. P., Folke, C., & Nyström, M. (2004). Confronting the coral reef crisis. *Nature*, *429*(6994), 827–833. https://doi.org/10.1038/nature02691

Belward, A. S., & Skøien, J. O. (2015). Who launched what, when and why; trends in global land-cover observation capacity from civilian earth observation satellites. *ISPRS Journal of Photogrammetry and Remote Sensing*, *103*, 115–128. https://doi.org/10.1016/j.isprsjprs.2014.03.009

Bermejo, R., Chefaoui, R. M., Engelen, A. H., Buonomo, R., Neiva, J., Ferreira-Costa, J., … Serrão, E. A. (2018). Marine forests of the Mediterranean-Atlantic Cystoseira tamariscifolia complex show a southern Iberian genetic hotspot and no reproductive isolation in parapatry. *Scientific Reports*, *8*(1), 10427. https://doi.org/10.1038/s41598-018-28811-1

Birkeland, C. (2015). *Coral reefs in the anthropocene*. *Coral Reefs in the Anthropocene*. https://doi.org/10.1007/978-94-017-7249-5

Blanfunï¿½, A., Boudouresque, C. F., Verlaque, M., Beqiraj, S., Kashta, L., Nasto, I., … Thibaut, T. (2016). Response of rocky shore communities to anthropogenic pressures in Albania (Mediterranean Sea): Ecological status assessment through the CARLIT method. *Marine Pollution Bulletin*, *109*(1), 409–418. https://doi.org/10.1016/j.marpolbul.2016.05.041

Boström, C., Pittman, S. J., Simenstad, C., & Kneib, R. T. (2011). Seascape ecology of coastal biogenic habitats: Advances , gaps, and challenges. *Marine Ecology Progress Series*, *427*, 191–217. https://doi.org/10.3354/meps09051

Boyd, D. S., & Danson, F. M. (2005). Satellite remote sensing of forest resources: Three decades of research development. *Progress in Physical Geography*. https://doi.org/10.1191/0309133305pp432ra

Brown, B. E. (1997). Coral bleaching: causes and consequences. *Coral Reefs*, *16*(0), S129–S138.

https://doi.org/10.1007/s003380050249

Bulleri, F., Cucco, A., Dal Bello, M., Maggi, E., Ravaglioli, C., & Benedetti-Cecchi, L. (2018). The role of wave-exposure and human impacts in regulating the distribution of alternative habitats on NW Mediterranean rocky reefs. *Estuarine, Coastal and Shelf Science*, *201*, 114–122. https://doi.org/10.1016/j.ecss.2016.02.013

Casella, E., Collin, A., Harris, D., Ferse, S., Bejarano, S., Parravicini, V., … Rovere, A. (2016). Mapping coral reefs using consumer-grade drones and structure from motion photogrammetry techniques. *Coral Reefs*. https://doi.org/10.1007/s00338-016-1522-0

Cheminée, A., Sala, E., Pastor, J., Bodilis, P., Thiriet, P., Mangialajo, L., … Francour, P. (2013). Nursery value of Cystoseira forests for Mediterranean rocky reef fishes. *Journal of Experimental Marine Biology and Ecology*, *442*, 70–79. https://doi.org/10.1016/j.jembe.2013.02.003

Cinner, J. E., Maire, E., Huchery, C., MacNeil, M. A., Graham, N. A. J., Mora, C., … Mouillot, D. (2018). Gravity of human impacts mediates coral reef conservation gains. *Proceedings of the National Academy of Sciences*. Retrieved from http://www.pnas.org/content/early/2018/06/12/1708001115

Coral Reef Remote Sensing. (2013). *Coral Reef Remote Sensing*. https://doi.org/10.1007/978-90-481-9292-2

Corcoran, P. L., Biesinger, M. C., & Grifi, M. (2009). Plastics and beaches: A degrading relationship. *Marine Pollution Bulletin*. https://doi.org/10.1016/j.marpolbul.2008.08.022

Davidson-Arnott, R. (2010). *An Introduction to Coastal Processes and Geomorphology*. Retrieved from www.cambridge.org

Dolan, A. H., & Walker, I. J. (2006). *Understanding Vulnerability of Coastal Communities to Climate Change Related Risks*. *Source: Journal of Coastal Research* (Vol. III). Retrieved from https://www.jstor.org/stable/pdf/25742967.pdf?refreqid=excelsior%3A29132cd7149feda67cb1ec4e8737ae1a

Fahrig, L. (2003). Effects of Habitat Fragmentation on Biodiversity. *Annual Review of Ecology, Evolution, and Systematics*, *34*(1), 487–515. https://doi.org/10.1146/annurev.ecolsys.34.011802.132419

Ferrari, R., Figueira, W. F., Pratchett, M. S., Boube, T., Adam, A., Kobelkowsky-Vidrio, T., … Byrne, M. (2017). 3D photogrammetry quantifies growth and external erosion of individual coral colonies and skeletons. *Scientific Reports*. https://doi.org/10.1038/s41598-017-16408-z

Ferrari, R., McKinnon, D., He, H., Smith, R. N., Corke, P., González-Rivero, M., … Upcroft, B. (2016). Quantifying multiscale habitat structural complexity: A cost-effective framework for underwater 3D modelling. *Remote Sensing*, *8*(2). https://doi.org/10.3390/rs8020113

Figueira, W., Ferrari, R., Weatherby, E., Porter, A., Hawes, S., & Byrne, M. (2015). Accuracy and Precision of Habitat Structural Complexity Metrics Derived from Underwater Photogrammetry. *Remote Sensing*, *7*(12), 16883–16900. https://doi.org/10.3390/rs71215859

Fine, M., Hoegh-Guldberg, O., Meroz-Fine, E., & Dove, S. (2019). Ecological changes over 90 years at Low Isles on the Great Barrier Reef. *Nature Communications*, *10*(1), 4409. https://doi.org/10.1038/s41467-019-12431-y

Foley, J. A. (2005). Global Consequences of Land Use. *Science*, *309*(5734), 570–574. https://doi.org/10.1126/science.1111772

Galgani, F., Leaute, J. P., Moguedet, P., Souplet, A., Verin, Y., Carpentier, A., … Nerisson, P. (2000). Litter on the sea floor along European coasts. *Marine Pollution Bulletin*. https://doi.org/10.1016/S0025-326X(99)00234-9

Galgani, Francois, Ryan, P. G., Moore, C. J., Eriksen, M., Borerro, J. C., Carson, H. S., … Thiel, M. (2014). Plastic Pollution in the World's Oceans: More than 5 Trillion Plastic Pieces Weighing over 250,000 Tons Afloat at Sea. *PLoS ONE*, *9*(12), e111913. https://doi.org/10.1371/journal.pone.0111913

Gardner, J. V., & Armstrong, A. A. (2011). The Mariana Trench: A new view based on multibeam echosounding. *American Geophysical Union, Fall Meeting 2011, Abstract Id. OS13B-1517*. Retrieved from http://adsabs.harvard.edu/abs/2011AGUFMOS13B1517G

Gianni, F. (2013). Conservation and restoration of marine forests in the Mediterranean Sea and the potential role of Marine Protected Areas. *Advances in Oceanography and Limnology*, *4*(2), 83–101. https://doi.org/10.1080/19475721.2013.845604

Green, E. P., Mumby, P. J., Edwards, A. J., & Clark, C. D. (1996). A review of remote sensing for the assessment and management of tropical coastal resources. *Coastal Management*. https://doi.org/10.1080/08920759609362279

Guannel, G., Arkema, K., Ruggiero, P., & Verutes, G. (2016). The power of three: Coral reefs, seagrasses and mangroves protect coastal regions and increase their resilience. *PLoS ONE*, *11*(7), e0158094. https://doi.org/10.1371/journal.pone.0158094

Hedley, J. D., Roelfsema, C., Brando, V., Giardino, C., Kutser, T., Phinn, S., … Koetz, B. (2018). Coral reef applications of Sentinel-2: Coverage, characteristics, bathymetry and benthic mapping with comparison to Landsat 8. *Remote Sensing of Environment*, *216*, 598–614. https://doi.org/10.1016/j.rse.2018.07.014

Hedley, J. D., Roelfsema, C. M., Chollett, I., Harborne, A. R., Heron, S. F., Weeks, S. J., … Mumby, P. J. (2016, February 6). Remote sensing of coral reefs for monitoring and management: A review. *Remote Sensing*. Multidisciplinary Digital Publishing Institute. https://doi.org/10.3390/rs8020118

Hicks, F. (2017). *Ecosystem Services Assessment of North Ari Atoll Ecosystem Services Assessment of North Ari Atoll Tundi Agardy*. IUCN. Retrieved from https://portals.iucn.org/library/sites/library/files/documents/2017-003_0.pdf#targetText=The key habitats that contribute,offshore pelagic areas and seamounts.

Hossain, M. S., Bujang, J. S., Zakaria, M. H., & Hashim, M. (2014). The application of remote sensing to seagrass ecosystems: an overview and future research prospects. *International Journal of Remote Sensing*, *36*(1). https://doi.org/10.1080/01431161.2014.990649

Hughes, T. P., Baird, A. H., Bellwood, D. R., Card, M., Connolly, S. R., Folke, C., … Roughgarden, J. (2003). Climate change, human impacts, and the resilience of coral reefs. *Science*. https://doi.org/10.1126/science.1085046

Hughes, Terence P., Rodrigues, M. J., Bellwood, D. R., Ceccarelli, D., Hoegh-Guldberg, O., McCook, L., … Willis, B. (2007). Phase Shifts, Herbivory, and the Resilience of Coral Reefs to Climate Change. *Current Biology*. https://doi.org/10.1016/j.cub.2006.12.049

Hughes, Terry P., Anderson, K. D., Connolly, S. R., Heron, S. F., Kerry, J. T., Lough, J. M., … Wilson, S. K. (2018). Spatial and temporal patterns of mass bleaching of corals in the Anthropocene. *Science*, *359*(6371), 80–83. https://doi.org/10.1126/science.aan8048

Hughes, Terry P., Kerry, J. T., Baird, A. H., Connolly, S. R., Chase, T. J., Dietzel, A., … Woods, R. M. (2019a). Global warming impairs stock–recruitment dynamics of corals. *Nature*, *568*(7752), 387–390. https://doi.org/10.1038/s41586-019-1081-y

Hughes, Terry P., Kerry, J. T., Baird, A. H., Connolly, S. R., Chase, T. J., Dietzel, A., … Woods, R. M. (2019b). Global warming impairs stock–recruitment dynamics of corals. *Nature*. https://doi.org/10.1038/s41586-019-1081-y

Hughes, Terry P., Kerry, J. T., Connolly, S. R., Baird, A. H., Eakin, C. M., Heron, S. F., … Torda, G. (2018). Ecological memory modifies the cumulative impact of recurrent climate extremes. *Nature Climate Change*, *9*(1), 40–43. https://doi.org/10.1038/s41558-018-0351-2

IPCC. (2019). Special Report on Climate Change and Land. *Ipcc*.

Jackson, J. B. C., & Sala, E. (2001). Unnatural Oceans. *Scientia Marina*, *65*(SUPPLEMENT 2), 273–281.

Jordà, G., Marbà, N., & Duarte, C. M. (2012). Mediterranean seagrass vulnerable to regional climate warming. *Nature Climate Change*, *2*(11), 821–824. https://doi.org/10.1038/nclimate1533

Kako, S., Isobe, A., Kataoka, T., & Hinata, H. (2014). A decadal prediction of the quantity of plastic marine debris littered on beaches of the East Asian marginal seas. *Marine Pollution Bulletin*. https://doi.org/10.1016/j.marpolbul.2014.01.057

Kako, S., Isobe, A., Seino, S., & Kojima, A. (2010). Inverse estimation of drifting-object outflows using actual observation data. *Journal of Oceanography*. https://doi.org/10.1007/s10872-010-0025-9

Kennedy, E. V., Perry, C. T., Halloran, P. R., Iglesias-Prieto, R., Schönberg, C. H. L., Wisshak, M., … Mumby, P. J. (2013). Avoiding Coral Reef Functional Collapse Requires Local and Global Action. *Current Biology*, *23*(10), 912–918. https://doi.org/10.1016/J.CUB.2013.04.020

Kovacs, E., Roelfsema, C., Lyons, M., Zhao, S., Phinn, S., Kovacs, E., … Phinn, S. (2018). Seagrass habitat mapping : how do Landsat 8 OLI ,. *Remote Sensing Letters*, *9*(7), 686–695. https://doi.org/10.1080/2150704X.2018.1468101

Laist, D. W. (1987). Overview of the biological effects of lost and discarded plastic debris in the marine environment. *Marine Pollution Bulletin*. https://doi.org/10.1016/S0025-326X(87)80019-X

Law, K. L., Morét-Ferguson, S. E., Goodwin, D. S., Zettler, E. R., Deforce, E., Kukulka, T., & Proskurowski, G. (2014). Distribution of surface plastic debris in the eastern pacific ocean from an 11-year data set. *Environmental Science and Technology*. https://doi.org/10.1021/es4053076

Law, K. L., Morét-Ferguson, S., Maximenko, N. A., Proskurowski, G., Peacock, E. E., Hafner, J., & Reddy, C. M. (2010). Plastic accumulation in the North Atlantic subtropical gyre. *Science*. https://doi.org/10.1126/science.1192321

Lewis, S. L., & Maslin, M. A. (2015). Defining the Anthropocene. *Nature*, *519*(7542), 171–180. https://doi.org/10.1038/nature14258

Manfreda, S., McCabe, M. F., Miller, P. E., Lucas, R., Madrigal, V. P., Mallinis, G., … Toth, B. (2018, April 20). On the use of unmanned aerial systems for environmental monitoring. *Remote Sensing*. Multidisciplinary Digital Publishing Institute. https://doi.org/10.3390/rs10040641

Mishra, D. R., & Gould, R. W. (2016). Preface: Remote sensing in coastal environments. *Remote Sensing*, *8*(8), 1–6. https://doi.org/10.3390/rs8080665

Moberg, F., & Folke, C. (1999). Ecological goods and services of coral reef ecosystems. *Ecological Economics*, *29*(2), 215–233. https://doi.org/10.1016/S0921-8009(99)00009-9

Moberg, F., & Rönnbäck, P. (2003). Ecosystem services of the tropical seascape: interactions, substitutions and restoration. *Ocean & Coastal Management*, *46*(1–2), 27–46. https://doi.org/10.1016/S0964-5691(02)00119-9

Mumby, P. J., Green, E. P., Edwards, A. J., & Clark, C. D. (1999). The cost-effectiveness of remote sensing for tropical coastal resources assessment and management. *Journal of Environmental Management*. https://doi.org/10.1006/jema.1998.0255

Murfitt, S. L., Allan, B. M., Bellgrove, A., Rattray, A., Young, M. A., & Ierodiaconou, D. (2017). Applications of unmanned aerial vehicles in intertidal reef monitoring. *Scientific Reports*, *7*(1). https://doi.org/10.1038/s41598-017-10818-9

National Academies, Cicerone, R. J., Barron, E. J., Dickinson, R. E., Fung, I. Y., Hansen, J. E., … Wallace, J. M. (2001). *Climate Change: An Analysis of Some Key Questions*. *Sciences-New York*.

Normile, D. (2016). El Niño's warmth devastating reefs worldwide. Science (New York, N.Y.), 352(6281), 15–16. https://doi.org/10.1126/science.352.6281.15

Nowak, M. M., Dziób, K., & Bogawski, P. (2019). Unmanned Aerial Vehicles (UAVs) in environmental biology: A review. *European Journal of Ecology*, *4*(2), 56–74. https://doi.org/10.2478/eje-2018-0012

Oreskes, N. (2004). The Scientific Consensus on Climate Change. *Science*. https://doi.org/10.1126/science.1103618

Pergent, G., Bazairi, H., Bianchi, C. N., Boudouresque, C. F., Buia, M. C., Calvo, S., … Verlaque, M. (2014, February 28). Climate change and Mediterranean seagrass meadows: A synopsis for environmental managers. *Mediterranean Marine Science*. https://doi.org/10.12681/mms.621

Perry, C. T., & Morgan, K. M. (2017). Bleaching drives collapse in reef carbonate budgets and reef growth potential on southern Maldives reefs. *Nature Publishing Group*, *7*(November 2016), 1–9.

https://doi.org/10.1038/srep40581

Perry, Chris T., & Alvarez-Filip, L. (2019). Changing geo-ecological functions of coral reefs in the Anthropocene. *Functional Ecology*. https://doi.org/10.1111/1365-2435.13247

Perry, Chris T., Murphy, G. N., Kench, P. S., Smithers, S. G., Edinger, E. N., Steneck, R. S., & Mumby, P. J. (2013). Caribbean-wide decline in carbonate production threatens coral reef growth. *Nature Communications*, *4*(1), 1402. https://doi.org/10.1038/ncomms2409

Pisapia, C., Burn, D., & Pratchett, M. S. (2019). Changes in the population and community structure of corals during recent disturbances (February 2016-October 2017) on Maldivian coral reefs. *Scientific Reports*, *9*(1), 8402. https://doi.org/10.1038/s41598-019-44809-9

Pisapia, C., Burn, D., Yoosuf, R., Najeeb, A., Anderson, K. D., & Pratchett, M. S. (2016). Coral recovery in the central Maldives archipelago since the last major mass-bleaching, in 1998. *Scientific Reports*, *6*(September), 34720. https://doi.org/10.1038/srep34720

Ramirez-Llodra, E., De Mol, B., Company, J. B., Coll, M., & Sardà, F. (2013). Effects of natural and anthropogenic processes in the distribution of marine litter in the deep Mediterranean Sea. *Progress in Oceanography*. https://doi.org/10.1016/j.pocean.2013.07.027

Roy, D. P., Wulder, M. A., Loveland, T. R., C.E., W., Allen, R. G., Anderson, M. C., … Zhu, Z. (2014). Landsat-8: Science and product vision for terrestrial global change research. *Remote Sensing of Environment*, *145*, 154–172. https://doi.org/10.1016/j.rse.2014.02.001

Ryan, P. G. (2015). A brief history of marine litter research. In *Marine Anthropogenic Litter*. https://doi.org/10.1007/978-3-319-16510-3_1

Savini, A., Vertino, A., Marchese, F., Beuck, L., & Freiwald, A. (2014). Mapping cold-water coral habitats at different scales within the Northern Ionian Sea (Central Mediterranean): an assessment of coral coverage and associated vulnerability. *PLoS One*, *9*(1), e87108. https://doi.org/10.1371/journal.pone.0087108

Shalaby, A., & Tateishi, R. (2007). Remote sensing and GIS for mapping and monitoring land cover and land-use changes in the Northwestern coastal zone of Egypt. *Applied Geography*, *27*(1), 28–41. https://doi.org/10.1016/j.apgeog.2006.09.004

Siddall, M., Rohling, E. J., Almogi-Labin, A., Hemleben, C., Meischner, D., Schmelzer, I., & Smeed, D. A. (2003). Sea-level fluctuations during the last glacial cycle. *Nature*. https://doi.org/10.1038/nature01690

Spalding, M. D., & Brown, B. E. (2015). Warm-water coral reefs and climate change. *Science*. https://doi.org/10.1126/science.aad0349

TANNER, J. E. (2005). Edge effects on fauna in fragmented seagrass meadows. *Austral Ecology*, *30*(2), 210–218. https://doi.org/10.1111/j.1442-9993.2005.01438.x

Traganos, D., Aggarwal, B., Poursanidis, D., Topouzelis, K., Chrysoulakis, N., & Reinartz, P. (2018). Towards global-scale seagrass mapping and monitoring using Sentinel-2 on Google Earth Engine: The case study of the Aegean and Ionian Seas. *Remote Sensing*, *10*(8), 1227. https://doi.org/10.3390/rs10081227

Traganos, D., & Reinartz, P. (2017). Mapping Mediterranean seagrasses with Sentinel-2 imagery. *Marine Pollution Bulletin*, (March), 0–1. https://doi.org/10.1016/j.marpolbul.2017.06.075

Vassallo, P., Paoli, C., Rovere, A., Montefalcone, M., Morri, C., & Bianchi, C. N. (2013). The value of the seagrass Posidonia oceanica: A natural capital assessment. *Marine Pollution Bulletin*, *75*, 157–167. https://doi.org/10.1016/j.marpolbul.2013.07.044

Ventura, D., Bonifazi, A., Gravina, M. F., Belluscio, A., & Ardizzone, G. (2018). Mapping and Classification of Ecologically Sensitive Marine Habitats Using Unmanned Aerial Vehicle (UAV) Imagery and Object-Based Image Analysis (OBIA). *Remote Sensing*, *10*(9), 1331. https://doi.org/10.3390/rs10091331

Zalasiewicz, J., Williams, M., Haywood, A., & Ellis, M. (2011). The Anthropocene: a new epoch of geological time? *Philosophical Transactions of the Royal Society A: Mathematical, Physical and Engineering Sciences*, *369*(1938), 835–841. https://doi.org/10.1098/rsta.2010.0339

Chapter 1

Satellite imagery: the power to map at a large scale

1.1

Fallati, L., Savini, A., Sterlacchini, S., & Galli, P. (2017). Land use and land cover (LULC) of the Republic of the Maldives: first national map and LULC change analysis using remote-sensing data. Environmental Monitoring and Assessment, 189(8), 417. https://doi.org/10.1007/s10661-017-6120-2

Land use and land cover (LULC) of the Republic of the Maldives: first National map and LULC change analysis using remote sensing data

FALLATI Luca [a,b,*], SAVINI Alessandra [a,b], STERLACCHINI Simone [c], GALLI Paolo [a,d]

[a] MaRHE Center (Marine Research and High Education Center). Magoodhoo Island, Faafu Atoll, Republic of Maldives

[b] Department of Earth and Environmental Sciences, University of Milan – Bicocca, Piazza della Scienza 2, 20126, Milan, Italy

[c] National Research Council of Italy, Institute for the Dynamic of Environmental Processes. Piazza della Scienza, 1 - 20126 Milano, Italy

[d] Department of Biotechnologies and Biosciences, University of Milan – Bicocca, Piazza della Scienza 2, 20126, Milan, Italy

Abstract

The Maldives islands in recent decades have experienced dramatic land-use change. Uninhabited islands were turned into new resort islands; evergreen tropical forests were cut, to be replaced by fields and new built-up areas. All these changes happened without a proper monitoring and urban planning strategy from the Maldivian government due to the lack of national land-use and land-cover (LULC) data. This study aimed to realize the first land-use map of the entire Maldives archipelago and to detect land-use and land-cover change (LULCC) using high-resolution satellite images and socioeconomic data. Due to the peculiar geographic and environmental features of the archipelago, the land-use map was obtained by visual interpretation and manual digitization of land-use patches. The images used, dated 2011, were obtained from Digital Globe's WorldView 1 and WorldView 2 satellites. Nine land-use classes and eighteen subclasses were identified and mapped. During a field survey, ground control points were collected to test the geographic and thematic accuracy of the land-use map. The final product's overall accuracy was 85%. Once the accuracy of the map had been checked, LULCC maps were created using images from the early 2000s derived from Google Earth historical imagery. Post-classification comparison of the classified maps showed that growth of built-up and agricultural areas resulted in decreases in forest land and shrubland. The LULCC maps also revealed an increase in land reclamation inside lagoons near inhabited islands, resulting in environmental impacts on fragile reef habitat.

The LULC map of the Republic of the Maldives produced in this study can be used by government authorities to make sustainable land-use planning decisions and to provide better management of land use and land cover.

Keywords: Republic of the Maldives - Land Use and Land Cover (LULC) - Remote sensing - Change detection - Coral reefs

Introduction

Worldwide, many regions are undergoing rapid, wide-ranging changes in land use and land cover (LULC) (Mas, 1999). Rural to urban land conversion through development is occurring at a rate unprecedented in recent history and is having a dramatic effect on natural ecosystem functioning (Dewan & Yamaguchi, 2009; Lambin et al., 2001). Land-use/land-cover change (LULCC) is significant to a range of themes and issues central to the study of global change (Turner, 1994), representing a crucial challenge that nature ecosystems have to deal with in this century (Brook, 2008). LULCC deeply influences indeed biotic diversity through habitat fragmentation and biodiversity loss, having an important and extensive effect on climate by altering the distribution of ecosystems and their associated energy fluxes (Dale, 1997). In tropical coastal regions, fragile marine coral reef ecosystems, already threatened by increasing carbon dioxide (Hoegh-Guldberg et al., 2007), are exposed to an increased load of terrestrial sediment, nutrients, and other pollutants (Game, Lipsett-Moore, Saxon, Peterson, & Sheppard, 2011; Klein et al., 2012; Rau, McLeod, & Hoegh-Guldberg, 2012) that compromise the resistance of corals to thermal stress and their potential to recover from bleaching events (Maina et al., 2013; Wiedenmann et al., 2012; Wooldridge, 2009).

LULCC due to human activities is proceeding more quickly in less-developed countries (Dewan & Yamaguchi, 2009), where lack of data and monitoring programs obstacle a global vision of LULC spatial and temporal patterns. Maldives is one of the Small Island Developing States (Ghina, 2003) with a unique geographic configuration: an archipelago composed of more than 1100 islands surrounded by coral reefs, grouped into a chain of atolls in the middle of the Indian Ocean. Healthy coral reefs are essential for the survival of the Maldivian islands because of their capability to significantly reduce wave energy and protect the island from massive erosion (Ferrario et al., 2014). The one-meter elevation of most of the islands makes the Maldives one of the countries at greatest risk for the effects of climate change (Gerrard & Wannier, 2013). Therefore monitoring and management of LULC and LULCC is extremely important to control sedimentation and reduce other stress factors on coral reefs (Maina et al., 2013), which may make the islands more susceptible to future sea-level and climate change.

The Republic of the Maldives has experienced an extraordinary growth of tourism in recent decades. Tourism was first introduced to the Maldives in 1972 with the opening of the first two resorts near Malé, the capital of the archipelago. The number of visitor arrivals has increased constantly from 1067 in 1972 to 1,200,000 in 2013 (Ministry of Tourism, 2014), which is

almost four times the indigenous population (338,400 in 2012) (World Bank, 2011). Tourism is the major source of foreign exchange and government revenue, with a contribution to Gross Domestic Product (GDP) of greater than 30% (Ministry of Tourism, 2013). This has led to an increase in anthropogenic pressure on the environment beyond the carrying capacity of the islands (Zubair, Bowen, & Elwin, 2011).The LULC of the islands has changed without a national monitoring program, and there are currently no national LULC maps or LULCC data. The paucity of LULC data leaves remote sensing as the only practical means of providing complete, accurate, quantitative, and cost-effective time-series data for systematic mapping and monitoring of spatial and temporal LULC dynamics using image processing and geographic information systems (GIS) (Were, Dick, & Singh, 2013). Because historic archives of remotely sensed data offer the opportunity to analyze historical LULC changes, the geographic pattern of these changes in relation to human factors can be evaluated (Dewan & Yamaguchi, 2009).

Classification (i.e.: the process that assigns meaningful categories to the pixels in an image) of LULC data can be done through automatic extraction or by visual interpretation of remote-sensing data (Meinel, Neubert, Sensing, & City, 2000). There are two broad type of automatic classification: supervised and unsupervised. Both these approaches are based on a pixel-based method that has played an important role in classifying low-resolution images (Das, 2009). LANDSAT remote-sensing data are widely used for automatic LULC classification. The spatial resolution of 30 m is sufficient to classify accurately a large variety of landscapes, and the open accessibility of the historical archives makes it possible to reconstruct LULCC over decades. Visual interpretation can be tedious and slow compared to automatic classification methods, and still remain a subjective process. Nevertheless determining the validity and accuracy of the results from automatic processing can be difficult and in some case automatic classification methods fail to precisely recognize differences in the “use” of a given land surface area; whereas the “human input” is somewhat instrumental in taking the ultimate decision on this kind of information. In addition, countries with a particular geographic situation such as the Maldives require visual interpretation of sub-metric and metric optical satellite images such as those provided by Ikonos, Geoeye, or Quickbird. These very high-resolution optical data deliver greater thematic accuracy than those provided by LANDSAT, which is useful in a country composed of islands of limited dimensions. Unfortunately, their use for regional mapping remains too expensive (Nascimento, Souza-Filho, Proisy, Lucas, & Rosenqvist, 2013). To overcome this limitation, it is possible to access free basemap services using ArcGIS Desktop 10. The World Imagery (ESRI) basemap provides one meter or better

satellite and aerial imagery for many parts of the world (ESRI). The service is metadata-enabled, and the resolution, collection date, and source of the imagery are available. Using the World Imagery basemap, it is thus possible to analyze and detect LULC on high-resolution images of countries with a paucity of remote-sensing data.

Post-classification comparison (PCC) is the main technique used to detect LULCC over time. PCC detects land-cover changes by comparing independently produced classifications of images from different dates (Lyon, Yuan, Lunetta, & Elvidge, 1998; Singh, 1989).

The aims of this study are as follows: (a) to create the first LULC map of the entire Maldivian archipelago through visual interpretation of free high-resolution remote-sensing data; to identify LULCC taking place on representative islands in the last 10 years and (c) analyzing the driving forces of the LULCC, with particular attention to tourism.

Study Area

The Maldives are an archipelago composed of coral reefs and reef islands, grouped in a double chain structure, in the middle of the Indian Ocean (Fig. 1). The islands stretch for 860 km from latitude 7°6'35"N to 0°42'24"S and lie between longitude 72°33'19"E to 73°46'13"E. The Republic of the Maldives covers an area of about 859,000 km2, of which only a little more than 1% is land, generally with a mean elevation of less than 1 m above sea level (Ministry of Planning and National Development, 2008).

The focus of this study is on the 1192 islands of the archipelago, which are grouped into 20 administrative atolls (26 geographic regions). They are mid-Holocene in age (Kench, McLean, & Nichol, 2005) and composed of carbonate sands and gravels derived from the surrounding reefs. The islands are typically small, varying in size from 0.1 km2 to 5 km2, and are situated on the periphery of atolls. The islands can be divided into three categories: uninhabited, inhabited, and resort islands.

The uninhabited islands are almost 900 in number and are characterized by the absence of urban settlements and covered by lush tropical vegetation.

The inhabited islands are 193 and accommodate villages for the local people. Only the biggest islands (e.g.: Goidhoo, Hithadhoo, Kalaidhoo) have also infrastructure for industrial and agricultural activities. The population of the Maldives is approximately 340,000, with a growth rate of 1.8%, which has remained constant over the last decade (http://data.worldbank.org/indicator/SP.POP.GROW). One-third of the population lives in the capital, Malé, an island with a surface of 2 km2 and a population density of more than 60,000 per km2, which is among the highest in the world.

The island resort appeared as a new category in the mid-1970s, with the establishment of mass tourism. Resorts are built only on uninhabited islands, since an island resort is completely dedicated to tourist accommodation; this rule was specified in the Quality Tourism Strategy (1978) to separate local people from tourists to protect the human environment and avoid "cultural pollution" (Scheyvens, 2011). An island resort is easily distinguishable in satellite images by the presence of peculiar accommodation structures: a staff area in the middle of the island, beach villas on the edge, and often water villas in the lagoon. Since the opening of the first two island resorts in 1972, the number has grown to 111 in 2015, with a total capacity of 23.917 beds (Tourism Yearbook, 2015).

The Maldivian reefs occupy an area of 4,513 km2 (Naseer & Hatcher, 2004). They are an outstanding reserve of marine biodiversity, with almost 250 species of scleractinian corals (Pichon & Benzoni, 2007) and more than 1200 reef fish species (Rajasuriya, Zahir, Venkataraman, Islam, & Tamelander, 2004). The reef systems are extremely vulnerable to anthropogenic stresses and global climate change. Their health is fundamental for the maintenance of land (erosion), provision of alimentary resources (fisheries and aggregates), and economic earnings (tourism) (Kench, 2011).

Materials and methods

World Imagery Basemap

The World Imagery (WI) basemap was used to detect LULC on the Maldivian islands. The free basemap service is provided by ESRI and is fully accessible using ArcGIS 10 (ESRI) or a higher version. The service coverage for the Maldivian archipelago is over 85% with high-resolution satellite images acquired between late 2010 and early 2011. The images, obtained from DigitalGlobe satellites WorldView-1 and WorldView-2, are panchromatic with a ground resolution of 1/0,5 m (see Figs. 2 and 3). This resolution makes it possible to recognize LULC categories on all the islands, including the smallest. The WI basemap uses the WGS 84 Web Mercator auxiliary spherical coordinate system.

The spatial accuracy of the basemap was checked using 50 ground control points previously acquired in Faafu atoll in October 2011. These points were overlaid on the basemap images, showing an extremely high correspondence with the ground elements (spatial error < 1 m).

Image Classification

To describe LULC classes on the Maldivian islands the Anderson land-use and land-cover classification scheme (Anderson, Hardy, Roach, Witmer, & Peck, 1976) has been used and adapted. The adopted classification is hierarchical with two levels of detail: Level I and Level II. These two levels describe all the LULC classes detectable in the remote-sensing data used for this study (Table 1). The nine classes of Level I describe all the main LULC types on the islands. Class 9, clouds, indicates the part of the satellite images covered by clouds that prevented identification of the underlying LULC classes. Level II is made up of 17 subclasses that provide more detail on the Level I types.

Visual interpretation and manual digitization

The ArcGIS Desktop 10.1 software (ESRI) was used to analyze the satellite images (DigitalGlobe satellites WorldView-1 and WorldView-2) and to create the LULC map, based on visual analysis (Shalaby & Tateishi, 2007), which proved to be efficient when the analysts are familiar with the area being classified (Singh, 1989) and when they are working on a basemap such as WI.

The database structure was created before starting visual interpretation of the images to enable storage of data associated with each LULC class. For the Maldivian archipelago, the interpretation proceeded island by island, digitizing LULC polygons and loading relative

information into the attribute table (i.e. LULC classes (Level I and Level II), the name of the island, the type (inhabited, uninhabited, resort), and the area for each LULC polygon). Using this procedure, LULC maps were created for each island and then grouped into atoll LULC maps.

Field data collection and accuracy assessment

Once completed, the LULC maps were checked to verify positional and thematic accuracy. The fieldwork took place in November 2013 in Faafu atoll with the help of MaRHE, the Marine Research and Higher Educational Center of the University of Milano-Bicocca, which was the base camp of this activity. Ground control points (GCPs) were acquired using the Garmin GPSMAP 62sc. GCPs for thematic accuracy were collected near the boundary between different LULC classes, whereas GCPs for position accuracy (or GPS) were taken on easily recognizable elements in the satellite images such as harbor corners, jetty edges, and football field corners. 168 GCPs were collected on the islands of the atoll: 88 GCPs were used to validate the thematic accuracy of the LULC classes (building an error matrix), and 80 points were used to check the positional accuracy of the map.

LULC change detection

The paucity of remote-sensing data for the Republic of the Maldives has made it difficult to find historical images suitable for detection of LULC changes. LANDSAT 7 (ETM+) imagery, with a spatial resolution of 30 m, was useful for detecting LULC changes only on a few of the larger islands. On the other hand, Google Earth offers free satellite images and allows access to historical images that can be used to detect changes over time. For the Maldivian islands, the historical database provides high-resolution images starting from 2001. Images of the islands were acquired from Google Earth historical imagery and geo-referenced in ArcGIS 10.1. Then these images were visually interpreted to detect LULC classes.

Finally, post-classification change detection was applied to the maps created. Land Change Modeler, which is integrated into the IDRISI 10.2 software (Clark Labs), provides tools for the assessment and trending of LULC changes. It was used to compare and analyze LULC maps of different ages representing the Maldivian islands. By comparing two LULC maps of an island created on two different dates, it was possible to quantify the gains, losses, and persistence of LULC classes both in a geographically distributed and a graphic format.

Results

LULC map, accuracy assessment, and data analysis

The accuracy of the LULC map was validated by means of fieldwork. According to (Foody, 2002), an error matrix was generated using the 88 GCPs collected on the islands in the Southern part of Faafu Atoll. The error matrix (Table 2) showed an overall accuracy of 85%. Only the Forest land and Shrubland classes showed higher errors, which were caused by the absence of an abrupt margin between the two classes.

The 80 GCPs collected for positional accuracy verification showed a high level of agreement with the same features on the map. The calculated positional error was less than one meter, which is an unexpected result for a map realized using only remote-sensing data from a basemap.

Table 3 reports the total extent in hectares of all the LULC classes of the Republic of the Maldives for the period between the end of 2010 and the first months of 2011. Detailed results on LULC of two representative atolls are reported in details in Figures 3 and 4. Figure 3 shows the LULC map of Laamu atoll, one of the largest in the southern part of the archipelago, composed of 64 islands, 11 of which are inhabited, with a total population of 13,395 (Ministry of Finance and Treasury, Department of National Planning, 2011). Tourism in this atoll is not massive due to the considerable distance from the international airport in Kaafu atoll. In fact, there are only two resorts, the LULC class Agricultural Land is well represented over in all the islands and covers one-third of the total land area of the atoll, occupying 612 ha out of 2162 ha (Figure 4 and Table 4).

Figure 4 represents the southern part of Kaafu atoll. Kaafu is an administrative atoll divided into two geographic atolls: North Kaafu and South Kaafu. In the northern part of the atoll, the capital of the archipelago and the international airport are located. For this reason, the first resorts were built in this atoll, and nowadays it has the highest bed capacity in the entire archipelago (Ministry of Tourism, 2013). Compared to Laamu, Kaafu is smaller, with a total land area of 1897 ha. One of the big differences between the two atolls is the high number of resort islands in Kaafu, 42 out of 90 islands in total, of which only 10 are inhabited. With regard to LULC classes, Urban or Built-up Land is the most representative class, with 738 ha, which is almost one-third of the total land area (Table 4). This value demonstrates the high anthropogenic impact for touristic purposes on the islands of this atoll.

LULC change detection

The LULC maps obtained from visual interpretation of the Google Earth historical images of 2001, 2002, 2005 and 2006 were analyzed and compared with those realized from the WI basemap using Land Change Modeler (IDRISI Selva Edition, Clarks Lab).

This study of LULC change has involved representative island typologies (inhabited, uninhabited and resort), which make it possible to detect spatial patterns of change in the archipelago. Fig. 6, 7 and 8 shows a synthesis of the main results obtained from the analysis and clearly show that the most evident changes in LULC occurred on resort islands, documenting a conversion from uninhabited island to resort islands and associated LULCC for inhabited island. It is also evident that the increased number of resort island is well correlated to the distance from the international airport: more is the distance less is the number of new resort island per atoll (Fig. 5).

Some example of LULCC detected at some representative islands are shown in Fig. 6, 7 and 8. Figure 6 represents Medhafushi, an island in the southern part of Noonu Atoll, as an example of the inhabited island category. The LULC map for 2002 (Google Earth imagery) shows an island covered entirely by Forest land (11 ha) and Shrubland (6 ha), both in the middle and along the shore. Anthropogenic impact was completely absent during this period. The LULC map for 2011 (WI basemap) highlights a drastic change in land use on the island: Medhafushi became Iru Fushi Resort & Spa, a resort island easily recognizable from the water villa jetty in the lagoon. The new LULC class of Urban and Built-up land developed over more than 8 ha at the expense of the natural environment, Shrubland (-6 ha) and lagoon (-3 ha). The Forest land class did not lose area. Actually, the coconut trees were simply transplanted along the shore, replacing Shrubland, to shade the beach villas, a necessity for the resort property to maintain the image of a luxuriant tropical island.

Figure 8 illustrates the LULC changes on Maamin'gili, an inhabited island in Alifu Dhaalu atoll. The LULC map for 2001 was created using the first historical satellite image available (Google Earth imagery). In this map, the Urban or Built-up land class occupies the eastern part of the island (28 ha) with an adjacent portion of Agricultural land (7 ha). The remaining area consists of Forest land (21 ha), Shrubland (11 ha), and Barren land (10 ha). Five year later, in 2006 (Google Earth imagery), the island appears unrecognizable. A huge part of the lagoon (100 ha) had been reclaimed from the sea, increasing the surface of the island from 77 ha to 180 ha. The most representative class had become Barren land (96 ha), followed by Urban or Built-up land (37 ha). Forest land lost 15 ha in favor of Urban and Agricultural land (10 ha). On the east side, a harbor was built. In 2011, the latest image analyzed (WI basemap) showed

a further increase in the island area, from 180 ha to 193 ha. This increment was due to land reclamation on the edge of the island. On Maamin'gili, the Barren land area to the south become the airfield (79 ha Infrastructure) for the new airport of the Alifu Atoll. On the other side of the island, Forest land and Shrubland lost further surface area to expansion of the Urban or Built-Up land (41 ha) and Agricultural land (16 ha) classes.

The last example shown (Fig. 7) is a resort island, Olhuveli Beach and Spa Resort, in Kaafu atoll. For this small island, the LULC change analysis was carried out using two satellite images dated 2005 and 2011. In 2005, the island was occupied by a resort with a capacity of 250 beds (Ministry of Tourism, 2006). In the LULC map (2005, Google Earth Imagery), the total area of the island was 8 ha: 3 ha of Urban and Built-Up land (guest villas, jetties, and staff area), 3 ha of Forest land, and 2 ha of Barren land (beaches). In 2011 (WI basemap), the island appeared different. The bed capacity of the resort was more than doubled, from 250 to 570 (Ministry of Tourism, 2011). Comparison of the two maps shows that this increment was provided by some land reclamation projects that increased the island surface and by building a new water villa jetty in the southern part of the lagoon. In addition, a new artificial island was built in the north-western part of the lagoon. The surface of the resort is now 19 ha, including the new island (3 ha). 11 ha of lagoon were occupied for accommodation purposes. The major increase was in Barren land, from 2 ha to 7 ha, and the appearance of the Shrubland class (3 ha). These elements are correlated with land reclamation: Barren land is the first LULC class that appears after reclamation, and Shrubland is the first vegetation type that starts to colonize the new land area.

Discussion

The LULC Map

The visual interpretation of satellite images using the WI basemap has proved to be a good method for LULC detection on the Maldivian islands. The high-resolution images of the basemap made it possible to detect LULC on the smallest islands of the archipelago. The LULC map created for the Republic of the Maldives showed very good accuracy considering the exclusive use of free remote-sensing data to generate it. The adopted classification scheme (Anderson et al., 1976) represents a comprehensive description of the LULC classes present on the islands. The only difficulties found during the classification process were detection of the border between the Shrubland and Forest land classes and the classification of Urban or Built-up land on resort islands. In the first situation, the problem was created by the progressive transition of Shrubland into Forest land: it is easy to digitize mistakenly a strip of Forest land that on the ground turns out to be Shrubland. Besides, on resort islands, the presence of built structures such as beach villas, bars, and restaurants with roofs made of coconut leaves may lead to errors. In fact, these structures are surrounded by bushy vegetation, and in some cases, especially when using WorldView 1 black and white RS data, it was difficult to classify them correctly as Urban or Built-up land. In these situations, to reduce the probability of interpretation errors, the LULC on the islands was analyzed at higher scale to increase the accuracy.

The LULC map created in this study made it possible for the first time to evaluate the surface area of LULC classes on the Maldivian islands. These quantitative data refer to the first months of 2011 and describe LULC status on 80% of the land surface of the archipelago: 22,389 ha out of almost 30,000 ha total land area (Official Atlas of the Maldives, 2008). The data in Table 3 show that most of the land area, 11,000 ha, was covered by natural vegetation, Forest Land, and Shrubland. Urban and Built-up land covered 4476 ha, distributed on inhabited and resort islands, and Agricultural land covered only 1442 ha.

The analysis highlighted that differences in LULC classes within the atolls are related to proximity to Ibrahim Nassir International Airport. Atolls that are closer, like Kaafu, Alifu (North and South), Baa, and Lhaviyani have been developed for tourist accommodation since the early 1980s. On these atolls, many inhabited islands were converted into resorts, and the main LULC class became Urban or Built-Up land. On the other atolls, distance from the international airport has slowed down the colonization of the tourist infrastructure, and as

shown for Laamu atoll (Table 4), Forest land appeared to be the main LULC class (667 ha). Agricultural land was also well represented, especially in atolls with large islands (612 ha, Laamu).

LULCC

Analysis of LULC changes over time revealed important variations on the surface of the islands, which were detectable in all categories: uninhabited, inhabited, and resort (Fig. 6, 7, 8). From the examples reported in this study, an increase in anthropogenic areas is evident at the expense of natural areas such as tropical forest and lagoon habitats. In particular, land reclamation processes were implemented to create new land reclaimed from the ocean to meet the needs of human activities. The PCC detection procedure has produced LULC change maps which describe the spatial patterns of change from 2001 to 2011. A spatial change trend observed in the entire archipelago was clearly visible in the three islands mentioned in this study. All the LULCC that has occurred on the islands in recent decades, caused by population growth and the exponential increase in tourism, has inevitably amplified the anthropogenic impact on the surrounding reefs.

On the inhabited islands, urban expansion, with increases in Urban or Built-up land and Agricultural land on the borders of villages, was noticeable. These changes have brought about an evident decline in the forest environment: loss of Forest land area and deterioration of this class to Shrubland. On islands with no more free surface for urban expansion, frequent use of land reclamation has been observed. The new reclaimed lands were used not only for expansion of urban settlements, but also to build new infrastructures like harbors and airports. On Maamin'gili (Fig. 8), all these changes were observed. In 2001, it was an island with a small village in the middle surrounded by Forest and Shrubland. Five years later, in 2006, huge land reclamation had been carried out in the lagoon all around the southern part of the island, a harbor had been built on the eastern side, and the Forest land class had almost disappeared. In 2011, on the Barren land class obtained from the land reclamation, the airfield of the Villa Domestic Airport had been built and was inaugurated in March 2013.

On the resort islands, the main LULC changes were connected to expansion of bed capacity related to tourism growth. To do this, the resort properties expanded guest accommodations by building new water villas or reclaiming land from the lagoon area. On Olhuveli Beach and Spa Resort, the resort island shown in Fig. 7, both solutions were adopted. From 2005 to 2011, a new large water villa jetty was built in the southern part of the lagoon, and in the western part, land reclamation was done to enlarge the island for future construction of beach villas. This

reorganization enabled the proprietor to more than double the bed capacity of the resort from 250 to 570 (Tourism Yearbook, 2013).

On uninhabited islands, which represent the majority of the archipelago (900 out of 1192 islands), LULC changes were related especially to expansion of Agricultural land or construction of new resorts. In the first case, islands were converted to farm islands, still uninhabited, but with plantations that have replaced Forest land area. Otherwise, when an uninhabited island was converted into a new resort island, its natural structure was completely altered. As on Medhafushi (Fig. 6), a pristine island in 2001, Urban or Built-Up land (for tourist purposes) had become the main LULC class in 2011; the Forest land area remained well represented, but in a completely anthropogenic environment designed for tourists' pleasure. The construction of three jetties, two for the water villas and one for the diving center, has also disturbed the lagoon environment.

The study revealed that LULC changes on the islands were relatively fast and radical, with a negative environmental impact not only on terrestrial, but also on near-shore ecosystems. These LULC changes were governed by socioeconomic factors, and tourist development has proved to be the primary cause. Census data show that from the beginning of the nineties, the population growth rate decreased from 3.0% in 1990 to 1.9% in 2013, stabilizing at an average of 1.7% during the last 10 years (http://data.worldbank.org/indicator/SP.POP.GROW). On the other hand, the presence of tourists in the archipelago has grown steadily from 195,000 per year in 1990 to 1,125,000 in 2013, a rate of increase of 470%. Figure 9 correlates the two growth lines and shows clearly the strong increase in tourists in the last 23 years. The only negative peak was registered between 2005 and 2006 due to the effect of the Asian tsunami that struck the archipelago. From 2009, growth started again because of the entrance of new emerging countries like China, Russia, and India into the tourism market. In 2010, the number of Chinese tourists surpassed that of European tourists, until then the most represented group in the Maldives (Ministry of Tourism, 2011). To support this growth, it was necessary to increase the number of resort islands and the global bed capacity. The number of resorts rose from 64 in 1990 to 86 in 2000 and to 109 in 2013, with an increase in bed capacity from 7,621 to 23,469; 45 pristine inhabited islands were converted to dedicated tourist islands, completely transforming their LULC. As for the 2007–2011 Tourism Master Plan, these resorts started to be built, not only on the islands in the atolls closer to the international airport, but in all atolls, which signaled the entrance of the Maldives into a new phase of tourist development (Sheyvens, 2011; Ministry of Tourism, 2007b). On the existing resort islands, expansion projects were necessary to satisfy the growth of tourist demand. This growth created a

migration flow inside the archipelago. Many citizens moved from the peripheral islands to the capital, Malé, looking for a job in the tourist industry. This led to a population increase of 58,000 from 2002 to 2012, representing a growth in population from 74,000 to 132,000 (http://data.un.org/Data.aspx?d=POP&f=tableCode%3A240).

Conclusions

The World Imagery basemap (ESRI) has proved to be an appropriate data source for LULC detection in a nation such as the Republic of the Maldives with its peculiar geographic configuration. It represents the first LULC map of the archipelago. Overall, the determined mapping accuracy of 85% indicates the effectiveness and the replicability of this method. The LULC map contributed to properly visualize the distribution and extent of various LULC classes throughout the atolls.

The study revealed that vegetated area, forest, and shrubland were still the most represented classes in 2011, followed by Urban or Built-Up areas. A clear difference was revealed in the extent of Urban or Built-Up areas for tourism purposes between atolls closer to the international airport and others. Data from the Ministry of Tourism related to the construction of new resorts have highlighted a concentric development from the central atolls to the peripheral ones, with an increase in the number of resorts from 89 in 2006 to 111 in 2014.

The LULCC analysis together with socioeconomic data has shown a common spatial dynamic for all the atolls. Urban or Built-Up areas have increased over the last decade in all the islands studied, followed by Agricultural lands and Infrastructure. This has caused a degradation of the natural environment, with the loss of vegetated surfaces or their deterioration into anthropogenic semi-natural areas. The analysis also revealed an increase in land reclamation both on inhabited and resort islands. This practice enlarged the exploitable surface of the islands, but with a negative impact on coral reef habitat, which is essential for the existence (economic and physical) of the Republic of the Maldives. Comparison of socioeconomic data has revealed that these changes have been driven by the growth of tourism, which has continued to increase from the seventies until today.

The land use and land cover map produced in this study together with change analysis can help to understand the impact of LULCC on coral reefs and the increase in erosion. It can also contribute to the development of sustainable land-use policies for forecasting the effects of climate change on the islands of the archipelago.

References

Anderson, J. R., Hardy, E. E., Roach, J. T., Witmer, R. E., & Peck, D. L. (1976). A Land Use And Land Cover Classification System For Use With Remote Sensor Data. A Revision of the Land Use Classification System as Presented in U.S. Geological Survey Circular 671, 964, 41.

Brook, B. W. (2008). Synergies between climate change, extinctions and invasive vertebrates. Wildlife Research. https://doi.org/10.1071/WR07116

Dale, V. H. (1997). The relationship between land-use change and climate change. Ecological Applications. https://doi.org/10.1890/1051-0761(1997)007[0753:TRBLUC]2.0.CO;2

Das, T. (2009). Land Use Land Cover Change Detection: an Object Oriented Approach. University of Munster.

Dewan, A. M., & Yamaguchi, Y. (2009). Land use and land cover change in Greater Dhaka, Bangladesh: Using remote sensing to promote sustainable urbanization. Applied Geography, 29(3), 390–401. https://doi.org/10.1016/j.apgeog.2008.12.005

Ferrario, F., Beck, M. W., Storlazzi, C. D., Micheli, F., Shepard, C. C., & Airoldi, L. (2014). The effectiveness of coral reefs for coastal hazard risk reduction and adaptation. Nature Communications, 5(May), 3794. https://doi.org/10.1038/ncomms4794

Foody, G. M. (2002). Status of land cover classification accuracy assessment. Remote Sensing of Environment, 80(1), 185–201. https://doi.org/10.1016/S0034-4257(01)00295-4

Game, E. T., Lipsett-Moore, G., Saxon, E., Peterson, N., & Sheppard, S. (2011). Incorporating climate change adaptation into national conservation assessments. Global Change Biology, 17(10), 3150–3160. https://doi.org/10.1111/j.1365-2486.2011.02457.x

Gerrard, M. B., & Wannier, G. E. (2013). Threatened Island Nations: Legal Implications of Rising Seas and a Changing Climate. Cambridge University Press. Retrieved from https://books.google.it/books?id=BuUvZK7L6q0C

Ghina, F. (2003). Sustainable-Development in Small Island Developing States. Environment Development and Sustainability, 5, 139–165.

Hoegh-Guldberg, O., Mumby, P. J., Hooten, A. J., Steneck, R. S., Greenfield, P., Gomez, E., … Hatziolos, M. E. (2007). Coral reefs under rapid climate change and ocean acidification. Science (New York, N.Y.), 318(5857), 1737–42. https://doi.org/10.1126/science.1152509

Kench, P. S., McLean, R. F., & Nichol, S. L. (2005). New model of reef-island evolution: Maldives, Indian Ocean. Geology, 33(2), 145. https://doi.org/10.1130/g21066.1

Klein, C. J., Jupiter, S. D., Selig, E. R., Watts, M. E., Halpern, B. S., Kamal, M., … Possingham, H. P. (2012). Forest conservation delivers highly variable coral reef conservation outcomes. Ecological Applications, 22(4), 1246–1256. https://doi.org/10.1890/11-1718.1

Lambin, E. F., Turner, B. L., Geist, H. J., Agbola, S. B., Angelsen, A., Bruce, J. W., … Xu, J. (2001). The causes of land-use and land-cover change: Moving beyond the myths. Global Environmental Change, 11(4), 261–269. https://doi.org/10.1016/S0959-3780(01)00007-3

Lyon, J. G., Yuan, D., Lunetta, R. S., & Elvidge, C. D. (1998). A change detection experiment using vegetation indices. Photogrammetric Engineering and Remote Sensing, 64(2), 143–150. https://doi.org/citeulike-article-id:7262520

Maina, J., de Moel, H., Zinke, J., Madin, J., McClanahan, T., & Vermaat, J. E. (2013). Human deforestation outweighs future climate change impacts of sedimentation on coral reefs. Nature Communications, 4(May), 1–7. https://doi.org/10.1038/ncomms2986

Mas, J.-F. (1999). Monitoring land-cover changes: A comparison of change detection techniques. International Journal of Remote Sensing, 20(1), 139–152. https://doi.org/10.1080/014311699213659

Meinel, G., Neubert, M., Sensing, R., & City, L. (2000). a Comparison of Segmentation Programs for High Resolution Remote Sensing Data. Spring, 35(Part B), 1097–1105. Retrieved from http://scholar.google.com/scholar?hl=en&btnG=Search&q=intitle:A+COMPARISON+OF+SEGMENTATION+PROGRAMS+FOR+HIGH+RESOLUTION+REMOTE+SENSING+DATA#0

Nascimento, W. R., Souza-Filho, P. W. M., Proisy, C., Lucas, R. M., & Rosenqvist, A. (2013). Mapping changes in the largest continuous Amazonian mangrove belt using object-based classification of multisensor satellite imagery. Estuarine, Coastal and Shelf Science, 117, 83–93. https://doi.org/10.1016/j.ecss.2012.10.005

Naseer, A., & Hatcher, B. G. (2004). Inventory of the Maldives? coral reefs using morphometrics generated from Landsat ETM+ imagery. Coral Reefs, 23(1), 161–168. https://doi.org/10.1007/s00338-003-0366-6

Pichon, M., & Benzoni, F. (2007). Taxonomic re-appraisal of zooxanthellate Scleractinian Corals in the Maldive Archipelago. Zootaxa, (1441), 21–33.

Rajasuriya, A., Zahir, H., Venkataraman, K., Islam, Z., & Tamelander, J. (2004). Status of coral reefs in South Asia: Bangladesh, Chagos, India, Maldives and Sri Lanka. Status of Coral Reefs of the World: 2004. Volume 1., (November), 213–233.

Rau, G. H., McLeod, E. L., & Hoegh-Guldberg, O. (2012). The need for new ocean conservation strategies in a high-carbon dioxide world. Nature Climate Change, 2(10), 720–724. https://doi.org/10.1038/nclimate1555

Scheyvens, R. (2011). The challenge of sustainable tourism development in the Maldives: Understanding the social and political dimensions of sustainability. Asia Pacific Viewpoint, 52(2), 148–164. https://doi.org/10.1111/j.1467-8373.2011.01447.x

Shalaby, A., & Tateishi, R. (2007). Remote sensing and GIS for mapping and monitoring land cover and land-use changes in the Northwestern coastal zone of Egypt. Applied Geography, 27(1), 28–41. https://doi.org/10.1016/j.apgeog.2006.09.004

Singh, A. (1989). Review Article: Digital change detection techniques using remotely-sensed data. International Journal of Remote Sensing, 10(6), 989–1003. https://doi.org/10.1080/01431168908903939

Turner, B. (1994). Local Faces, Global Flows - the Role of Land-Use and Land-Cover in Global Environmental-Change. Land Degradation and Rehabilitation, 5(2), 71–78. https://doi.org/10.1002/ldr.3400050204

Were, K. O., Dick, T. B., & Singh, B. R. (2013). Remotely sensing the spatial and temporal land cover changes in Eastern Mau forest reserve and Lake Nakuru drainage basin, Kenya. Applied Geography, 41, 75–86. https://doi.org/10.1016/j.apgeog.2013.03.017

Wiedenmann, J., D'Angelo, C., Smith, E. G., Hunt, A. N., Legiret, F.-E., Postle, A. D., & Achterberg, E. P. (2012). Nutrient enrichment can increase the susceptibility of reef corals to bleaching. Nature Climate Change, 3(2), 160–164. https://doi.org/10.1038/nclimate1661

Wooldridge, S. A. (2009). Water quality and coral bleaching thresholds: Formalising the linkage for the inshore reefs of the Great Barrier Reef, Australia. Marine Pollution Bulletin, 58(5), 745–751. https://doi.org/10.1016/j.marpolbul.2008.12.013

Zubair, S., Bowen, D., & Elwin, J. (2011). Not quite paradise: Inadequacies of environmental impact assessment in the Maldives. Tourism Management, 32(2), 225–234. https://doi.org/10.1016/j.tourman.2009.12.007

Tables and Figures

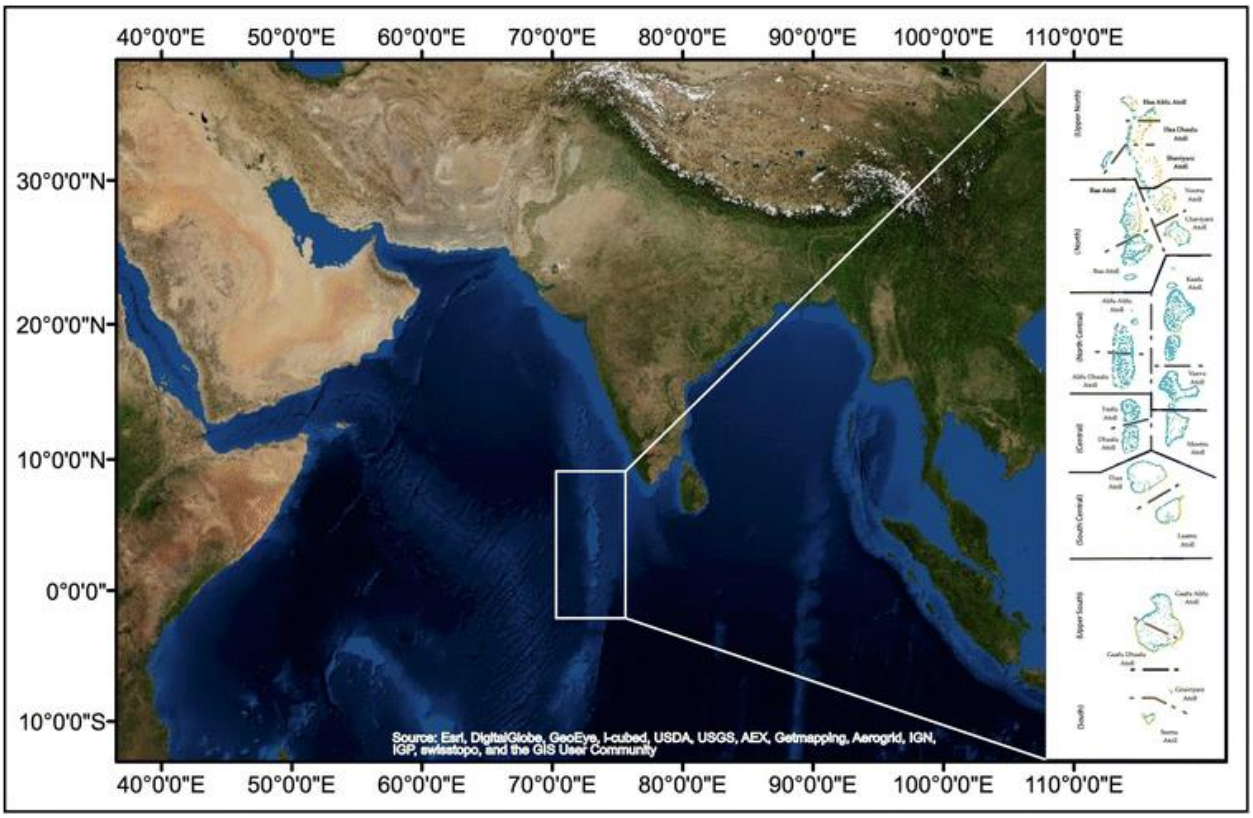

Fig.1 Geographical location ofthe study area. Republic ofthe Maldives is highlighted in the rectangle and in the zoomed area on the right are the represented subdivisions of the archipelago in geographic and administrative atolls

Fig. 2 Panchromatic satellite images of the basemap World Imagery. a An inhabited island captured by the satellite WorldView 1 (DigitalGlobe). b An uninhabited island is shown in a WorldView 2 (DigitalGlobe) image. In both the high-resolution images can be easily identified the LULC classes

Table 1 Hierarchical LULC classification scheme adopted for the Maldivian islands

Land Use-Cover Class	
Level I	**Level II**
1 URBAN OR BUILD UP LAND	
	11 Low density residential
	12 High density residential
	13 Resort
2 AGRICULTURAL LAND	
	21 Cropland
	22 Nursery (Greenhouse)
	23 Non natural-woody
3 HERBACEUS UP-LAND	
	31 Grassland
4 SHRBLAND	
	41 Shrubland
5 FOREST LAND	
	51 Evergreen tropical forest
	52 Tropical forest patch
6 BARREN LAND	
	61 Beach
	62 Transitional
	63 Land reclamation
7 WETLAND	
	71 Water
8 INFRASTRUCTURE	
	81 Airport
	82 Harbour
9 CLOUD	
	91 Cloud

Table 2 Error matrix and overall accuracy for the classified map

Contingency Table								
		Satellite Map Class						
		Urban	Shrubland	Forest Land	Barren Land	Infrastructure (Harbour)	TOT	Producers Accuracy
Ground Reference	Urban	11	0	0	0	0	11	100%
	Shrubland	0	12	3	0	0	15	80%
	Forest Land	2	8	21	1	0	32	66%
	Barren Land	0	0	0	20	0	20	100%
	Infrastructure (Harbour)	0	0	0	0	10	10	100%
	TOTAL	13	20	24	21	10	88	
								Overall Accuracy
	Users Accuracy	85%	60%	87,50%	96%	100%		85%

Table 3
Extension in hectares of the different land use and la cover classes on the entire study area

LULC Classes	2011
	Area (ha)
1 URBAN OR BUILD UP LAND	4476
2 AGRICULTURAL LAND	1442
3 HERBACEUS UP-LAND	648
4 SHRBLAND	4632
5 FOREST LAND	6436
6 BARREN LAND	3161
7 WETLAND	240
8 INFRASTRUCTURE	769
9 CLOUD	585
Total area (ha)	22389

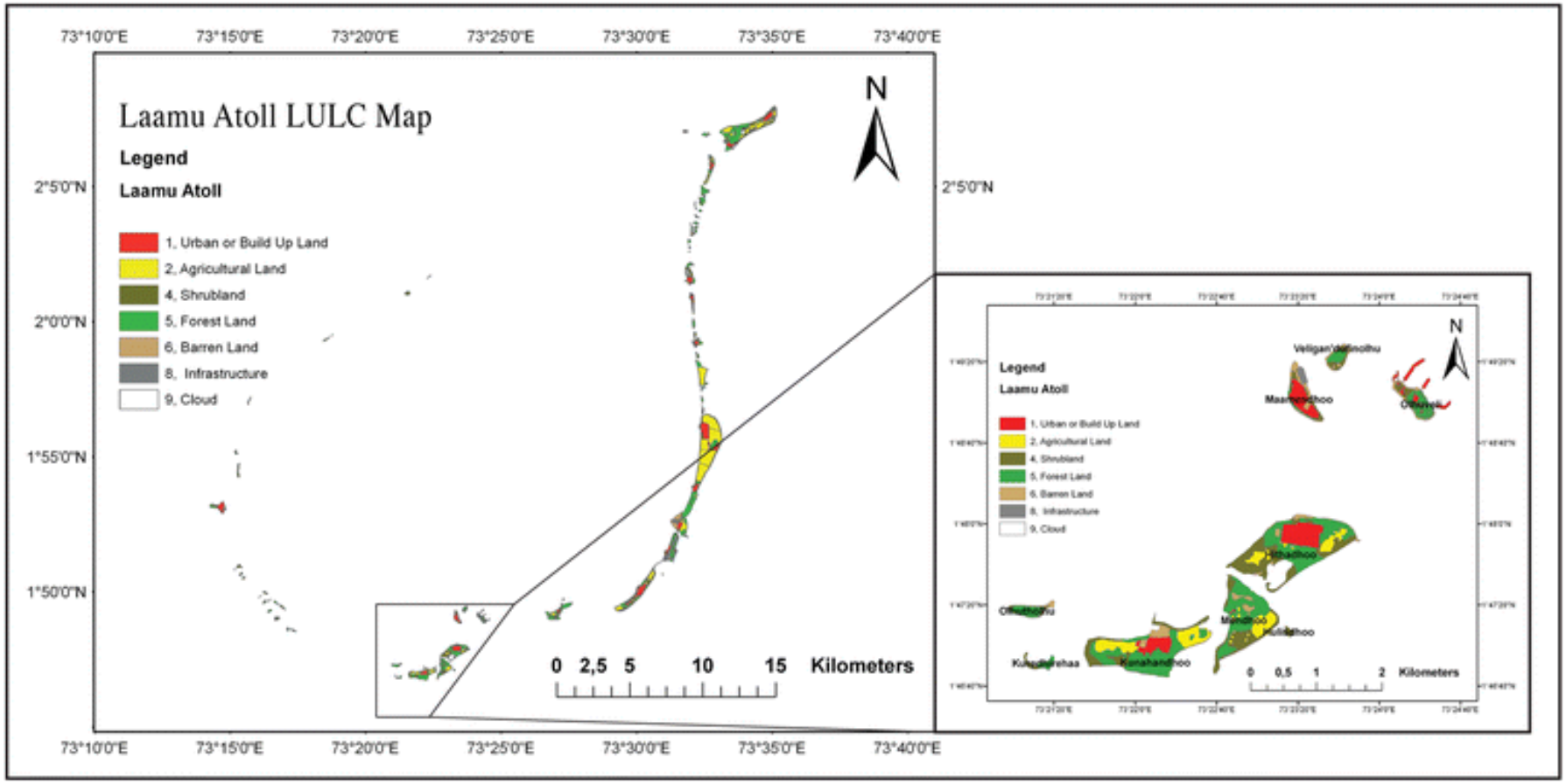

Fig. 3 Land use land cover classified m ap of Laamu Atoll. In the zoomed area, a group of islands in detail

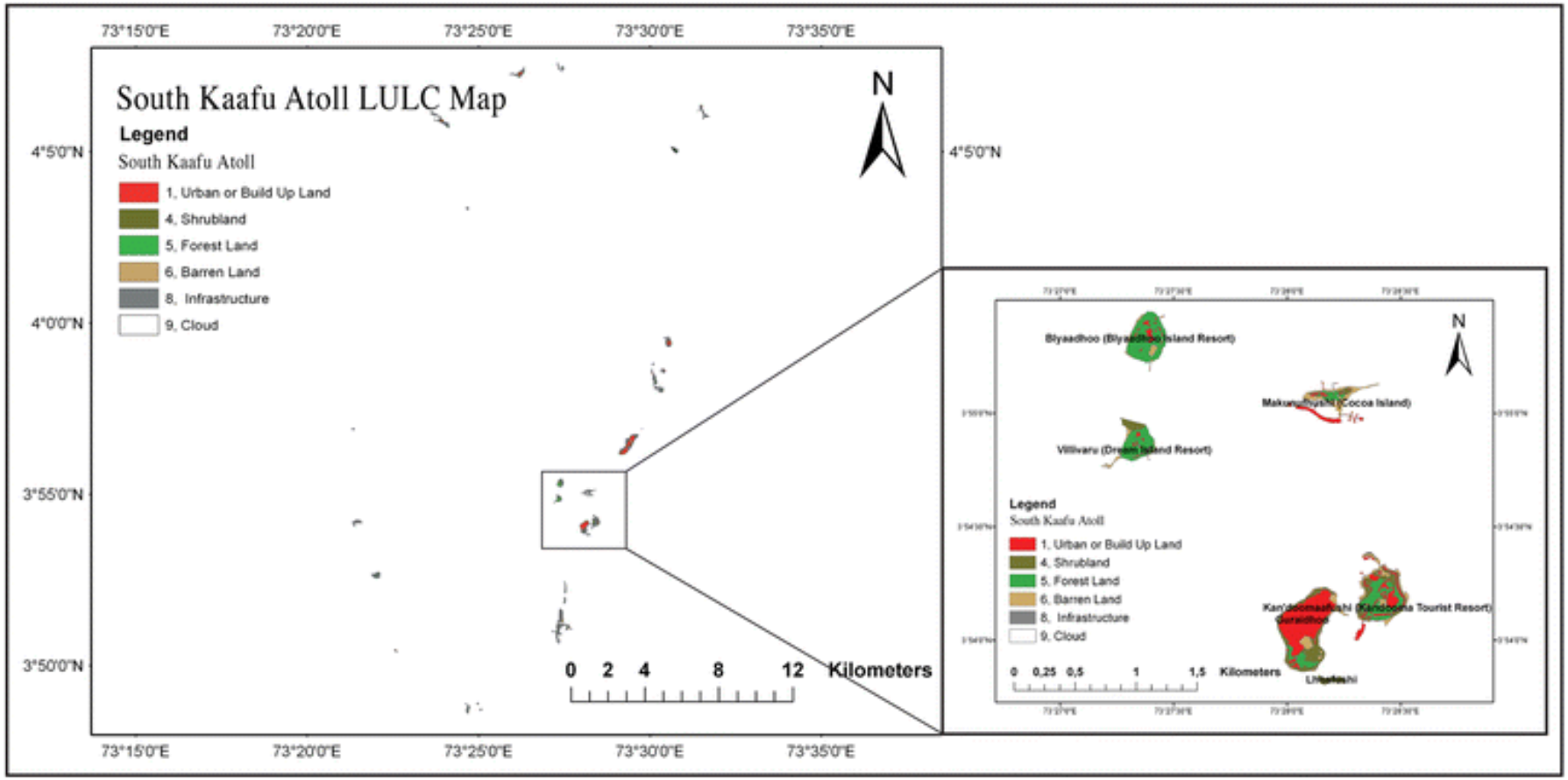

Fig. 4 Land use land cover classified map of the southern part of Kaafu Atoll. In the zoomed area, a group of islands in detail

Table 4 Land use and land cover classification for Kaafu Atoll, in the central part of the archipelago, and Laamu Atoll on the southern part

LULC Classes Kaafu Atoll	2011 Area (ha)	LULC Classes Laamu Atoll	2011 Area (ha)
1 URBAN OR BUILD UP LAND	738	1 URBAN OR BUILD UP LAND	264
3 HERBACEUS UP-LAND	6	2 AGRICULTURAL LAND	612
4 SHRBLAND	159	4 SHRBLAND	364
5 FOREST LAND	164	5 FOREST LAND	667
6 BARREN LAND	262	6 BARREN LAND	168
7 WETLAND	2	8 INFRASTRUCTURE	67
8 INFRASTRUCTURE	236	9 CLOUD	20
9 CLOUD	285		
Total area (ha)	1897	Total area (ha)	2162

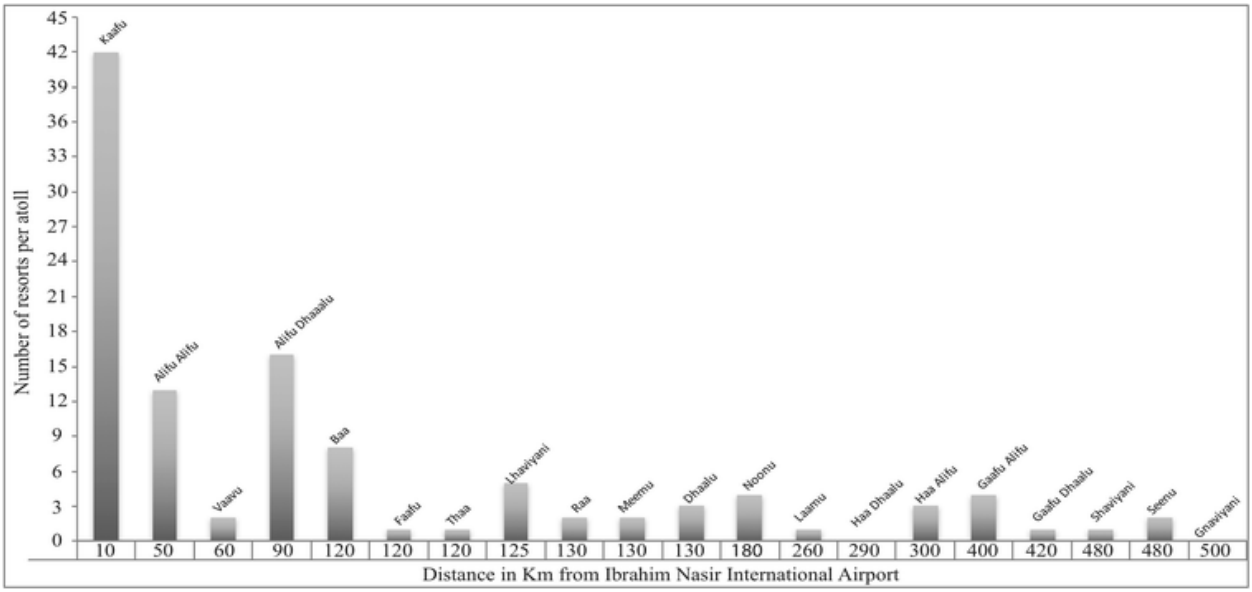

Fig. 5 Comparison of numbers of resorts per atoll and the average distance from the centre of each atolls to Ibrahim Nassir International Airpor

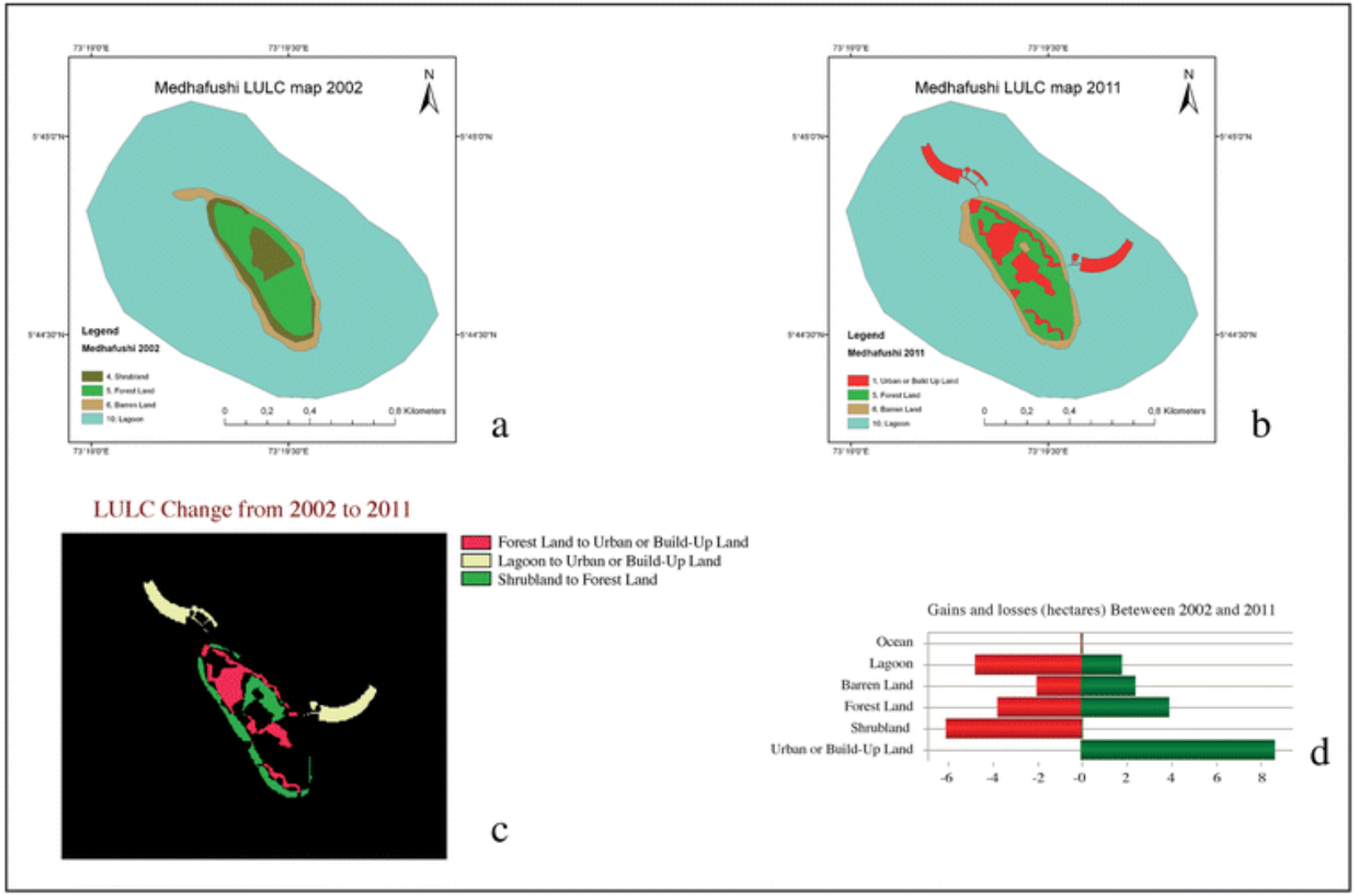

Fig. 6 Classified land-use and land-cover maps of Medhufushi (Noonu Atoll) in 2002 (a) and 2011 (b); bar graph representing gains and losses (d) and LULC chance map (c)

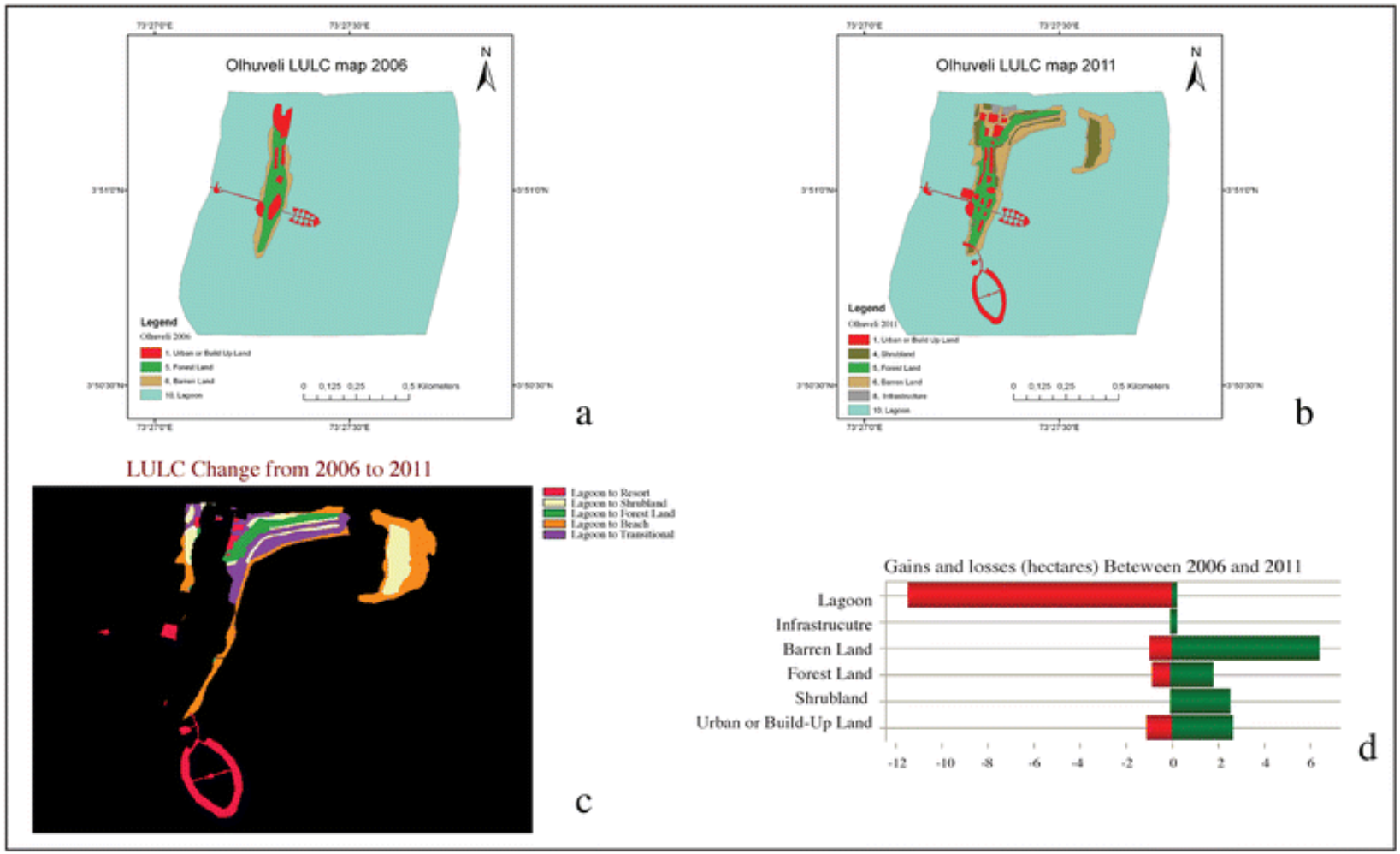

Fig. 7 Classified land-use and land-cover maps ofOlhuveli (Kaafu Atoll) in 2006 (a) and 2011 (b); bar graphs representing gains and losses (d) and LULC chance map (c)

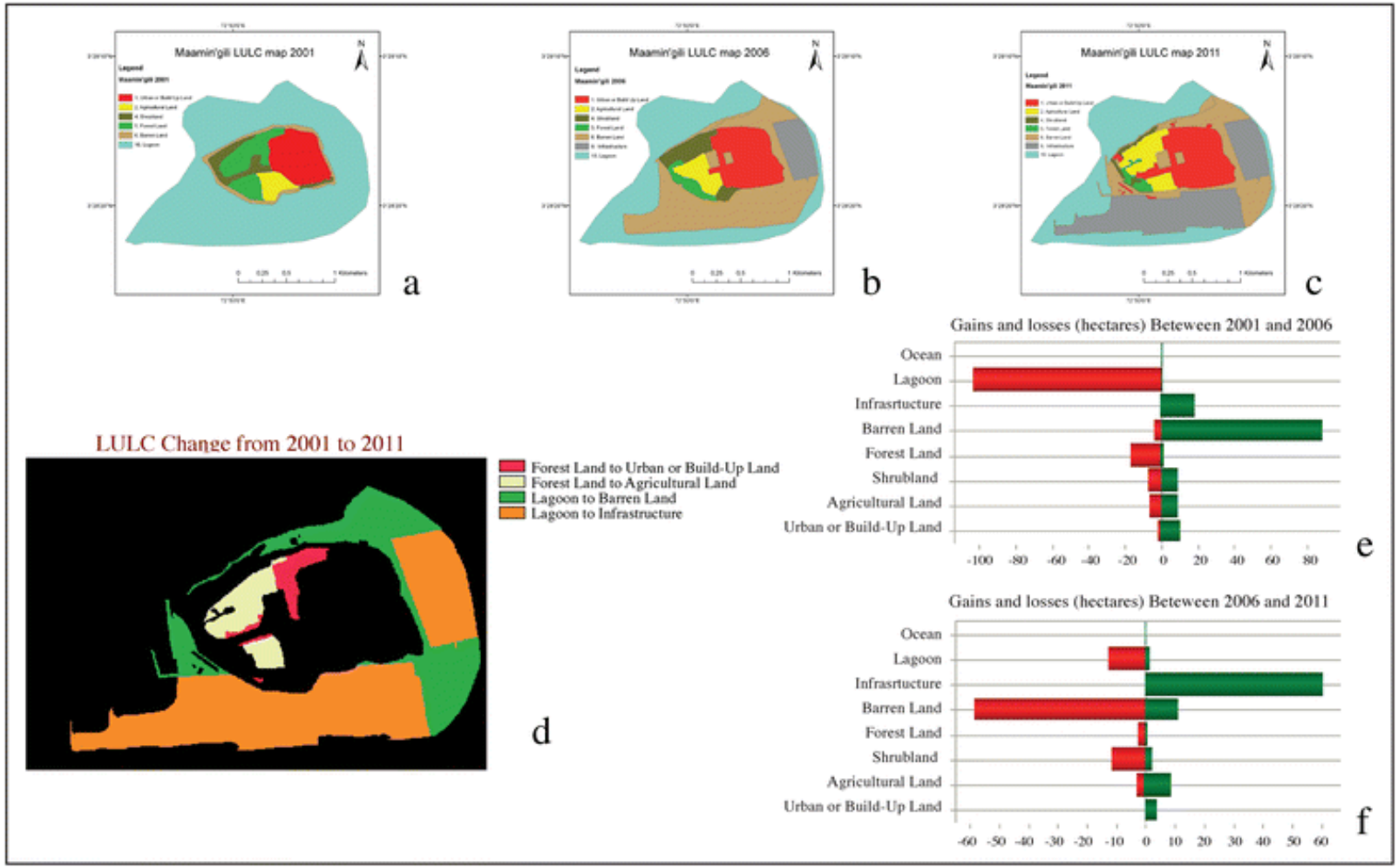

Fig. 8 Classified land-use and land-cover maps of Maamin'gili (Alifu Dhalu Atoll) in 2001 (a), 2006 (b), and 2011 (c); bar graphs representing gains and losses (e, f) and LULC chance map (d) between 2001 and 2011

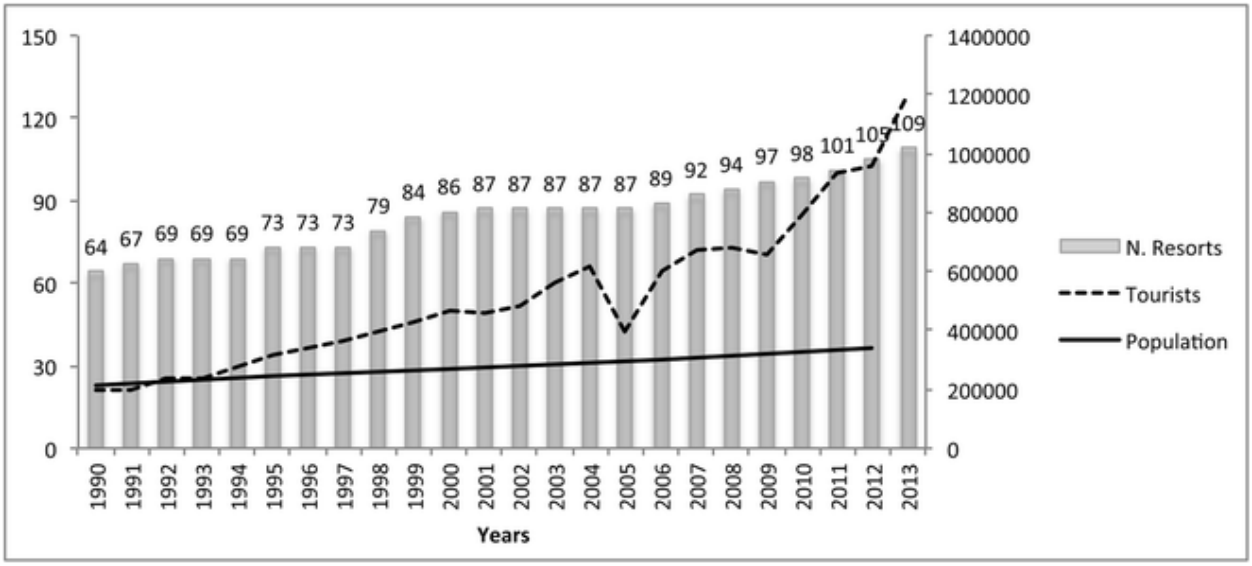

Fig. 9 Comparison between the growths in tourist arrivals, population, and number of resorts built from 1990 to 2013

Chapter 2

Unmanned Aerial Vehicles (UAVs) coupled with innovative processing algorithms and machine learning: new frontiers in high-resolution monitoring of coastal environments

2.1

Fallati L., Savini A., Saponari L., Marchese F., Corselli C., Galli P. (2019). A glance at the catastrophe: Unmanned Aerial Vehicle imagery and Object Base Image Analysis to map habitat shifts on shallow-water coral reefs in a post-bleaching period. (**Under Submission)**

A glance at the catastrophe: Unmanned Aerial Vehicle imagery and Object Base Image Analysis to map habitat shifts on shallow-water coral reefs in a post-bleaching period

Luca Fallati [a,b], Luca Saponari [a,b], Fabio Marchese [a], Cesare Corselli [a], Paolo Galli [a,b] Alessandra Savini [a,b]

[a] Department of Earth and Environmental Sciences, University of Milan-Bicocca, Milan, Italy
[b] MaRHE Center (Marine Research and High Education Center), Magoodhoo Island, Faafu Atoll, Maldives

Abstract

Coral reefs are worldwide undergoing a decline due to the effects of multiple natural and anthropogenic stressors such as increasing water temperature, ocean acidification, overfishing and land reclamation. Among those, temperature-induced bleaching has been reported to cause major coral mortality. According to their severity, these impacts may lead to an evident structural collapse of the reef and to benthic communities shifts. Under this scenario, reasonable monitoring techniques and reproducible protocols are essential to improve data collection in order to enhance our knowledge of spatial and temporal patterns of coral reefs after a major bleaching impact. Our study determined for the first time the potential of consumer-grade Unmanned Aerial Vehicles, coupled with Structure from Motion and Object Base Image Analysis, as a tool to monitor over time shallow-water coral reefs communities. The spatial resolution achieved from the orthomosaics allowed us to classify benthic community types with good accuracy and the comparison of the maps through time (February 2017, November 2018) has shown clearly the deterioration of the fore reef environments after 2016 mass bleaching event. Moreover, the methodology described in this study can be used to generate maps for long term monitoring programs to check the dynamics of shallow water coral assemblages.

Introduction

Coral reefs are worldwide undergoing a decline due to the effects of multiple natural and anthropogenic stressors such as increasing water temperature, ocean acidification, overfishing and land reclamation (Fallati et al., 2017; Hughes et al., 2019; Fine et al., 2019). Among those, temperature-induced bleaching has been reported to cause major coral mortality in the Indo-Pacific Ocean with two main destructive events in 1998 and 2016 (Ateweberhan & McClanahan, 2010; Cowburn et al., 2019; Harrison et al., 2018; Weiler et al., 2019; Pisapia et al., 2019). Coral loss after a bleaching event has important consequences on ecological functionality of the ecosystem. Live coral decline is related to the loss of structural complexity provided by the different coral colony shapes. Complex structures support high diversity and abundance of coral related organisms such as fish, molluscs, echinoderms, and other invertebrates(Alvarez-Filip et al., 2015; Graham & Nash, 2013; Wilson et al., 2006). Further, coral reef structural complexity absorbs wave energy reducing shoreline erosion (Sheppard et al., 2002). Thus, coral mortality reduces the diversity of reef marine organisms and increase erosion of coastline. Structural complexity loss has been reported both after 1998 and 2016 coral bleaching events (Graham et al., 2006; Magel et al., 2019). However, most of the studies on structural complexity are qualitative (Graham et al., 2009; Graham et al., 2006; Sheppard et al., 2002) the majority of the quantitative measurements are made using the chain-and-type method (Risk, 1972) which is time-intensive and suffer of high variation (Friedman et al., 2012). Recently, new technologies, specifically, Structure from Motion (SfM) photogrammetry, have been used to simplify the structural measurements to widen the spatial scale of the survey and to increase the resolution of the data (Burns et al., 2015; Ferrari et al., 2016; Leon et al., 2015; Magel et al., 2019; Storlazzi et al., 2016). However, underwater SfM is limited to a small spatial scale reducing our understanding of a wide process even if at very high-resolution scale (Burns et al., 2016; Couch et al., 2017; Ferrari et al., 2017). Thus, we aimed at use a novel technique to widen the spatial scale of the monitoring process for the effect of the coral bleaching event on structural complexity of a reef in the Maldives. We used an Unmanned Aerial Vehicle (UAV) to collect high-resolution shallow-reef pictures and the SfM and Object Base Image Analysis to process the data and obtain a time-efficient, high-resolution and at reef-spatial scale monitoring of the change in reef structural complexity.

Materials and Methods

Study Area

The Republic of Maldives is an archipelago composed of coral reef islands, grouped in a double chain structure, in the middle of the Indian Ocean (Fig. 1, a.). The 1192 islands of the archipelagos are extended along 860 km from latitude 7° 6′ 35″ N to 0°42′ 24″ S. The Maldives cover an area of about 859,000 km2, but only 227.45 km2 are the land areas (Godfrey, 2018; Naseer & Hatcher, 2004). The majority of the territorial area consists of sea and coral reefs. The islands, generally with a mean elevation of less than 2 m above sea level, can be divided into three groups: inhabited, resort islands and uninhabited (Fallati et al., 2017). Therefore, coral reef ecosystems are vital for the Maldives in terms of economic income and shoreline protection from the erosion. Fisheries and tourism industries are both depending on the health status of the coral reefs and are numerous the ecosystem services/benefits provide by the coral reefs to the local population (Agardy et al., 2017). However, in the last two decades, anthropogenic and natural impacts and global climate change had increased the threats on the Maldivian reefs. Sea Surface Temperature (SST) anomalies and the resulting bleaching events are among the main stress factor for the integrity of the coral reefs of the archipelagos (Pisapia et al., 2016). In the middle of 2016 (April-June) was registered as the largest bleaching event since 1998, which had led to pronounced changes in coral communities in the following months (Pisapia et al., 2019). Further, predation by corallivores, such as the seastars *Acanthaster planci* (Saponari et al., 2018) and *Culcita* spp. (Montalbetti et al., 2019) and the snail *Drupella* spp. (Bruckner et al., 2017), had enhanced the effect of the bleaching event increasing coral mortality and delaying coral recovery.

Fieldwork and data collection was carried out on the Southern part of Faafu Atoll (Fig. 1, b.), on the shallow reef environments around Magoodhoo islands (Fig. 1, c.). These environments, with a depth of maximum 2 m and highly transparent water, offer optimal condition for UAV data collection (Casella et al., 2016; Levy et al., 2018; Doukari et al., 2019). Besides, on this island, since 2009, operates MaRHE Center (http://marhe.unimib.it), a Research and High Educational Centre of the University of Milan-Bicocca. Therefore, thanks to the numerous research activities carried out from different researchers through time, the ecology and biology of the surrounded coral reef are well known (Montalbetti et al., 2019; Montano et al., 2012; Montano et al., 2017; Saliu et al., 2019; Seveso et al., 2014)

As a case study, we monitored four reef portions (Fig. 1, C) a few months after the bleaching event (February and March 2017) and at the end of 2018 (October/November), more than two years later. Area 1 and Area 2 are both parts of the same reef flat on the South of the island. These environments are exposed to the waves and the currents from the oceanic channel between Faafu and Dhaalu atolls. Instead, Area 3 and Area 4 are two internal reefs of Faafu Atoll lagoons. Area 3 is a small semicircular patch reef in a small and sheltered lagunar system on the East side of the island. Area 4 consists in a reef system, elongated in North-West direction, on the central lagoon of the atoll.

UAV Data Collection and Field Survey

DJI Phantom4 drone was chosen for data acquisition. This consumer-grade UAV is a quadcopter with high sensing characteristics. It is equipped with a 1/2.3″ CMOS camera sensor (12.4 MP) that can collect RGB images with a resolution of 4000 × 3000 pixels and an integrated GPS/GLONASS system. DJI Phantom 4 is lightweight, easy to carry, and can efficiently fly at low altitude to obtain good quality ground-resolution images. Additionally, easy take-off and landing procedures make this drone a remarkable solution for low height and short-range surveys. Metadata of the acquired images are recorded in an EXIF (Exchangeable Image File Format) file, which incorporates information such as shutter speed, apertures, ISO and GPS coordinates.

In addition to the UAV surveys were performed visual snorkelling transect across the four monitored areas (Fig 1, c.) in order to validate the remote sensing data and identify the composition of the benthic community

Flights Planning

The surveys were designed using DJI GS PRO (www.dji.com/it/ground-station-pro) a flight planner for iPad device distributed by DJI. This application allows planning in detail all the aspects of the drone mission: generate flight paths, set camera parameters and directly check data acquisition on the iPad display. For all the surveys, we set a fix flight and images acquisition parameters (Tab. 1).

Besides, all the UAV reefs assessments were planned to minimise the differences in environmental conditions between 2017 and 2018 surveys. We always flew during low tide, to reduce water column effect, and with low sun position to the horizon to avoid the glint effect on images (Casella et al., 2016). Moreover, we chose days with no or little wind (less than 5m/s) and consequently a calm sea state: waves strongly influenced the possibility to recognise

and map benthic communities (Doukari et al., 2019). These precautions allow us to reduce errors during the post-processing and the comparison of the output data.

SfM processing and geo-referencing

Agisoft PhotoScan (www.agisoft.com), a commercial Structure from Motion (SfM) software, was used to process UAV images of each area. The software was chosen for the affordable price of the licence and its spontaneous workflow, user-friendly interface and the excellent quality of the outputs (Benassi et al., 2017). These features have made it widely used by the scientific community (Burns and Delparte, 2017; Cook, 2017; Bonali et al., 2019). The images were processed following four main steps: alignment of the photos using high accuracy setting and creation of sparse point cloud; then, generation of a dense point cloud and creation of a Digital Terrain Model (DTM) from the dense could. As final outputs, high-resolution orthomosaic were obtained from the DTM. Processing parameters and outputs are provided in Table 1. For additional information on the SfM procedure, see Verhoeven (2011) and Brunier et al. (2016).

In order to accurately georeferenced the orthomosaics resulting from SfM processing, we collected Ground Control Points (GCPs) in all the monitored areas. At least 8 GCPs per area were deployed over structures easily visible and identifiable in the UAV imagery (Fig. 3). GNSS coordinates were recorded with Emlid Reach RS© (https://emlid.com/reachrs/), a low-cost single-frequency RTK GNSS receivers, with centimetre-level accuracy. This GNSS can operate in Long Range Radio (LoRa 868/915 MHz) mode with one receiver working as a base station that is set up on a fix position (on a distance up to 8 km) and sends real-time correction to the second receiver acting as a rover (Hill et al., 2019). The LoRa mode is useful for RTK GCPs collecting in a country like the Maldives, with no network of International GNSS Service (IGS) or Continuously Operating Reference Stations (CORS). Moreover, the receivers are waterproof (IP67) and for this reason, perfect for GCPs collection in coastal environments. The orthomosaics were then georeferenced in ArcGis 10.6 (Esri).

OBIA Segmentation and Classification

The analysis and classification of the orthomosaics were performed trough Trimble eCognition Developer 9.4 (http://www.ecognition.com/suite/ecognition-developer). The use of this software allowed to carry out a robust image analysis in order to create comparable benthic communities maps. Application of Object-Based Image Analysis (OBIA) algorithms followed

the methods described in previous studies by Roelfsema et al. (2018) on satellites images and Ventura et al. (2018a) on UAV data.

On the high-resolution orthomosaics were applied a multiresolution segmentation algorithm based on homogeneity criteria. Classification takes advantage of the features calculated for each segment such as spectral value but also size, shape, texture and proximity (Liu & Xia, 2010). Using the thresholds between these parameters we define a ruleset for the classification algorithms that allowed us to classify and to label the three benthic cover types present in the area: Hard Coral, Sand, and Coral Rubble. The class composition was established by visual transects collected by snorkelers. Sand class was classified based on the spectral difference (mainly in brightness level and band ratio) between Coral Rubbles and Hard Coral. Instead, Hard Coral and Coral Rubbles were classified considering both the difference in brightness, band ratio, standard deviation, saturation and the form and texture of the segments. Unfortunately, it was not possible to discriminate only from the RGB channels between dead and alive colonies for the inaccuracy of the analysis based only on the visible colours.

Map Accuracy Assessment

The map's accuracy was assessed comparing the outputs with 732 randomly distributed points that proportionally cover all the monitored areas. The points were manually classified, and the accuracy of the maps was evaluated visually using the orthomosaics; this was possible due to the high resolution of the UAV images that allowed an on-screen check conducted by an expert in coral reefs and with good knowledge of the study area (Kattenborn, et al., 2019; Ventura et al., 2018). Then, the accuracy evaluation was done comparing the outputs with the reference data in a confusion matrix (Table 3) to estimate the user and producer accuracy, the overall accuracy of the maps and calculate the Kappa Index (Congalton and Green, 2008). Finally, the benthic cover maps from 2017 and 2018 were compared in ArcGis 10.6 to highlight the differences between the two years and calculate the gain and loss in the three classes (Table 2).

Results

High-Resolution Orthomosaics and Benthic Assemblages Maps

The processing of the UAV images has led to the realisation of high-resolution orthomosaics (1.5 cm/px) of 16 hectares of shallow-water coral reef environments around the island of Magoodhoo for the years 2017 and 2018. The achieved detail of the models provides an overview of the benthic communities dynamic obtained with low-cost surveys. Moreover, the quality of the data allowed to highlight the difference in benthic assemblages extension between the two years from the simple visual comparison of the orthomosaics (Fig. 4)

The benthic assemblages maps realised from the OBIA analysis define the distribution of Hard Coral, Coral Rubble and Sand on selected portions of the fours monitored areas a few months after 2016 bleaching events and more than two years later (Fig. 4). The comparison of the maps revealed a general loss of Hard Corals frameworks extension, from 25% to 44%, with a total loss of 6119 m^2. Consequently, it is evident the increase of the other two classes, Sand and Coral Rubble. Particularly Coral Rubble, a class closely linked with the degradation and fragmentation of the corals' colonies, shows a significant increase in Area 1, Area 2 and Area 4 the most affected by the reduction of Hard Coral.

Maps accuracy

The benthic community maps had an overall accuracy of 79 % and a Kappa index of 56% (Tab. 3), which represent a moderate agreement level, according to Congalton & Green (2008). Individual classes had a user accuracy of 85% for Sand, 66% for Coral Rubbles and 86% for Hard Corals. The lower accuracy of the Coral Rubble is mainly due to the absence of precise boundaries between the other two classes. In some areas, the mixture of sand with corals rubbles form a transition zone which may lead to misclassification. This also applies to the margin between Hard Coral and Rubble. During the map processing in eCognition the jagged margins of the segments have been smoothed. This processed may have created some centimetric imprecision on the boundaries between the class that in several cases can contribute to an accuracy reduction.

Discussion

AUV surveys and image processing

The use of UAV data combined with SfM algorithms is increasing in the last years for environmental researches in different fields: plastic and marine litter monitoring (Fallati et al., 2019; Martin et al., 2018), marine megafauna surveys (Colefax et al., 2018; Kiszka et al., 2016; Raoult et al., 2018), coastal geomorphology (Laporte-Fauret et al., 2019; Lowe et al., 2019), structural geology (Bonali et al., 2019), forestry sciences (Baron et al., 2018; Kattenborn et al., 2019). From the first description of the great potential of this coupled techniques in monitoring ecology and geomorphology of the coral reefs by Casella et al. (2016) are still few the studies that have improved this methodology in this field (Collin et al., 2019; Levy et al., 2018; Parsons et al, 2018).

In our study, we used for the first time UAV images coupled with SfM and OBIA algorithms to monitor and map changes in coral reefs benthic assemblages following a mass bleaching event. The high-resolution orthomosaics produced in our study confirm the potential of these low-cost and versatile tools for the monitoring of shallow-water reefs environments. Besides, no temporal survey limits allowed to observe through time environmental impacts and the resulting changes. Consumer-grade UAV, like DJI Phantom 4, can take off from the shore or a small boat. This flexibility allowed to easily monitor reef structure, such as patch reefs in the lagoon, far from the coast. Obviously, UAVs cannot be compared to a satellite in terms of spatial cover: satellite imagery analysis allowed to map an entire reef system (Hedley et al., 2012; Roelfsema et al., 2018; Roelfsema et al., 2013). However, even if the spatial and temporal resolutions of the satellite sensors has improved in the last decade (Sentinel 2 offer 10 m/pix in visible bands and a revisit time of 5 days) is not even comparable to the centimetric resolution obtain from the UAV surveys. This level of detail placed the monitoring activities of marine environments with the UAVs on a scale that lies between a satellite and a snorkelling/diving survey (Casella et al., 2016; Ventura et al., 2018).

On the other hand, the main limitations of this type of UAV are the low accuracy of the built-in GPS and the restriction in data analysis for RGB images. Regarding the precision of the GPS, the unmodified geolocation is expected to have an error up to 3 m (Kalacska et al., 2018). This level of inaccuracy does not allow to compare the same area, monitored during two different flights, without precise GCPs. To overcome this limitation, we georeferenced our models with RTK GCPs collected in all the areas. Instead, problems in the classification system

for high-resolution UAVs RGB imagery (e.g. the extremely time spending on-screen manual classification) can be overcome with the application of OBIA algorithms. OBIA processing considers not only the spectral information but also the geometrical and spatial relation between pixels or group of them (Blaschke, 2010) and allowed us to manage RGB spatial data with low spectral separation between the classes (e.g. Hard Coral and Coral Rubbles). Moreover, the use of OBIA helped to speed up the classification process: once the ruleset has been developed, it can be applied to all the orthomosaics that represent the same environments with slights changes in features parameters.

Another critical factor that may restrict the potential of the UAVs benthic habitats surveys is the influence of environmental conditions on the water column. Thus, it is important to monitor weather conditions and oceanographic parameters before the flight. Therefore, we planned the surveys to minimise class misclassification errors, and the data acquisition were performed for all the monitored areas during the same optimal conditions in 2017 and 2018.

Classification and maps comparison

The benthic assemblage maps produced from the processing of orthomosaics with OBIA had a good overall accuracy, 79%, that confirm the validity of the classification process. The process allows classifying benthic cover types (Sand, Coral Rubble and Hard Coral) with higher accuracy than maps realised from satellite images with the same methodology (Roelfsema et al., 2018; Roelfsema et al., 2018).

The maps represent the composition of the fore reef benthic assemblages, around Magoodhoo islands, few months after the 2016 coral bleaching event and more than two years later. Before the bleaching, coral reefs around Magoodhoo were composed of flourished frameworks of *Acropora* spp colonies (mainly branching but with some tabular) (Fig. 6, a-b) with an increase of massive *Porites* spp colonies moving from the shore towards the reef crest. During the bleaching, the most affected corals were tabular and branching *Acropora* spp, the primary habitat-forming species of shallow reef environments in the Maldives (Pisapia et al., 2016). Mortality rates in this genus reached 80% (Marine Research Center, 2016) and signs in colonies desegregation were already recorded a few months after the event (Perry & Morgan, 2017). The benthic maps (Fig.4) described an environment where most of the extension of Hard Coral class consists of dead Acropora still in living position (Fig.6, c-d). In addition, this category was composed by 35% of dead coral and only 14% by alive corals (Saponari et al., in prep.). Unfortunately, it was not possible to discriminate the status of corals just from UAV images but were necessary direct snorkelling observations.

The comparison of the maps between 2017 and 2018 show a substantial reduction in Hard Coral class. The dead colonies gradually lose their structure due to the impairment caused by the action of bioeroders and the mechanical action of currents and waves. Therefore was evident a shrinking of the coral frameworks in all the monitored areas from 25% to 44% (Tab 2). Most of the decline was driven by the degradation of branching and tabular colonies that in some areas entirely disappeared from the reef (Fig. 6, a-b). Consequently, an expansion of Coral Rubble was recorded. The extension of these degraded areas can lead to an increase of algal cover and the formation of unstable substrate unsuitable for coral larvae settlement (Roth et al., 2018).

In Area 3, the trends of the benthic assemblages, from 2017 to 2108, are slightly different from the other three (Tab. 2). This because the reef is more sheltered than the other three for its position inside a small lagoon, and the mechanical action of waves and currents on colonies is less pronounced.

Nevertheless, the general effect observed in all the mapped environments was a marked transformation in benthic assemblages with a resulting flattening of the reefs. Rugosity is a crucial ecological factor since biodiversity is strongly correlated to habitat complexity (Anelli et al., 2017; Newman et al., 2015; Perry & Alvarez-Filip, 2019). The negative variation in this parameter due to the transition from healthy coral reefs to a post bleaching degraded environments can have significant implications on reef-associated organisms such as fish. Moreover, the described changes in the structural complexity of the fore reef can lead to an increase in the rates of coastline erosion as a result of the loss of their coastal protection functions (Harris et al., 2018; Perry & Alvarez-Filip, 2019). The comparison of the selected portions of the DTM models obtained from the SfM workflow let us detect the decline in substrate rugosity (Fig 6, c-d.). Unluckily, we were not able to compare the DTMs of the entire areas in order to obtain lost rugosity rates due to the inaccuracy of the Z values. In future studies, this limitation can be overcome with accurate water depth GCPs collection to scale the Z value correctly in all the models.

Final remarks

The future of the coral reefs in the Anthropocene is unknown. The increase of the extreme heating events driven by climate change could make the coral assemblages recovery after a bleaching event more challenging (Hughes et al., 2018). In the Maldives, the full recovery from

the 2016 mortality could take decades (Gilmour et al., 2013; Graham et al., 2011; Hughes et al., 2019) and may be adversely affected by the increase of coral reefs exploitation from fisheries activities, tourism and land reclamation (Aslam & Kench, 2017; Fallati et al., 2017; Naylor, 2015). Moreover, the action of corallivorous organisms, such as *Culcita* sp (Montalbetti et al., 2019), on small coral colonies and recruits can further increase the recovery time. In this scenario, affordable monitoring techniques and reproducible protocol are essential to improve data collection in order to enhance our knowledge of spatial and temporal patterns of coral reefs after a major impact.

Our study determined for the first time the enormous potential of UAV data coupled with SfM and OBIA analysis as a tool to monitor over time shallow-water coral reef assemblages. The protocol that we described is efficient and reliable and confirmed the capability of commercial UAV to acquire high-resolution data in a fast and easy way. The spatial resolution achieved from the orthomosaics allowed us to classify benthic community types with good accuracy and the comparison of the maps through time has shown clearly the deterioration of the fore reef environments.

There are still some limitations, as the difficulty in the calibration of DTMs in order to calculate an accurate rugosity variation, that can easily overcome in the future thanks to a better GCPs collection plan and the continuous increase of the efficiency of UAV platforms. However, the maps generated in this work can be used as a starting point for a long term monitoring program to check the dynamics of shallow water coral assemblages in this new human-dominated era.

References

Alvarez-Filip, L., Paddack, M. J., Collen, B., Robertson, D. R., & Côté, I. M. (2015). Simplification of Caribbean reef-fish assemblages over decades of coral reef degradation. *PLoS ONE*. https://doi.org/10.1371/journal.pone.0126004

Anelli, M., Julitta, T., Fallati, L., Galli, P., Rossini, M., & Colombo, R. (2017). Towards new applications of underwater photogrammetry for investigating coral reef morphology and habitat complexity in the Myeik Archipelago, Myanmar. *Geocarto International*, *6049*(December), 1–14. https://doi.org/10.1080/10106049.2017.1408703

Aslam, M., & Kench, P. S. (2017). Reef island dynamics and mechanisms of change in Huvadhoo Atoll, Republic of Maldives, Indian Ocean. *Anthropocene*, *18*, 57–68. https://doi.org/10.1016/j.ancene.2017.05.003

Ateweberhan, M., & McClanahan, T. R. (2010). Relationship between historical sea-surface temperature variability and climate change-induced coral mortality in the western Indian Ocean. *Marine Pollution Bulletin*. https://doi.org/10.1016/j.marpolbul.2010.03.033

Baron, J., Hill, D. J., & Elmiligi, H. (2018). International Journal of Remote Sensing Combining image processing and machine learning to identify invasive plants in high-resolution images Combining image processing and machine learning to identify invasive plants in high-resolution images. *Remote Sensing*, *39*, 5099–5118. https://doi.org/10.1080/01431161.2017.1420940

Benassi, F., Dall'Asta, E., Diotri, F., Forlani, G., Cella, U. M. di, Roncella, R., & Santise, M. (2017). Testing accuracy and repeatability of UAV blocks oriented with gnss-supported aerial triangulation. *Remote Sensing*, *9*(2), 172. https://doi.org/10.3390/rs9020172

Blaschke, T. (2010). Object based image analysis for remote sensing. *ISPRS Journal of Photogrammetry and Remote Sensing*, *65*(1), 2–16. https://doi.org/10.1016/j.isprsjprs.2009.06.004

Bonali, F. L. L., Tibaldi, A., Marchese, F., Fallati, L., Russo, E., Corselli, C., & Savini, A. (2019). UAV-based surveying in volcano-tectonics: An example from the Iceland rift. *Journal of Structural Geology*, *121*(February), 46–64. https://doi.org/10.1016/j.jsg.2019.02.004

Bruckner, A. W., Coward, G., Bimson, K., & Rattanawongwan, T. (2017). Predation by feeding aggregations of Drupella spp. inhibits the recovery of reefs damaged by a mass bleaching event. *Coral Reefs*. https://doi.org/10.1007/s00338-017-1609-2

Brunier, G., Fleury, J., Anthony, E. J., Gardel, A., & Dussouillez, P. (2016). Close-range airborne Structure-from-Motion Photogrammetry for high-resolution beach morphometric surveys: Examples from an embayed rotating beach. *Geomorphology*, *261*, 76–88. https://doi.org/10.1016/j.geomorph.2016.02.025

Burns, J. H. R., Delparte, D., Gates, R. D., & Takabayashi, M. (2015). Integrating structure-from-motion photogrammetry with geospatial software as a novel technique for quantifying 3D ecological characteristics of coral reefs. *PeerJ*, *3*, e1077. https://doi.org/10.7717/peerj.1077

Burns, J. H. R., Delparte, D., Kapono, L., Belt, M., Gates, R. D., & Takabayashi, M. (2016). Assessing the impact of acute disturbances on the structure and composition of a coral community using innovative 3D reconstruction techniques. *Methods in Oceanography*, *15–16*, 49–59. https://doi.org/10.1016/j.mio.2016.04.001

Casella, E., Collin, A., Harris, D., Ferse, S., Bejarano, S., Parravicini, V., … Rovere, A. (2016). Mapping coral reefs using consumer-grade drones and structure from motion photogrammetry techniques. *Coral Reefs*. https://doi.org/10.1007/s00338-016-1522-0

Colefax, A. P., Butcher, P. A., & Kelaher, B. P. (2018, January 1). The potential for unmanned aerial vehicles (UAVs) to conduct marine fauna surveys in place of manned aircraft. *ICES Journal of Marine Science*. Oxford University Press. https://doi.org/10.1093/icesjms/fsx100

Collin, A., Dubois, S., James, D., & Houet, T. (2019). Improving Intertidal Reef Mapping Using UAV Surface, Red Edge, and Near-Infrared Data. *Drones*, *3*(3), 67. https://doi.org/10.3390/drones3030067

Congalton, R. G., & Green, K. (2008). *Assessing the Accuracy of Remotely Sensed Data*. *Assessing the Accuracy of Remotely Sensed Data*. https://doi.org/10.1201/9781420055139

Couch, C. S., Burns, J. H. R., Liu, G., Steward, K., Gutlay, T. N., Kenyon, J., … Kosaki, R. K. (2017). Mass coral bleaching due to unprecedented marine heatwave in Papahānaumokuākea Marine National Monument (Northwestern Hawaiian Islands). *PLoS ONE*. https://doi.org/10.1371/journal.pone.0185121

Cowburn, B., Moritz, C., Grimsditch, G., & Solandt, J. (2019). Evidence of coral bleaching avoidance, resistance and recovery in the Maldives during the 2016 mass-bleaching event. *Marine Ecology Progress Series*. https://doi.org/10.3354/meps13044

Doukari, M., Batsaris, M., Papakonstantinou, A., & Topouzelis, K. (2019). A Protocol for Aerial Survey in Coastal Areas Using UAS. *Remote Sensing*, *11*(16), 1913. https://doi.org/10.3390/rs11161913

Fallati, L., Polidori, A., Salvatore, C., Saponari, L., Savini, A., & Galli, P. (2019). Anthropogenic Marine Debris assessment with Unmanned Aerial Vehicle imagery and deep learning: A case study along the beaches of the Republic of Maldives. *Science of The Total Environment*, 133581. https://doi.org/10.1016/j.scitotenv.2019.133581

Fallati, Luca, Savini, A., Sterlacchini, S., & Galli, P. (2017). Land use and land cover (LULC) of the Republic of the Maldives: first national map and LULC change analysis using remote-sensing data. *Environmental Monitoring and Assessment*, *189*(8), 417. https://doi.org/10.1007/s10661-017-6120-2

Ferrari, R., Figueira, W. F., Pratchett, M. S., Boube, T., Adam, A., Kobelkowsky-Vidrio, T., … Byrne, M. (n.d.). 3D photogrammetry quantifies growth and external erosion of individual coral colonies and skeletons. https://doi.org/10.1038/s41598-017-16408-z

Ferrari, R., McKinnon, D., He, H., Smith, R. N., Corke, P., González-Rivero, M., … Upcroft, B. (2016). Quantifying multiscale habitat structural complexity: A cost-effective framework for underwater 3D modelling. *Remote Sensing*, *8*(2). https://doi.org/10.3390/rs8020113

Friedman, A., Pizarro, O., Williams, S. B., & Johnson-Roberson, M. (2012). Multi-Scale Measures of Rugosity, Slope and Aspect from Benthic Stereo Image Reconstructions. *PLoS ONE*, *7*(12), e50440. https://doi.org/10.1371/journal.pone.0050440

Gilmour, J. P., Smith, L. D., Heyward, A. J., Baird, A. H., & Pratchett, M. S. (2013). Recovery of an isolated coral reef system following severe disturbance. *Science*. https://doi.org/10.1126/science.1232310

Godfrey, Timothy J. Atlas of the Maldives: A reference for Travellers, Divers and Sailors. Atoll Editions, 2018.

Graham, N. A.J., Nash, K. L., & Kool, J. T. (2011). Coral reef recovery dynamics in a changing world. *Coral Reefs*. https://doi.org/10.1007/s00338-010-0717-z

Graham, N. A.J., Wilson, S. K., Pratchett, M. S., Polunin, N. V. C., & Spalding, M. D. (2009). Coral mortality versus structural collapse as drivers of corallivorous butterflyfish decline. *Biodiversity and Conservation*. https://doi.org/10.1007/s10531-009-9633-3

Graham, N. A J, & Nash, K. L. (2013). The importance of structural complexity in coral reef ecosystems. *Coral Reefs*, *32*(2), 315–326. https://doi.org/10.1007/s00338-012-0984-y

Graham, Nicholas A.J., Wilson, S. K., Jennings, S., Polunin, N. V. C., Bijoux, J. P., & Robinson, J. (2006). Dynamic fragility of oceanic coral reef ecosystems. *Proceedings of the National Academy of Sciences of the United States of America*. https://doi.org/10.1073/pnas.0600693103

Harris, D. L., Rovere, A., Casella, E., Power, H., Canavesio, R., Collin, A., … Parravicini, V. (2018). Coral reef structural complexity provides important coastal protection from waves under rising sea levels. *Science Advances*, *4*(2). https://doi.org/10.1126/sciadv.aao4350

Harrison, H. B., Álvarez-Noriega, M., Baird, A. H., Heron, S. F., MacDonald, C., & Hughes, T. P. (2018). Back-to-back coral bleaching events on isolated atolls in the Coral Sea. *Coral Reefs*. https://doi.org/10.1007/s00338-018-01749-6

Hedley, J., Roelfsema, C., Koetz, B., & Phinn, S. (2012). Capability of the Sentinel 2 mission for tropical coral reef mapping and coral bleaching detection. *Remote Sensing of Environment*, *120*, 145–155. https://doi.org/10.1016/j.rse.2011.06.028

Hicks, F. (2017). *Ecosystem Services Assessment of North Ari Atoll Ecosystem Services Assessment of North Ari Atoll Tundi Agardy*. IUCN. Retrieved from https://portals.iucn.org/library/sites/library/files/documents/2017-003_0.pdf#targetText=The key habitats that contribute,offshore pelagic areas and seamounts.

Hill, A. C., Limp, F., Casana, J., Laugier, E. J., & Williamson, M. (2019). A New Era in Spatial Data Recording: Low-Cost GNSS. *Advances in Archaeological Practice*, *7*(2), 169–177. https://doi.org/10.1017/aap.2018.50

Hughes, T. P., Anderson, K. D., Connolly, S. R., Heron, S. F., Kerry, J. T., Lough, J. M., … Wilson, S. K. (2018). Spatial and temporal patterns of mass bleaching of corals in the Anthropocene. *Science*, *359*(6371), 80–83. https://doi.org/10.1126/science.aan8048

Hughes, T. P., Kerry, J. T., Baird, A. H., Connolly, S. R., Chase, T. J., Dietzel, A., … Woods, R. M. (2019). Global warming impairs stock–recruitment dynamics of corals. *Nature*. https://doi.org/10.1038/s41586-019-1081-y

Kalacska, M., Lucanus, O., Sousa, L., Vieira, T., & Arroyo-Mora, J. (2018). Freshwater Fish Habitat Complexity Mapping Using Above and Underwater Structure-From-Motion Photogrammetry. *Remote Sensing*, *10*(12), 1912. https://doi.org/10.3390/rs10121912

Kattenborn, T., Lopatin, J., Förster, M., Braun, A. C., & Fassnacht, F. E. (2019). UAV data as alternative to field sampling to map woody invasive species based on combined Sentinel-1 and Sentinel-2 data. *Remote Sensing of Environment*, *227*, 61–73. https://doi.org/10.1016/j.rse.2019.03.025

Kiszka, J. J., Mourier, J., Gastrich, K., & Heithaus, M. R. (2016). Using unmanned aerial vehicles (UAVs) to investigate shark and ray densities in a shallow coral lagoon. *Marine Ecology Progress Series*, *560*, 237–242. https://doi.org/10.3354/meps11945

Laporte-Fauret, Q., Marieu, V., Castelle, B., Michalet, R., Bujan, S., & Rosebery, D. (2019). Low-Cost UAV for high-resolution and large-scale coastal dune change monitoring using photogrammetry. *Journal of Marine Science and Engineering*, *7*(3), 63. https://doi.org/10.3390/jmse7030063

Leon, J. X. X., Roelfsema, C. M., Saunders, M. I., & Phinn, S. R. (2015). Measuring coral reef terrain roughness using "Structure-from-Motion" close-range photogrammetry. *Geomorphology*, *242*, 21–28. https://doi.org/10.1016/j.geomorph.2015.01.030

Levy, J., Hunter, C., Lukacazyk, T., & Franklin, E. C. (2018). Assessing the spatial distribution of coral bleaching using small unmanned aerial systems. *Coral Reefs*, pp. 1–15. https://doi.org/10.1007/s00338-018-1662-5

Liu, D., & Xia, F. (2010). Assessing object-based classification: Advantages and limitations. *Remote Sensing Letters*, *1*(4), 187–194. https://doi.org/10.1080/01431161003743173

Lowe, M. K., Adnan, F. A. F., Hamylton, S. M., Carvalho, R. C., Woodroffe, C. D., Lowe, M. K., … Woodroffe, C. D. (2019). Assessing Reef-Island Shoreline Change Using UAV-Derived Orthomosaics and Digital Surface Models. *Drones*, *3*(2), 44. https://doi.org/10.3390/drones3020044

Magel, J. M. T., Burns, J. H. R., Gates, R. D., & Baum, J. K. (2019). Effects of bleaching-associated mass coral mortality on reef structural complexity across a gradient of local disturbance. *Scientific Reports*, *9*(1), 2512. https://doi.org/10.1038/s41598-018-37713-1

Marine Research Center. (2016). *Status of Coral Bleaching in the Maldives*.

Martin, C., Parkes, S., Zhang, Q., Zhang, X., McCabe, M. F., & Duarte, C. M. (2018). Use of unmanned aerial vehicles for efficient beach litter monitoring. *Marine Pollution Bulletin*, *131*, 662–673. https://doi.org/10.1016/j.marpolbul.2018.04.045

Montalbetti, E., Saponari, L., Montano, S., Maggioni, D., Dehnert, I., Galli, P., & Seveso, D. (2019). New insights into the ecology and corallivory of Culcita sp. (Echinodermata: Asteroidea) in the Republic of Maldives.

Hydrobiologia, *827*(1), 353–365. https://doi.org/10.1007/s10750-018-3786-6

Montano, S., Seveso, D., Strona, G., Arrigoni, R., & Galli, P. (2012). Acropora muricata mortality associated with extensive growth of Caulerpa racemosa in Magoodhoo Island, Republic of Maldives. *Coral Reefs*. https://doi.org/10.1007/s00338-012-0895-y

Montano, Simone, Fattorini, S., Parravicini, V., Berumen, M. L., Galli, P., Maggioni, D., … Strona, G. (2017). Corals hosting symbiotic hydrozoans are less susceptible to predation and disease. *Proceedings of the Royal Society B: Biological Sciences*. https://doi.org/10.1098/rspb.2017.2405

Naseer, A., & Hatcher, B. G. (2004). Inventory of the Maldives? coral reefs using morphometrics generated from Landsat ETM+ imagery. *Coral Reefs*, *23*(1), 161–168. https://doi.org/10.1007/s00338-003-0366-6

Naylor, A. K. (2015). Island morphology, reef resources, and development paths in the Maldives. *Progress in Physical Geography*, *39*(6), 728–749. https://doi.org/10.1177/0309133315598269

Newman, S. P., Meesters, E. H., Dryden, C. S., Williams, S. M., Sanchez, C., Mumby, P. J., & Polunin, N. V. C. (2015). Reef flattening effects on total richness and species responses in the Caribbean. *Journal of Animal Ecology*, *84*(6), 1678–1689. https://doi.org/10.1111/1365-2656.12429

Parsons, M., Bratanov, D., Gaston, K. J., & Gonzalez, F. (2018). UAVs, hyperspectral remote sensing, and machine learning revolutionizing reef monitoring. *Sensors (Switzerland)*, *18*(7), 2026. https://doi.org/10.3390/s18072026

Perry, C. T., & Morgan, K. M. (2017). Bleaching drives collapse in reef carbonate budgets and reef growth potential on southern Maldives reefs. *Nature Publishing Group*, *7*(November 2016), 1–9. https://doi.org/10.1038/srep40581

Perry, Chris T., & Alvarez-Filip, L. (2019). Changing geo-ecological functions of coral reefs in the Anthropocene. *Functional Ecology*. https://doi.org/10.1111/1365-2435.13247

Pisapia, C., Burn, D., & Pratchett, M. S. (2019). Changes in the population and community structure of corals during recent disturbances (February 2016-October 2017) on Maldivian coral reefs. *Scientific Reports*, *9*(1), 8402. https://doi.org/10.1038/s41598-019-44809-9

Pisapia, C., Burn, D., Yoosuf, R., Najeeb, A., Anderson, K. D., & Pratchett, M. S. (2016). Coral recovery in the central Maldives archipelago since the last major mass-bleaching, in 1998. *Scientific Reports*, *6*(September), 34720. https://doi.org/10.1038/srep34720

Raoult, V., Tosetto, L., & Williamson, J. (2018). Drone-Based High-Resolution Tracking of Aquatic Vertebrates. *Drones*. https://doi.org/10.3390/drones2040037

Risk, M. J. (1972). Fish Diversity on a Coral Reef in the Virgin Islands. *Atoll Research Bulletin*. https://doi.org/10.5479/si.00775630.153.1

Roelfsema, C., Kovacs, E., Ortiz, J. C., Wolff, N. H., Callaghan, D., Wettle, M., … Phinn, S. (2018). Coral reef habitat mapping: A combination of object-based image analysis and ecological modelling. *Remote Sensing of Environment*, *208*, 27–41. https://doi.org/10.1016/j.rse.2018.02.005

Roelfsema, C., Kovacs, E., Roos, P., Terzano, D., Lyons, M., & Phinn, S. (2018a). Use of a semi-automated object based analysis to map benthic composition, Heron Reef, Southern Great Barrier Reef. *Remote Sensing Letters*, *9*(4), 324–333. https://doi.org/10.1080/2150704X.2017.1420927

Roelfsema, C., Kovacs, E., Roos, P., Terzano, D., Lyons, M., & Phinn, S. (2018b). Use of a semi-automated object based analysis to map benthic composition, Heron Reef, Southern Great Barrier Reef. *Remote Sensing Letters*, *9*(4), 324–333. https://doi.org/10.1080/2150704X.2017.1420927

Roelfsema, C., Phinn, S., Jupiter, S., Comley, J., & Albert, S. (2013). Mapping coral reefs at reef to reef-system scales, 10s-1000s km2, using object-based image analysis. *International Journal of Remote Sensing*. https://doi.org/10.1080/01431161.2013.800660

Roth, F., Saalmann, F., Thomson, T., Coker, D. J., Villalobos, R., Jones, B. H., … Carvalho, S. (2018). Coral reef

degradation affects the potential for reef recovery after disturbance. *Marine Environmental Research*, *142*, 48–58. https://doi.org/10.1016/j.marenvres.2018.09.022

Saliu, F., Montano, S., Leoni, B., Lasagni, M., & Galli, P. (2019). Microplastics as a threat to coral reef environments: Detection of phthalate esters in neuston and scleractinian corals from the Faafu Atoll, Maldives. *Marine Pollution Bulletin*, *142*, 234–241. https://doi.org/10.1016/j.marpolbul.2019.03.043

Saponari, L., Montalbetti, E., Galli, P., Strona, G., Seveso, D., Dehnert, I., & Montano, S. (2018). Monitoring and assessing a 2-year outbreak of the corallivorous seastar Acanthaster planci in Ari Atoll, Republic of Maldives. *Environmental Monitoring and Assessment*. https://doi.org/10.1007/s10661-018-6661-z

Seveso, D., Montano, S., Strona, G., Orlandi, I., Galli, P., & Vai, M. (2014). The susceptibility of corals to thermal stress by analyzing Hsp60 expression. *Marine Environmental Research*. https://doi.org/10.1016/j.marenvres.2014.06.008

Sheppard, C. R. C., Spalding, M., Bradshaw, C., & Wilson, S. (2002). Erosion vs. recovery of coral reefs after 1998 El Niño: Chagos reefs, Indian Ocean. *Ambio*. https://doi.org/10.1579/0044-7447-31.1.40

Storlazzi, C. D., Dartnell, P., Hatcher, G. A., & Gibbs, A. E. (2016). End of the chain ? Rugosity and fine-scale bathymetry from existing underwater digital imagery using structure-from-motion (SfM) technology. *Coral Reefs*, *35*(3), 887–892. https://doi.org/10.1007/s00338-016-1462-8

Ventura, D., Bonifazi, A., Gravina, M. F., Belluscio, A., & Ardizzone, G. (2018a). Mapping and classification of ecologically sensitive marine habitats using unmanned aerial vehicle (UAV) imagery and Object-Based Image Analysis (OBIA). *Remote Sensing*, *10*(9), 1331. https://doi.org/10.3390/rs10091331

Ventura, D., Bonifazi, A., Gravina, M. F., Belluscio, A., & Ardizzone, G. (2018b). Mapping and Classification of Ecologically Sensitive Marine Habitats Using Unmanned Aerial Vehicle (UAV) Imagery and Object-Based Image Analysis (OBIA). *Remote Sensing*, *10*(9), 1331. https://doi.org/10.3390/rs10091331

Ventura, D., Bonifazi, A., Gravina, M. F., Belluscio, A., & Ardizzone, G. (2018c). Mapping and Classification of Ecologically Sensitive Marine Habitats Using Unmanned Aerial Vehicle (UAV) Imagery and Object-Based Image Analysis (OBIA). *Remote Sensing*, *10*(9), 1331. https://doi.org/10.3390/rs10091331

Verhoeven, G. (2011). Taking computer vision aloft - archaeological three-dimensional reconstructions from aerial photographs with photoscan. *Archaeological Prospection*, *18*(1), 67–73. https://doi.org/10.1002/arp.399

Weiler, B. A., Van Leeuwen, T. E., & Stump, K. L. (2019). The extent of coral bleaching, disease and mortality for data-deficient reefs in Eleuthera, The Bahamas after the 2014–2017 global bleaching event. *Coral Reefs*. https://doi.org/10.1007/s00338-019-01798-5

Wilson, S. K., Graham, N. A. J., Pratchett, M. S., Jones, G. P., & Polunin, N. V. C. (2006). Multiple disturbances and the global degradation of coral reefs: Are reef fishes at risk or resilient? *Global Change Biology*. https://doi.org/10.1111/j.1365-2486.2006.01252.x

Tables and Figures

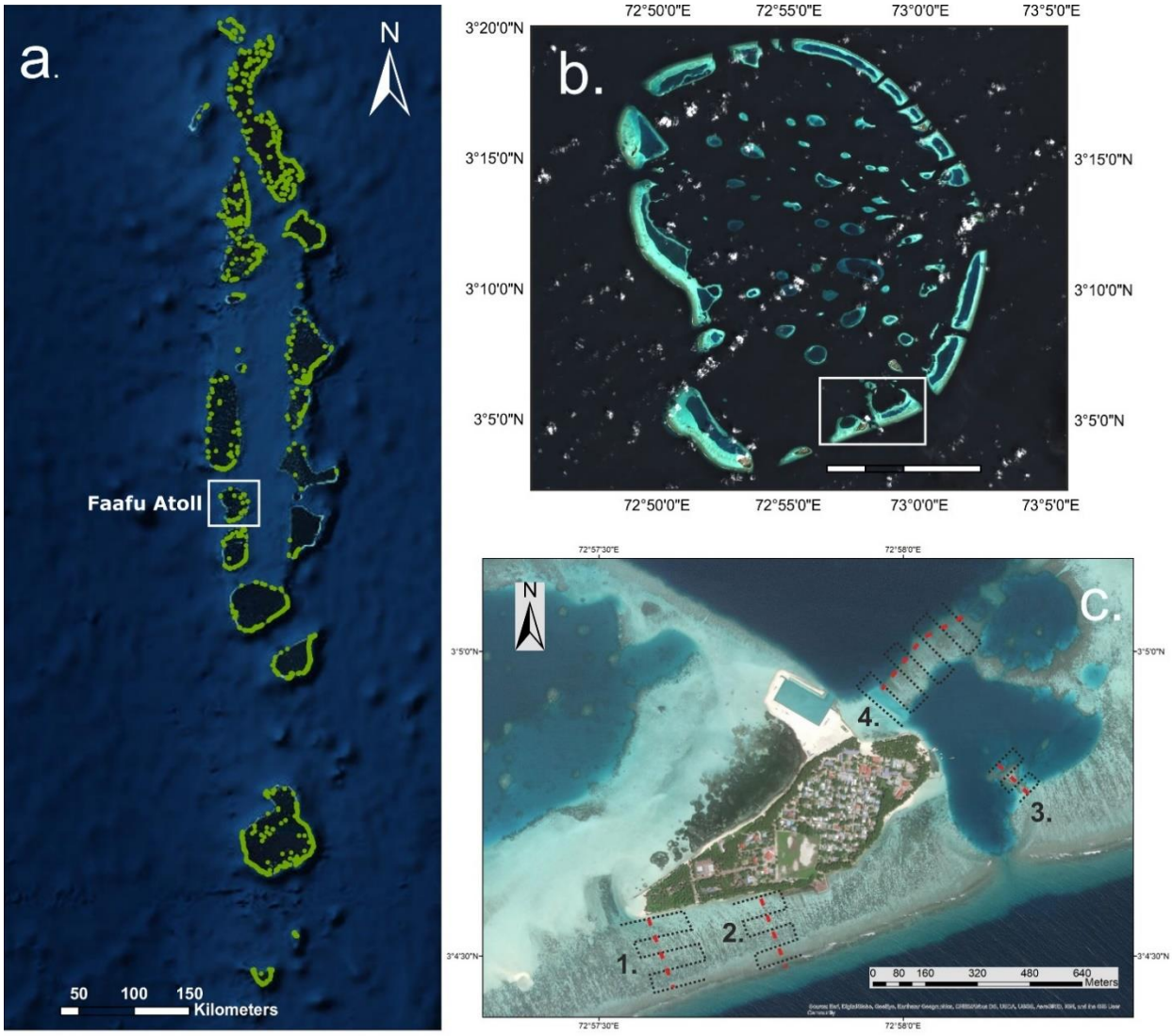

Fig. 1 (a.) Geographic location of the study area, Republic of Maldives; **(b.)** Faafu Atoll**. (c.)**The four monitored reef areas around Magoodhoo island: red dashed lines indicated the snorkelling transects.

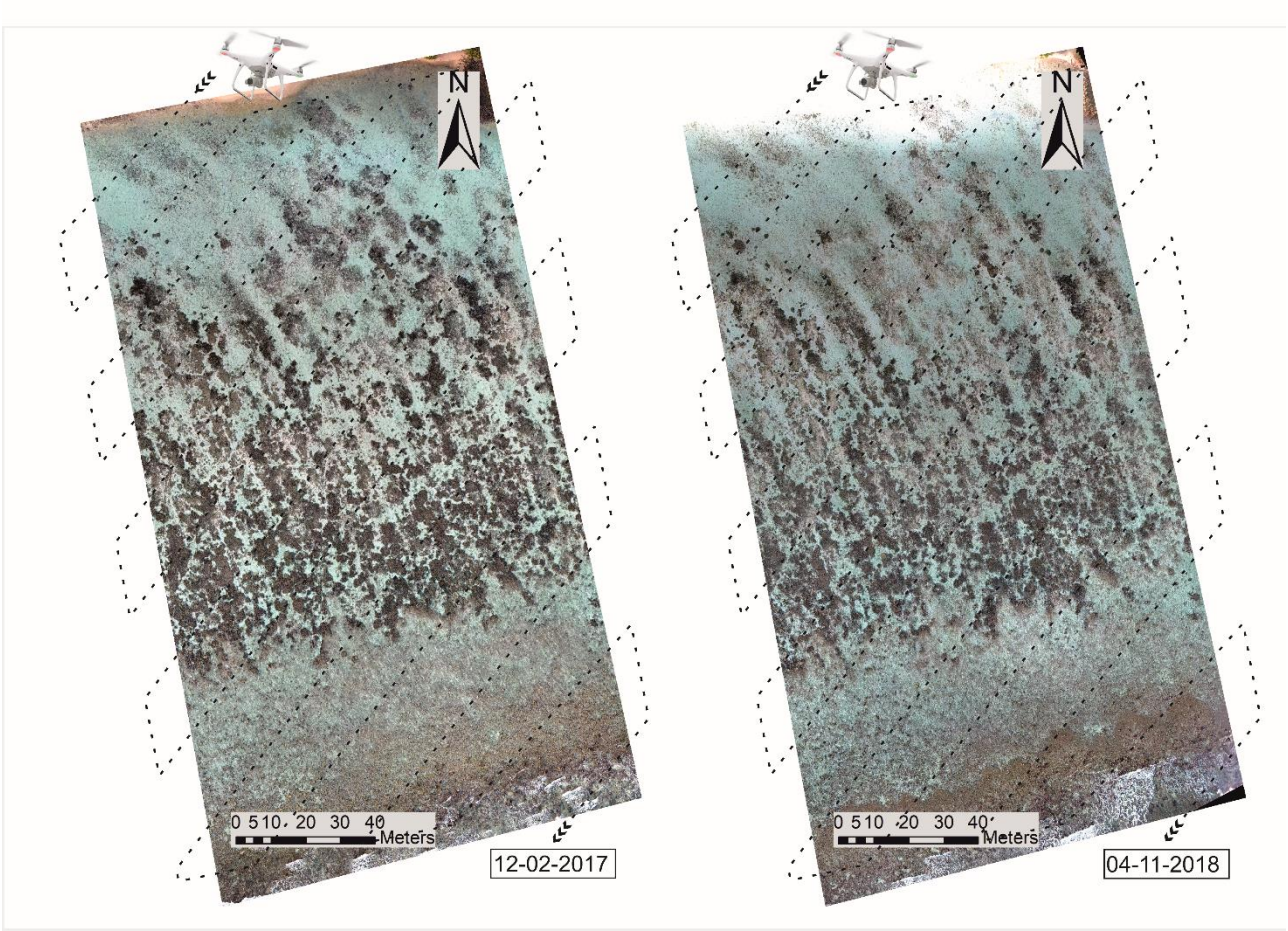

Fig.2 Example of UAV flight paths over Area 2 in 2017 and 2018

Tab.1 Date of UAV surveys, flight acquisition parameters and SfM processing specifications of selected areas.

		2017				2018			
		AREA 1	**AREA 2**	**AREA 3**	**AREA 4**	**AREA 1**	**AREA 2**	**AREA 3**	**AREA 4**
UAV Images Acquisition	Flying Date	11-Feb	12-Feb	05-Feb	18-Feb	04-Nov		14-Oct	05-Nov
	Flying Altitude	35 m				35 m			
	Frontal Overlap	85%				85%			
	Lateral Overlap	75%				75%			
	Speed	2.2 m/s				2.2 m/s			
	Shutter Interval	2.0 s				2.0 s			
	Image Resolution	1.5 cm/px				1.5 cm/px			
	Covered Area	4.98 Ha	4.46 Ha	1.20 Ha	5.37 Ha	5.52 Ha	4.38 Ha	1.49 Ha	5.39 Ha
	Images Numbers	495	431	123	662	550	425	186	664
SfM Processing	Alignment and Dense Cloud processing accuracy	High				High			
	Dense Cloud Points	87,138,680	56,885,927	12,412,455	96,498,907	89,836,998	54,737,644	15,038,040	96,149,457
	DTM Resolution cm/pix	2.94	3.16	2.97	2.86	3.08	3.17	3.1	2.9
	Ortomosaic Resolution cm/pix	1.49	1.58	1.43	1.36	1.54	1.58	1.55	1.45

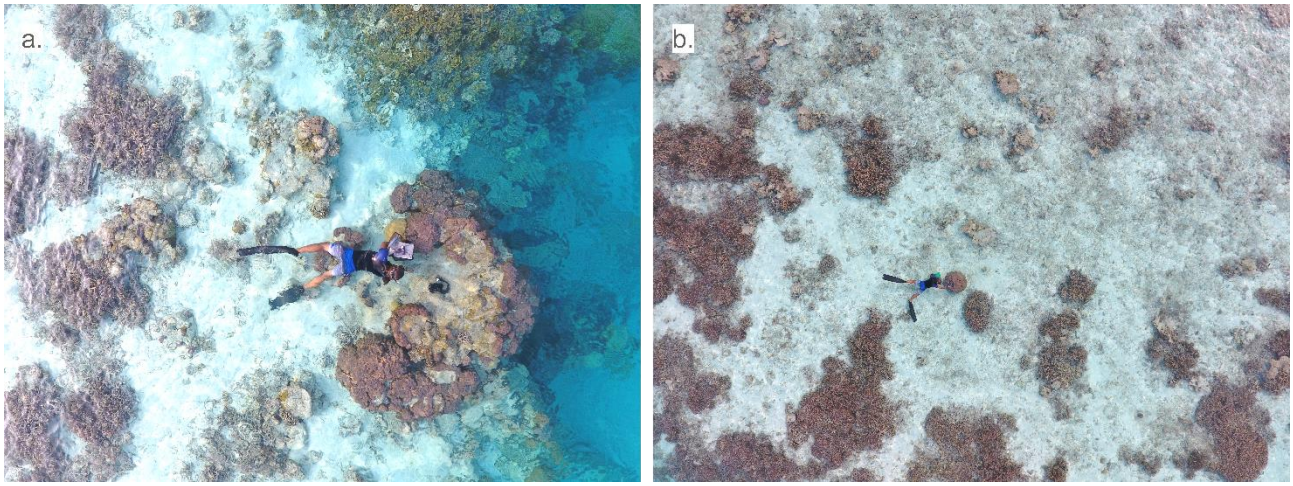

Fig. 3 Deploy of Ground Control Points over easily recognisable features from drone images

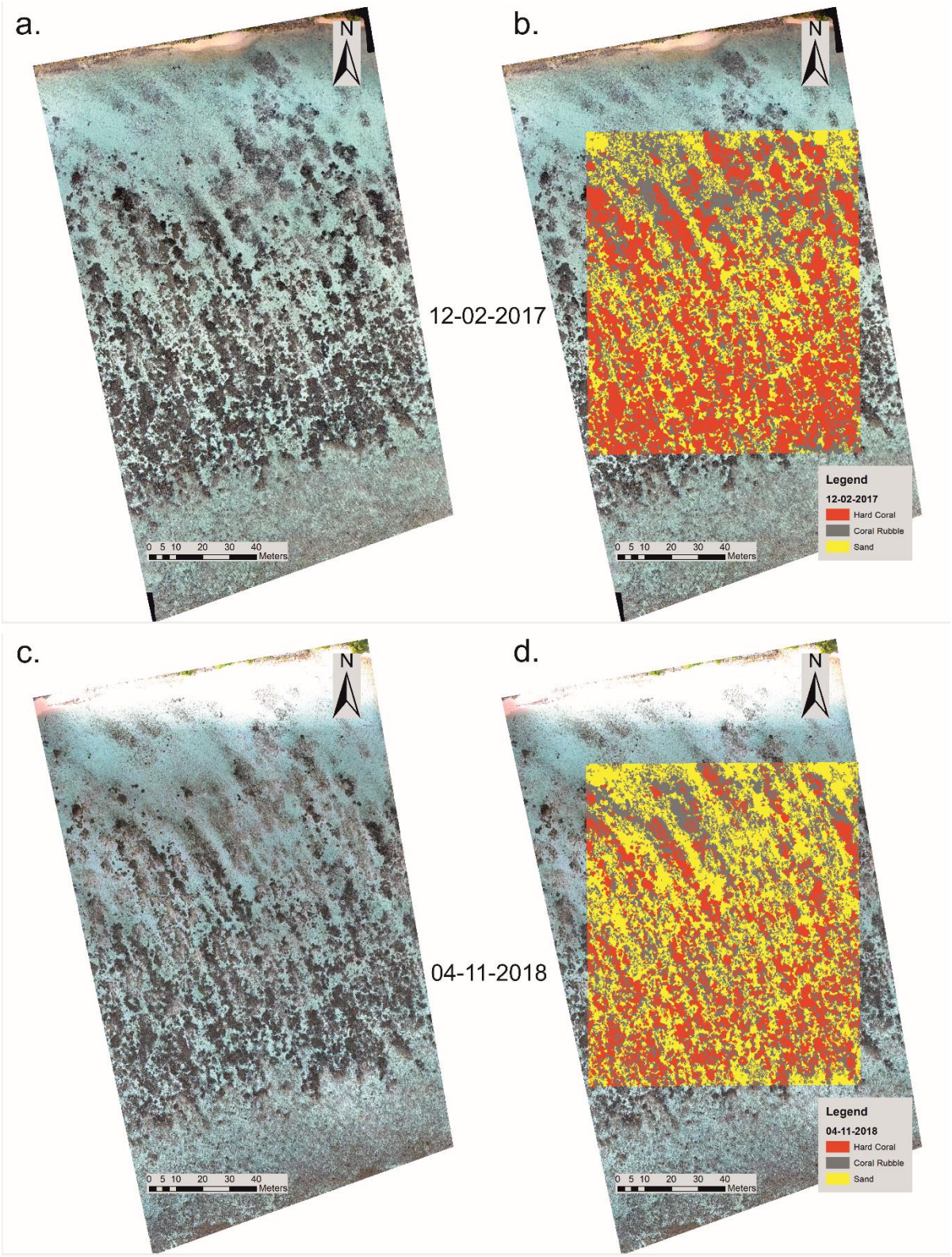

Fig. 4 High-resolution orthomosaics of Area 2 (a. and c.) and OBIA classification of benthic assemblages (c. and d.) on February 2017 and November 2018

Tab. 2 Extension of the cover of benthic assemblages on the monitored areas trough years obtained. The loss of Hard Coral class is expressed in percentage for the total mapped area.

	Area 1		Area 2		Area 3		Area 4	
	2017	**2018**	**2017**	**2018**	**2017**	**2018**	**2017**	**2018**
Hard Coral	28%	15%	41%	26%	56%	42%	35%	20%
Coral Rubble	41%	54%	30%	32%	5%	4%	34%	54%
Sand	31%	31%	29%	42%	39%	54%	31%	26%
Loss of Hard Corals on the total area	11 % (-2811 m^2)		14 % (-1733 m^2)		14 % (-290 m^2)		15 % (-1285 m^2)	

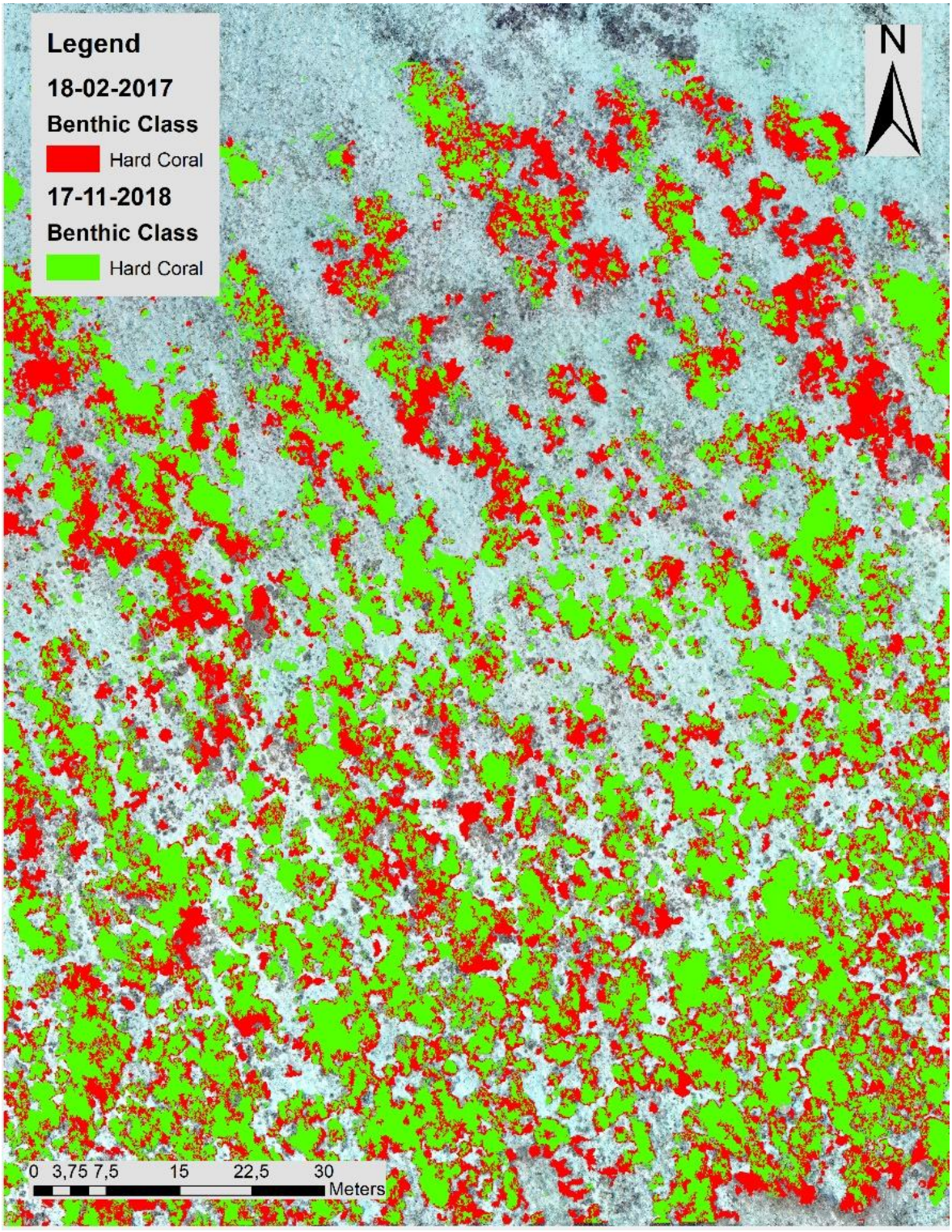

Fig. 5 Comparison of Coral class mapped in February 2017 (polygons in RED) and November 2018 (polygons in GREEN). The overlap of the two maps highlights the reduction of the extension of the coral colonies over the years.

Tab. 3 Error matrix and accuracy index for the classified maps.

Accuracy Table							
		Control Reference					
		Hard Coral	Coral Rubble	Sand	Total	User Accuracy %	Producer Accuracy %
	Hard Coral	**349**	39	21	409	85	86
	Coral Rubble	52	**169**	35	256	66	78
Benthic maps	Sand	2	7	**58**	67	86	51
	Total	403	215	114	**732**		
						Overall Accuracy	Kappa Index
						79%	0.56

Fig. 6 **a. – b.** Underwater pictures of branching and tabular *Acropora spp.* colonies took before bleaching (February 2016) on the reef flat of Magoodhoo. **c. – d.** Dead branching and tabular corals still in living position on the same areas few months after the bleaching event (February 2017)

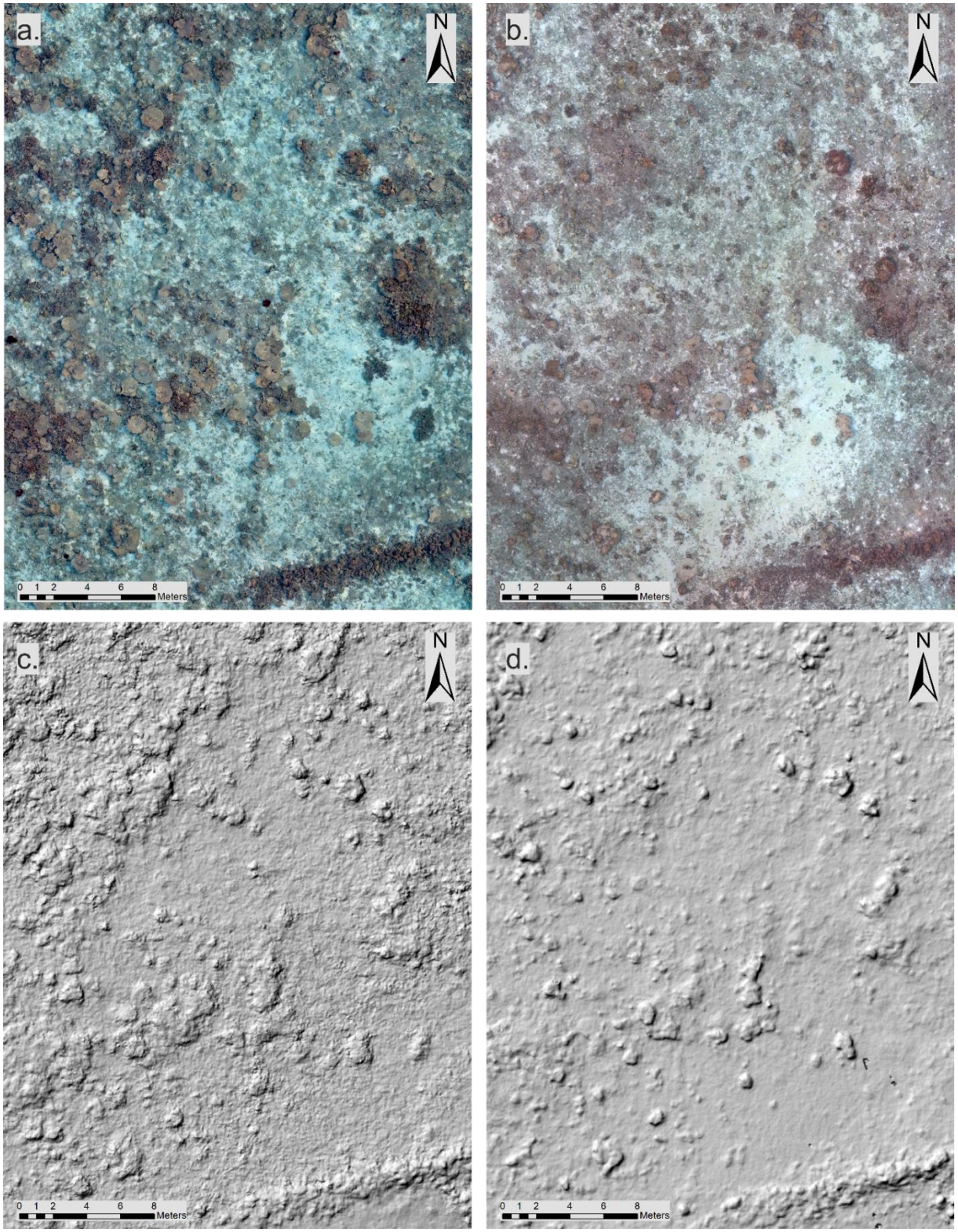

Fig. 7 Same portions of orthomosaic and DTM of reef flat Area 4 in February 2017 (a.-c.) and November 2018 (b.-c.). By comparison of images **a. – b.** is possible to notice the partially disappearance of Acropora table colonies and the increase of rubble areas. **c. – d.** DTM models comparison highlight an overall flattening of the area due to the disintegrationof tabula coral colonies.

2.2

Grech D., Fallati L., Farina S., Guala, I. (2019). The Matrix Reloaded: CARLIT assessment ten years later in the Sinis Coast (Sardinia, Italy) coupled with drone technology. SPA - RAC 6th Symp. on Mar. Veg. Marine Key Habitats and NIS Symp.. Antalya Turkey 14-18 January 2019 (*Conference Paper*)

The matrix reloaded: CARLIT assessment ten years later in the Snis coast (sardinia, italy) coupled with drone technology

Daniele GRECH[1*], Luca FALLATI[2], Simone FARINA[1], Ivan GUALA[1]

[1] IMC - International Marine Centre, Oristano, ITALY

[2] DISAT - Department of Earth And Environmental Sciences, Università degli Studi di Milano-Bicocca, ITALY

*e-mail: d.grech@fondazioneimc.it

Abstract

Mapping and monitoring of marine habitats are crucial tools for coastal management and the implementation of conservation measures. CARLIT index is based on the cartography of littoral assemblages and their sensitivity to changes of environmental conditions. It has been widely tested and applied in the Mediterranean Sea since its introduction in 2007, to assess the ecological status of water bodies within the Water Framework Directive (WFD). Sinis coast (Sardinia, Western Mediterranean) comprises Penisola del Sinis - Isola di Mal di Ventre MPA, being a poorly inhabited and almost devoid of man-made structures. The methodology was for the first time applied in 2008, representing the first application in Sardinia and among the first ever. In 2018, we re-monitored the same coastline coupling a drone technology integration of the classic methodology. The aim of the study was to compare the ecological status 10 years later and to develop a GIS database with more detailed information respect to previous data that will be available at high resolution for future monitoring and developments (e.g. coverage, DTM). Data were gathered by boat or by walking along the coast and high-resolution images were acquired by a commercial drone, elaborated using Structure from Motion (SfM) technique and georeferenced. CARLIT revealed an overall stability of ecological status of water bodies 10 years later, with some slight differences along restricted stretches of coast. The implementation of high resolution GIS based mapping of littoral habitats will allow to obtain

more detailed data on the vertical zonation and extent of the most abundant assemblages. Furthermore, the drone technology will represent even more a historical baseline to follow temporal dynamics of marine vegetation, for both the early detection of native species regression and the spreading of non-indigenous one.

Introduction

The Mediterranean coastal seascape has sharply changed in the last decades, mainly due to the disappearance of sensitive species to local anthropogenic disturbances and global climate changes. Benthic communities associated with rocky littoral habitats are known to significantly respond to slight changes of environmental conditions, thus they are considered good bioindicators of water quality for the implementation of Water Framework Directive (WFD) 2000/60/EC. Their occurrence is taken into account for the assessment of the ecological status of water bodies in the Mediterranean Sea, according to the Cartography of littoral and upper-sublittoral rocky-shore communities (CARLIT) method (Ballesteros et al. 2007). They include shallow species, such as *Cystoseira* spp., threatened (UNEP/MAP-SPA/RAC, 2018) because experiencing a huge decline in Mediterranean Sea (Thibaut et al. 2015). This is especially noticeable where an historical baseline of long phycological tradition is present, allowing to recognise an appropriate reference point and correctly interpret the possible decline. On the contrary, this is not evident when proper dated historical records are lacking. Despite the CARLIT methodology is widespread all around the Mediterranean Sea (Badreddine et al. 2018 and reference therein), only a few examples of re-surveys after many years have been reported in literature, namely for France (Blanfuné et al. 2017) and Spain (Torras et al. 2015).

The method proposed by Ballesteros et al. (2007) has been modified, simplified (Blanfuné et al. 2017 and references therein) and empirically adjusted (Lasinio et al. 2017). Notwithstanding, to date, no technological improvements have been yet considered to increase the amount and resolution of collected information during the monitoring of rocky shore communities, especially for detailed shift detection. In recent years, commercial drones became a powerful tool for environmental applications including surveying and monitoring, that are essential for the implementation of habitat mapping and conservation measures (Lorah et al. 2018; Ventura et al. 2018).

In the Sinis Peninsula (Western Sardinia, Italy), apart from former punctual references, i.e. phycological lists (Cossu, 1992; Gueneau et al. 1992), the CARLIT assessment of Guala et al. (2010) performed during spring 2008 is the most significant oldest semiquantitative baseline

of macroalgal assemblages.

This paper aims to re-evaluate the CARLIT along the same strength of the coast, exactly 10 years later, in order to assess historical change of macroalgal communities and water quality along the Sinis Peninsula. Additionally, the potential of Unmanned Aerial Vehicles (UAVs) or briefly 'drones' have been assessed i) to test the feasibility of data aquisition for the addition to the CARLIT protocol; ii) to explore new type of data available from this type of approach; iii) to built a detailed reference baseline for future comparisons in the study area.

Material and methods

This study was carried out along the Marine Protected Area of Penisola del Sinis - Isola Mal di Ventre (thereafter, MPA) located in the Middle-West coast of Sardinia (Italy). The shoreline is characterized by different coast typology: rocks and cliffs alternating with sandy beaches for about 27 km of coastline. Northwards the MPA is exposed to western winds, while southwards (inside the Gulf of Oristano) is sheltered from dominant winds and waves. The study area is contiguous to a wide wetland system (Cabras and Mistras lagoons) and the Tirso mouth, the main river in Sardinia, both affecting the Gulf of Oristano, where they flow into. Along the exposed shoreline some freshwater springs flow by rocky cliffs (Su Tingiosu) and by the outback behind some main beaches (Is Arutas and Funtana Meiga). The area is scarcely urbanised with a demographic density of about 90 inhabitants/km^2 almost stable during the decade 2008-2017 (ISTAT, 2017). As a matter of fact, it can be considered very low compared to other Mediterranean sites where Fucales assemblages were assessed (Thibaut et al. 2015; Grech, 2017) such as Portici in the Gulf of Naples (Italy) with 12,000 inhabitants/km^2. In the entire Sinis coast, 12,000 is the mean number of touristic influx per season. A treatment plant system, devoted to civil and industrial wastewater, is located about 10 km apart from the MPA. It was settled in the 80s and was dedicated at the beginning to the industrial area and the Oristano city. Between the years 1990-2000, the plant system was extended to treat also neightbouring municipalities wastewater outputs. The treatment plant receives wastewater for a Population Equivalent or unit per capita loading (PE) of 79.423 (N. ab/eq) with a flow of 31.111 mc/g. (Provincia di Oristano, 2014). Discharge outlet flows into the industrial port channel and then into the sea. The water circulation is mainly forced by the NW wind and is characterised by a short water-residence time (Cucco et al. 2006), with a fast and intense exchange of water masses with the open sea. Under the most common wind forcing, 1.5 days is required to renew the 70% of the gulf water.

The re-monitoring of CARLIT was carried out along the entire coastline of the MPA through the traditional method, by assigning the sensitivity level (SL) to benthic communities per each stretch of rocky coast and assessing the Ecological Quality Ratio (EQR) according to Ballesteros et al. (2007). The EQR values were calculated for each of the two water bodies (WB1 and WB2, respectively inside and outside the gulf) as defined by Guala et al. (2010) on the basis of the different geographic orientation and exposure to prevailing winds. In addition, we used a DJI Phantom4, a consumer grade drone, to collect macroalgal assemblage orthophotos. Take-off and landing were controlled manually from a small boat or by walking along the coastline. Different geomorphological relevant features (*sensu* Ballesteros et al., 2007) were selected to test the cruise feasibility and the cartographic rendering (i.e. accuracy, distortion, coverage) at different flying height (from 5 to 20 m a.s.l.). All the images were edited using the photogrammetric software Agisoft PhotoScan Professional and Structure from Motion (SfM) techniques to obtain a digital model of the coast and analysed through free and open source Geographic Information System (QGIS) to compute the surfaces covered by the most abundant assemblages.

Results

The EQR values were maintained both in WB1 (from 0.64 to 0.60) and WB2 (from 0.97 to 0.95), with the same 'Good' and 'High' ecological status respectively, after 10 years. Superimposing the stretches of coastline with corresponding SL assigned to thriving communities in 2008 and 2018, some slight differences were detected and are represented in Fig. 1.

Through the drone survey, more than 2,500 high-resolution orthophotos of macroalgal assemblages were collected. The best compromise between sampled area and resolution was found at 15 m of flying height. Through the image processing, high-resolution ortho-mosaics (0,5 cm/px; Fig. 1) and digital terrain models (DTMs) were obtained. From the digital models and orthophotos of the coast, the coverages of the shallow subtidal communities and terrain attributes (slope, aspect, rugosity) were estimated with a cenimetric accuracy and a sampling effort of 2.6 h/km. As additional result, here we defined the Index of Cystoseirety (IoC), namely the ratio between surface of the species and the coastal length (see example reported in Fig. 1).

Discussion and conclusions

The CARLIT index shows that the water quality did not changed from the first assessment in the MPA. The drone survey allowed to integrate the CARLIT data with more accurate information on the distribution and the surfaces covered by the most abundant communities.

This study demonstrated the high stability of the 10-years-later-CARLIT assessment (among the first in the Mediterranean Sea and the first reported in Italy). Despite this index could be performed every 3 years across all the water bodies without significant reduction in the confidence of EQR classification (Cavallo et al. 2016), it was no longer monitored in the study area after 2008 and this contribution updated the information to 2018.

Our results point out once more, as suggested by Guala et al. (2010), that Sinis coast (outside the gulf) is the ideal candidate to represent a proper reference site, at least for the biogeographic area that includes the coastline of Sardinia and the north Tyrrhenian sea (see Bianchi, 2004), with higly biodiverse stands along a very heterogenous geomorphological coastline. Considering the high level of EQR in WB2, with lushy forests of *C. amentacea* and *C. crinita*, the area is worth of conservation measures, detailed investigations and more frequent monitoring programmes. On the contrary, higher trophic conditions are evident inside the gulf, probably because of the influence of surrounding inland water systems. Although the assessment of the anthropic pressure was beyond the scope of this work, tourism activities in the Sinis area have shown a definitely slight increase in recent past. We felt confident that habitat destruction could be exluded at present, however human trampling should be monitored as some patterns may be significant and no data are currently available.

The slight difference of SLs recorded along a few stretches of coast (Fig.1), could be due to both natual temporal dinamics of algal communities and the influence of human pressure. Notwithstanding we cannot exclude the bias of the subjectivity of the CARLIT index assessors.

The innovative technique of post-processing images from drone allowed us to compute coastal surfaces covered by the most abundant community assemblages with a decimetric accuracy, through a relatively low sampling effort considering also the increased amount of information acquired. The current contribution is far to propose a further integration of CARLIT, that is complete for the purpose for which it was conceived. However, the information coming from otho-mosaics and terrain attributes allow to detaily characterize the forests and open new scenarios of studies and analysis such as the IoC and the computation of spatial patterns through a seascape ecology approach.

This study suggests that new developments are available for the assessments of shallow rocky shores and complementary data collected by drone could be coupled to raise the amount and the quality of data from standard monitoring. The use of this instrument, in conjunction with SfM algorithms, will offer a powerful contribution, that is additional to the EQR assessment, used until now. Furthermore the post processing workflow could be remarkably improved and the selection with mapping of the communities could be considerably simplified through algorithms (Adams, 2008), i.e. Object-based Image Analysis (OBIA; Ventura, 2018). Once implemented, such an analysis could automatically detect CARLIT categories on the ortho-mosaics to be furtherly validated by an expert and trained eye. Future habitat mapping, with improved sensors and longer battery life of drones, will easily advance the classic visual method, adding detailed and georeferenced data about assemblage coverage and terrain attributes (i.e. slope, aspect, bathymetry and DTM) with relatively low cost, sampling effort and high accuracy. These achievements will give a detailed baseline to follow temporal dynamics (e.g. the early detection of macroalgal community shifts and slight SL change with high resolution models of coastline), and could allow to disentangle global changes to local one (punctual pollution or habitat destruction) in a study area that is still far from to be properly studied from a phycological point of view.

1).

References

Adams, W. M. (2018). Conservation by Algorithm. Oryx, 52(1), 1-2.

Badreddine, A., Saab, M. A. A., Gianni, F., Ballesteros, E., & Mangialajo, L. (2018). First assessment of the ecological status in the Levant Basin: Application of the CARLIT index along the Lebanese coastline. *Ecol. Indic.*, 85, 37-47.

Ballesteros, E., Torras, X., Pinedo, S., Garcia, M., Mangialajo, L., & De Torres, M. (2007). A new methodology based on littoral community cartography dominated by macroalgae for the implementation of the European Water Framework Directive. *Mar. Pollut. Bull.*, 55(1-6), 172-180.

Bianchi C.N., (2004). Proposta di suddivisione dei mari italiani in settori biogeografici. *Notiziario SIBM*, 46: 57-59.

Blanfuné, A., Thibaut, T., Boudouresque, C. F., Mačić, V., Markovic, L., Palomba, L., Verlaque, M., Boissery, P. (2017). The CARLIT method for the assessment of the ecological quality of European Mediterranean waters: Relevance, robustness and possible improvements. *Ecological Indicators*, 72, 249-259.

Cavallo, M., Torras, X., Mascaró, O., & Ballesteros, E. (2016). Effect of temporal and spatial variability on the classification of the Ecological Quality Status using the CARLIT Index. *Mar. Pollut. Bull.*, 102(1), 122-127.

Cossu, A., Gazale, V., & Baroli, M. (1992). La flora marina della Sardegna: inventario delle alghe bentoniche. *Plant Biosyst.*, 126(5), 651-707.

Cucco, A., Perilli, A., De Falco, G., Ghezzo, M., & Umgiesser, G. (2006). Water circulation and transport timescales in the Gulf of Oristano. *Chem. Ecol.*, 22 (sup1), S307-S331.

Grech, D. (2017). Historical Records and current status of Fucales (*Cystoseira* and *Sargassum* spp.) in the Gulf of Naples., The Open University, PhD thesis, 350 pp.

Guala, I., Torras, X., Simeone, S., Ballesteros, E. (2010). Valutazione della qualità ecologica delle acque costiere nell'Area Marina Protetta Penisola del Sinis -Isola di Mal di Ventre (Sardegna occidentale) secondo il metodo¨CARLIT¨. *In*: 32°Atti S.It.E. XVIII *Congresso Nazionale Società Italiana di Ecologia*, Parma 1–3 settembre 2008 (G. Giordani,V. Rossi & P. Viaroli). pp. 61–67.

Gueneau P., Mastinu C., Grisorio M.R., Dadea C. (1992) Riassunto delle escursioni a Tharros e sullo Stagno di Santa Giusta, IMC September 1992 (Report interno).

Istat (2017). Rapporto annuale 2017. La situazione del Paese. Roma: Istat.

Lasinio, G. J., Tullio, M. A., Ventura, D., Ardizzone, G., Abdelahad, N. (2017). Statistical analysis of the distribution of infralittoral Cystoseira populations on pristine coasts of four Tyrrhenian islands: Proposed adjustment to the CARLIT index. Ecol. Indic., 73, 293-301.

Lorah, Paul; Ready, Alice; and Rinn, Emma (2018) "Using Drones to Generate New Data for Conservation Insights," *Int. J. of Geosp. and Env. Res.*: Vol.5:No.2, Article 2. https://dc.uwm.edu/ijger/vol5/iss2/2.

Provincia di Oristano (2014) Autorizzazione allo scarico dell'impianto di depurazione del Consorzio Industriale Provinciale di Oristano ubicato in Localita' Cirras del Comune di Santa Giusta. *Determ. Dirig. N. 1199 del 09/06/2014.* Pp.6.

Thibaut, T., Blanfuné, A., Boudouresque, C. F., & Verlaque, M. (2015). Decline and local extinction of Fucales in French Riviera: the harbinger of future extinctions?. *Mediterr. Mar. Sci.*, 16(1), 206-224.

Torras, X., Pinedo, S., García, M., Weitzmann, B., & Ballesteros, E. (2015). Environmental quality of Catalan coastal waters based on macroalgae: The interannual variability of CARLIT index and its ability to detect changes in anthropogenic Pressures over time. *In:* Experiences from Ground, Coastal and Transitional Water Quality Monitoring (pp. 183-199). *Springer*, Cham.

UNEP/MAP-SPA/RAC, (2018). SAP/RAC: SPA-BD Protocol - Annex II: List of endangered or threatened species.

Ventura, D., Bonifazi, A., Gravina, M., Belluscio, A., & Ardizzone, G. (2018). Mapping and Classification of Ecologically Sensitive Marine Habitats Using Unmanned Aerial Vehicle (UAV) Imagery and Object-Based Image Analysis (OBIA). *Remote Sens.*, 10(9), 1331.

Tables and Figures

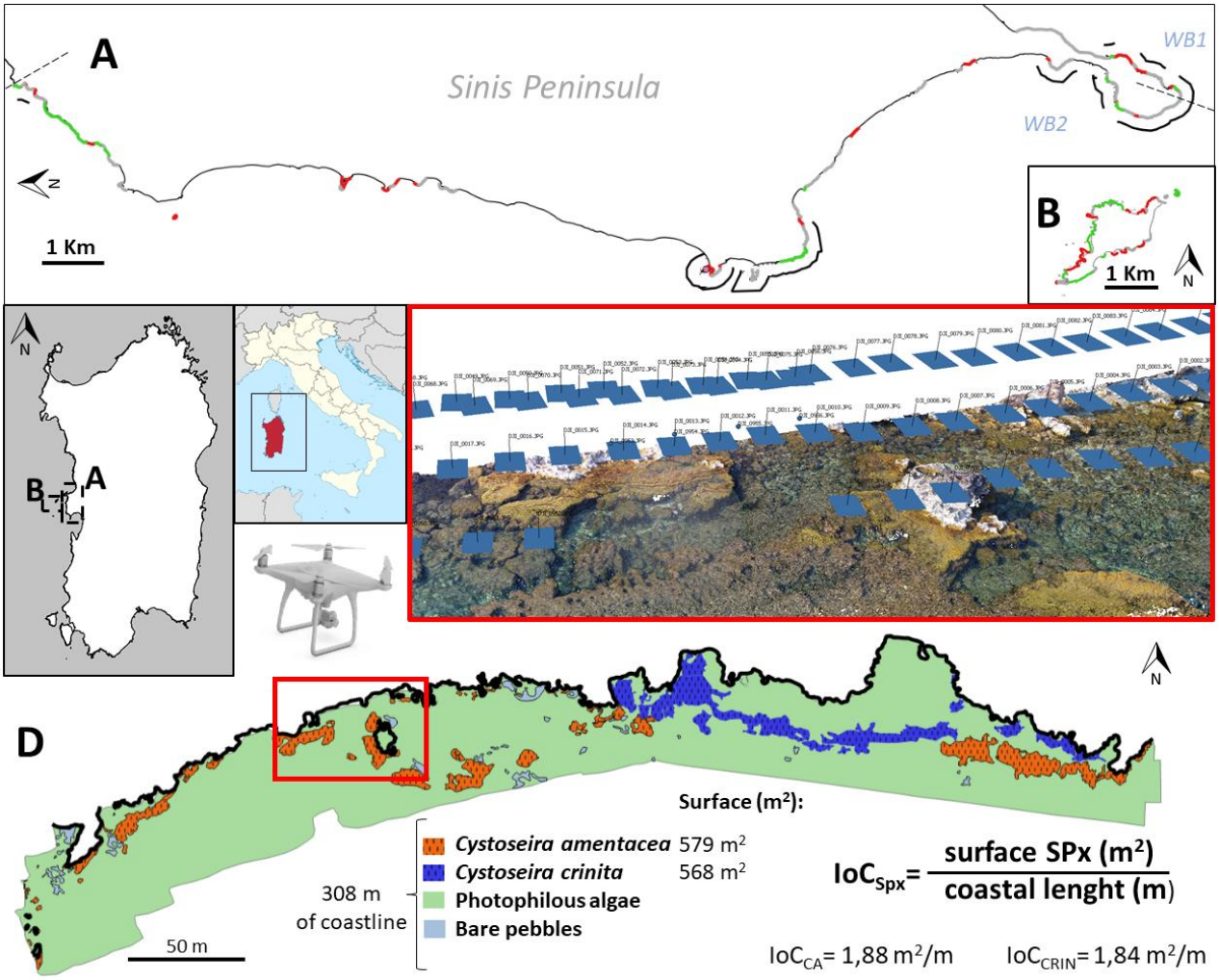

Fig. 1: SL variation after 10 year along the Sinis coastline (Red=decrease; Green=increase; Grey=stable). Black line below the coastline indicate the sectors where othomosaic photos where acquired (A, B). Example of a 3D model coastline with the superimposed orthophotos (C). Final result of drone survey with delimited macroalgal assemblages (D)

2.3

Grech, D., Fallati, L., Farina S., Cabana, D., Guala, I. (2019). Marine Forests (Fucales, Ochrophyta) in a low impacted Mediterranean coastal area: current knowledge and future perspectives. INPUT aCAdemy 2019 - Planning, nature and ecosystem services Cagliari 24-26 June 2019 (*Conference Paper*)

Marine forests (fucales, ochrophyta) in a low impacted Mediterranean coastal area: current knowledge and future perspectives

A phycological review in Sinis peninsula and the Gulf of Oristano (Sardinia Island, Italy)

DANIELE GRECH [*a], LUCA FALLATI [b], SIMONE FARINA [a], DAVID CABANA [a], IVAN GUALA [a]

[a] IMC - International Marine Centre, Oristano, Italy

[*] E-mail: d.grech@fondazioneimc.it - URL: https://www.fondazioneimc.it/

[b] Università degli Studi di Milano-Bicocca - Department of Earth and Environmental Sciences - DISAT, Italy,

E-mail: l.fallati@campus.unimib.it

ABSTRACT

Mediterranean seascapes are currently facing massive changes, with the disappearance of sensitive species responding to local anthropogenic disturbances and global climate changes. Mapping and monitoring of marine habitats are crucial tools for highlighting the occurrence of community shift that should be taken into account in coastal management and the implementation of conservation measures. Proper reference baselines are generally lacking, especially for marine forests of brown macroalgae (Fucales, Ochrophyta). They are considered among the most important marine ecosystem-engineers, forming extended stands comparable to land forests. They increase three-dimensional complexity and spatial heterogeneity of rocky bottoms, thus providing directly or indirectly substrate, refuge, shelter and food for a lot of animal and plant species at different life history stages. Despite their ecological importance, sensitiveness to anthropogenic disturbances and conservation interest, in the Sinis Peninsula (Western Sardinia, Italy), Fucales are historically understudied compared to other Mediterranean areas. A review of historical records and current research has been performed

in order to shed light on the gaps in our knowledge and to discuss future possibilities for their management and conservation.

KEYWORDS:
Sinis Peninsula (Sardinia, Italy); Cystoseira; Habitat Conservation; Coastal Ecosystems; Cutting-edge Technology

Introduction

In the last decades, Mediterranean seascapes have faced massive changes. Responding to local anthropogenic disturbances and global climate changes, many sensitive species are in decline throughout the basin with some reported cases of local extinction (Thibaut et al., 2015 and references therein). Mapping and monitoring of marine habitats are crucial tools for highlighting the occurring community shift and should be taken into account in coastal management and for the implementation of conservation measures. The lack of proper reference baselines in marine ecosystems is rather common and generally leads to the so called 'Shifting Baseline Syndrome' (Pauly 1995) which is hampering the proper assessment of the status of an ecosystem.

In vegetated sub-littoral systems, the best-known dramatic change is the shift from complex, three-dimensional forests of brown macroalgae (Fucales, Ochrophyta) to turf species. Fucales are considered among the most important marine ecosystem-engineers, forming extended stands comparable to land forests, increasing three-dimensional complexity and spatial heterogeneity of rocky bottoms, thus providing substrate for many other algae and refuge, shelter and food for a lot of species at different life history stages. Reference baselines of marine forests have been described along the most frequented and investigated study areas of the Mediterranean Sea, where the first marine biological stations were located (Sauvageau, 1912; Funk, 1927, 1955; Ercegovic, 1952). Conversely, suitable studies on marine macroalgae in remote areas (or those not easily accessible from the mainland), have been historically complex or absent. This is the case of the Sinis Peninsula, located along the western coast of Sardinia (Italy), an area historically far from both mainstream access and the scientific community. Thus, this area is rarely taken into account by phycological research. At the beginning of the 1900s, the entire Sardinian population was comparable to that of Naples (Italy) (among the biggest cities in Europe, with 600,000 inhabitants). Here the Prussian Zoologist Felix Anton Dohrn founded the visionary project of the 'Stazione Zoologica di Napoli' in 1872. This is a marine station which has hosted thousands of international researchers since its institution. In the following years, other marine stations (i.e. in Banyuls, Roscoff, Endoume, Split, and Rovinj) would be settled close to populated coastlines, where many researchers worked year after year in the continuous study of marine algal flora and fauna. The algal vegetation of the Western Mediterranean was initially studied by dredging near these marine biology research centers. These studies built important baselines for marine ecology, allowing

in recent times for the comparison of historical records with current ones and evidencing the abrupt changes (Thibaut et al., 2015 and references therein; Grech, 2017).

The Sinis Peninsula is currently one of the less densely populated coastal area of Sardinia. Because of the non-negligible pressure of fisheries (Vandeperre et al., 2008), it cannot be considered a pristine area. However, it could be assumed to be low impacted seascape, at least for benthic communities of the intertidal zone. Here, in 1988, the International Marine Centre (IMC) was founded in Torregrande (Oristano, Italy).

The aim of this study is to review all the past records concerning the marine forests and to summarize recent findings and achievements. Given the presence of the 'Penisola del Sinis - Isola di Mal di Ventre' Marine Protected Area (MPA), these findings should serve as baseline for future management and conservation perspectives of these communities.

Methodology

A review on Cystoseira and Sargassum has been conducted for the Sinis Peninsula and the Gulf of Oristano. A frequent problem while studying fucalean forests is the lack of data with enough taxonomic resolution. Therefore, also grey literature as well as peer-reviewed journals was considered for this study. Records have been collected and a geodatabase has been developed (including all the historical and current information) on the basis of past experience of FuCart DB (Fucales Cartography DataBase; Grech, 2017).

Results

The first historical records of marine forests in Sardinia are relatively few and sparse, consisting of algal lists (Barbey, 1884). Here, the record of *C. amentacea* in Capo Mannu is the oldest one for the study area. Other historical records for the Sinis Peninsula were published more than 100 years later and are spotted (Cossu et al., 1992; Gueneau et al., 1992; Sales, 2010) with some of them doubtful. Cossu et al., (1992) reported 18 fucalean species (15 *Cystoseira spp.* and 3 *Sargassum spp.*) in Sardinia. Cormaci et al., (2005) afterwards reported the rare C. squarrosa in Castelsardo (Northern Sardinia) that is the only place in the Western Mediterranean Sea (another one is in Sicily) where populations of this species are known to occur.

In the study area, *C. barbata* was reported by Addis et al., (2004) and Casu et al., (2006) in 'Penisola del Sinis - Isola di Mal di Ventre' MPA. Nonetheless, based on this study we contemplate the possibility that this may be a misidentification of a late summer habitus of *C. amentacea*, which is rather abundant in the area. This uncertainty about the records is also exacerbated by the lack of abundant Herbaria vouchers and samples collection of the area, and by a lack of clear and unequivocal reported sites of presence (GPS coordinates, pictures in references) that could be examined and resurveyed by specialists after decades, i.e. as was properly done by Cormaci et al., (2005). Moreover, if *C. barbata* is present in the study area it is considered rare, since we have only collected stranded specimens until now in two sites in the Gulf of Oristano (Mare Morto and Mistras). The most likely source of this species is close to the mouth of the wetland system in the gulf. However, we cannot exclude surface drifting of detached thallus from sites outside the study area. *C. foeniculacea* and *C. compressa* have also been reported in the lagoons of Santa Giusta (Magni et al., 2008) and Curru de S'Ittiri (Provincia di Oristano, 2013), respectively. Their occurrence should be confirmed and checked along the complex wetland systems.

The only proper reference baseline of this study area (concerning upper sublittoral species) is the cartography of littoral and upper-sublittoral rocky-shore communities, performed by applying the CARLIT method in 2008 (Guala et al., 2010). Although it is not entirely appropriate to consider this work as a historical baseline, it represents the starting point for our studies, at least for the upper subtidal species. In addition, some punctual records on the lower subtidal species have been reported by ENEA (1990), in the framework of the feasibility study

of “Penisola del Sinis - Isola Mal di Ventre” MPA. Nevertheless, it is worth stressing that after Guala et al., (2010), no other studies were performed in the area.

Recently, within the GIREPAM project (Integrated Management of Ecological Networks through Parks and Marine Areas, Programme Interreg Maritime Italy-France 2014-20, http://interreg-maritime.eu/web/girepam), surveys on habitats 1120 (Posidonia beds) and 1170 (Reefs) have been carried out in the MPA to assess possible disturbances from anthropic activities and to define management guidelines. These activities lead to the re-implementation of the CARLIT method during the year 2018 (Grech et al., 2019) and confirmed the high stability of the index after 10 years, testifying even today by a high ecological quality of the upper sublittoral habitats of the Sinis Peninsula, with continuous lush forests of the most sensitive species *C. amentacea* and *C. crinita*. As an integration of the CARLIT index, Unmanned Aerial Vehicles (UAVs) were tested in 2018 (Grech et al., 2019) to map the shallow communities and to compute Cystoseira species coverage along the study area. All the information reviewed and recent achievements are represented in Figure 1.

Moreover, detailed surveys have recently been conducted and the distribution of rare species such as *C. algeriensis* has been mapped extensively along the coastline. Additionally, recently new records have been reported (Grech, 2019). On the basis of this review, along the Sinis Peninsula, 8 taxa of Cystoseira have been reported in the upper sublittoral fringe, namely: *C. algeriensis, C. amentacea, C. barbata (stranded), C. brachycarpa, C. compressa var. compressa, C. compressa var. pustulata, C. crinita, C. sp.*. Below the water mark 7 taxa are reported: *C. algeriensis, C. brachycarpa, C. crinita, C. foeniculacea, C. montagnei, C. usneoides, C. zosteroides*. Overall, 12 taxa occur, 4 of them are Mediterranean endemism.

Further study on marine forests is currently underway within the project ‘Amelioration by Benthic habitat-formers under Climate Change’ (ABC2; Bulleri et al., 2018) in order to understand the extent to which marine belts and forests can reduce environmental stress, regulate and maintain associated benthic assemblages, through the establishment of a network of experimental setups along Mediterranean and Atlantic coasts of Europe (Bulleri et al., 2018). Data logging is currently in progress (Figure 2).

Discussion and Conclusions

Although most marine forests are under protection within the framework of international agreements (Berne Convention, 1979, Habitats Directive, 1992; Barcelona Convention, 1995) fucalean species are currently not effectively protected on a Mediterranean scale, not even within marine reserve zones. Moreover, there is a lack of knowledge about their distribution, due to the paucity of continuous and widespread data.

This contribution sheds light on the marine forests of the Sinis Peninsula and the Gulf of Oristano. Here, the upper subtidal species do not seem to be threatened by local stressors, although some of them (e.g. human trampling) may be increasing in recent years and should be quantified in future. The deep species, on the other hand, are quite vulnerable to fisheries: the branched species can be detached by fishing gears (i.e. trammel nets) that could be one of the main factors of decline (Thibaut et al., 2015; Grech, 2017). The study area, although scarcely studied from an algological point of view, is characterized by a high biodiversity of marine forest (Grech et al., 2019) and deserves further study. Deep species distribution data is lacking in the study areas as in most of the deep Mediterranean habitats (Ballesteros et al., 2009 and references therein; Capdevila et al., 2016 and references therein). Moreover, there is paucity of information on how climate change could potentially affect marine forests and how they can cope with these stressors. Recent studies suggested that climate change could influence some critical steps of their life cycle and a create susceptibility of marine forests to climate change, forecasting that up to 94% of originally suitable areas could be lost (Buonomo et al., 2017). Marine forests display clear signs of regression that are still not clearly understood across their distribution range (Thibaut et al., 2015 and references therein). The risk of losing these forests before gaining awareness about them and their extension is high. There is an urgent need for a detailed mapping all along the Mediterranean Sea. The putatively low local human impact in the study area makes the Sinis Peninsula the ideal candidate to represent a natural laboratory for testing the response of marine forests facing climate change. Therefore, the current research addressed at improving knowledge of distribution, extent, status of these forests and the environmental variables (e.g. temperature, light, water motion) affected by climate change, is crucial. The area, with its high abundance of very sensitive species, can be useful for the scientific community as a source of reproductive stages for in situ and ex situ pilot restoration projects of degraded habitats, which are recently becoming more common along the Mediterranean Sea (Falace et al., 2018). In-depth knowledge of natural systems and

increased awareness of the ecosystem services they provide are crucial for an effective integrated management of coastal and marine areas aimed at reducing biodiversity loss and ecosystem degradation. As for marine forests, an effective tool can be represented by dissemination and outreach activities through participatory methodologies, e.g. Citizen Science projects (Grech, Buia, 2017) aimed at marine forest reporting (https://www.facebook.com/ProgettoFucales/; http://www.progetto-fucales.it/) and/or to their decline. Reconstructing historical baselines engaging citizens through Local Ecological Knowledge (LEK) and Citizen Science is feasible in highly populated zones (i.e. Grech, Buia, 2017) with many stakeholders (e.g. the sharing of old and current photos from underwater photographers), strongly engaged with marine research institute activities. In the context of Sardinia, this approach is still in its infancy and seems complex at the moment, especially because the area is scarcely populated, with relatively low touristic influx and fishermen are generally not prone to collaboration and cooperation.

References

Addis, P., Ceccherelli, G., Murenu, M., Farci, S., Ferrari, A., Olita, A., Ortu, A., Poma, S., Canu, B., Casu, D., Greco, S., Sechi, N. (2004). Caratterizzazione delle biocenosi associate a *Cystoseira* in tre Aree Marine Protette della Sardegna. *Biologia Marina Mediterranea* 11.2, 397-399.

Barbey, W. (1884). *Florae Sardoae Compendium*. - Lausanne.

Ballesteros, E., Garrabou, J., Hereu, B., Zabala, M., Cebrian, E., Sala, E. (2009). Deep-water stands of *Cystoseira zosteroides* C. Agardh (Fucales, Ochrophyta) in the Northwestern Mediterranean: Insights into assemblage structure and population dynamics. *Estuarine Coastal and Shelf Science*, 82, 477-484. doi: http://doi.org/10.1016/j.ecss.2009.02.013

Brambilla, W., Conforti, A., Simeone, S., Carrara, P., Lanucara, S., De Falco, G. (2019). Data set of submerged sand deposits organised in an interoperable spatial data infrastructure (Western Sardinia, Mediterranean Sea). *Earth System Science Data*, 11(2), 515-527. doi: http://doi.org/10.5194/essd-11-515-2019

Bulleri, F., Eriksson, B. K., Queirós, A., Airoldi, L., Arenas, F., Arvanitidis, C., Bouma, T. J., Crowe, T. P., Davoult, D., Guizien, K., Ivesa, L., Jenkins, S. R., Michalet, R., Olabarria, C., Procaccini, G., Serrão, E. A., Wahl, M., Benedetti-Cecchi L. (2018). Harnessing positive species interactions as a tool against climate-driven loss of coastal biodiversity. *PLoS biology*, 16(9). doi: http://doi.org/10.1371/journal.pbio.2006852.g002

Buonomo, R., Assis, J., Fernandes, F., Engelen, A. H., Airoldi, L., Serrão, E. A. (2017). Habitat continuity and stepping-stone oceanographic distances explain population genetic connectivity of the brown alga *Cystoseira amentacea*. *Molecular ecology*, 26(3), 766-780. doi: http://doi.org/10.1111/mec.13960

Capdevila, P., Hereu, B., Riera, J. L., Linares, C. (2016). Unravelling the natural dynamics and resilience patterns of underwater Mediterranean forests: insights from the demography of the brown alga *Cystoseira* zosteroides. *Journal of Ecology*. doi: http://doi.org/10.1111/1365-2745.12625

Casu, D., Ceccherelli, G., Sechi, N. (2006). Different structure of assemblages understoried by three *Cystoseira* species occurring on the same upper-infralittoral platforms. *XVI Conferenza della Società Italiana di Ecologia*, Viterbo/Civitavecchia.

Cormaci, M., Furnari, G., Giaccone, G., Serio, D. (2005). Su due rare specie della macroflora algale mediterranea presenti in Sardegna: *Laurencia pyramidalis* (Rhodophyta, Rhodomelaceae) e *Cystoseira squarrosa* (Ochrophyta, *Cystoseiraceae*). Biol. Mar. Medit., 12 (1), 265-268.

Cossu, A., Gazale, V., Baroli, M. (1992). La flora marina della Sardegna: inventario delle alghe bentoniche. *Plant Biosystem*, 126(5), 651-707. doi: http://doi.org/10.1080/11263509209440371

ENEA (1990). I*ndagine sulla situazione ambientale delle aree destinate a riserve marine di Porto Cesareo, Capo Rizzuto e Penisola del Sinis – Isola di Mal di Ventre*. Convenzione del 23.2.1986 con il Ministero della Marina Mercantile. La spezia. pp. 638 + Allegati + Tavole.

Ercegovic, A. (1952). *Jadranske cistozire: njihova morfologija, ekologija i razvitak*. Institut za oceanografiju i ribarstvo.

Falace, a., Kaleb, s., De la Fuente, g., Asnaghi, v., Chiantore, m. (2018). Ex situ cultivation protocol for *Cystoseira amentacea* var. *stricta* (Fucales, Phaeophyceae) from a restoration perspective. *PloS One*, 13(2), doi: http://doi.org/10.1371/journal.pone.0193011

Funk, G. (1927). *Die Algenvegetation des Golfs von Neapel*. Pubblicazioni della Stazione Zoologica di Napoli, 7, 1-507 + 20 Tavv.

Funk, G. (1955). *Meeresalgen von Neapel*. Pubblicazioni della Stazione Zoologica di Napoli, 25, 1-178 + 30 Tavv.

Grech, D. (2019) *Cystoseira usneoides:* a new protected species for the Penisola del Sinis – Isola di Mal di Ventre MPA and Sardinia. *50° Congresso della Società Italiana di Biologia Marina.* Livorno, Italy 10-14 June 2019.

Grech D., Fallati L., Farina S., Guala, I. (2019). The Matrix Reloaded: CARLIT assessment ten years later in the Sinis Coast (Sardinia, Italy) coupled with drone technology. *SPA-RAC 6th Symp. on Mar. Veg. Marine Key Habitats and NIS Symp.*. Antalya Turkey 14-18 January 2019.

Grech, D. (2017). *Historical records and current status of Fucales (*Cystoseira *and* Sargassum *spp.) in the Gulf of Naples*. PhD Thesis - Open University, London - SZN, Naples: 350 pp.

Grech, D., Buia M.C. (2017). Progetto Fucales: un progetto pilota di scienza partecipata per la valutazione di macroalghe in regressione - *Biologia Marina Mediterranea*, 24 (1), 146-147.

Guala, I., Torras, X., Simeone, S., Ballesteros, E. (2010). Valutazione della qualità ecologica delle acque costiere nell'AMP Penisola del Sinis -Isola di Mal di Ventre (Sardegna occidentale) secondo il metodo¨CARLIT¨. In: *32°Atti S.It.E. XVIII Congr. Naz. SItE*, 2008.

Gueneau P., Mastinu C., Grisorio M.R., Dadea, C. (1992). *Riassunto delle escursioni a Tharros e sullo Stagno di Santa Giusta, IMC September 1992* (Report interno).

Magni, P., Rajagopal, S., Van der Velde, G., Fenzi, G., Kassenberg, J., Vizzini, S., Mazzola, A. Giordani, G. (2008). Sediment features, macrozoobenthic assemblages and trophic relationships (δ13C and δ15N analysis) following a dystrophic event with anoxia and sulphide development in the Santa Giusta lagoon (western Sardinia, Italy). *Marine Pollution Bulletin*, 57(1-5), 125-136. doi: http://doi.org/10.1016/j.marpolbul.2007.10.015

Pauly D. (1995). Anecdotes and the shifting baseline syndrome of fisheries. *Trends Ecol. Evol*. 10, 430. doi: http://doi.org/10.1016/S0169-5347(00)89171-5

Provincia di Oristano (2013). *Piano Faunistico Venatorio Provinciale. Prima e seconda Parte: Finalità e Quadro Conoscitivo. Settore Attività produttive Sviluppo Sostenibile*. Servizio Gestione Fauna selvatica.

Sales, M. (2010). Cystoseira-*dominated assemblages from sheltered areas in the Mediterranean Sea: diversity, distribution and effects of pollution*. PhD Universitat de Girona, Spain.

Sauvageau, C., (1912). *A propos des* Cystoseira *de Banyuls et de Guéthary*. Bull. de la Station Biologique d'Arcachon 14, 133–556.

Thibaut, T., Blanfuné, A., Boudouresque, C. F., Verlaque, M. (2015). Decline and local extinction of Fucales in French Riviera: the harbinger of future extinctions?. *Mediterranean marine science*, 16(1), 206-224. doi: http://doi.org/10.12681/mms.1032

Vandeperre F., Higgins R., Santos R.S., Marcos C., Pérez-Ruzafa A. Coord., (2008). *Fishery Regimes in Atlanto-Mediterranean European Marine Protected Areas*. EMPAFISH Project, Booklet nº 2. Editum. 108 pp.

WEB SITES

http://interreg-maritime.eu/web/girepam/-/fondazione-imc-e-girepam-al-festival-della-scienza-di-oristano
https://www.facebook.com/ProgettoFucales/
http://www.progetto-fucales.it/

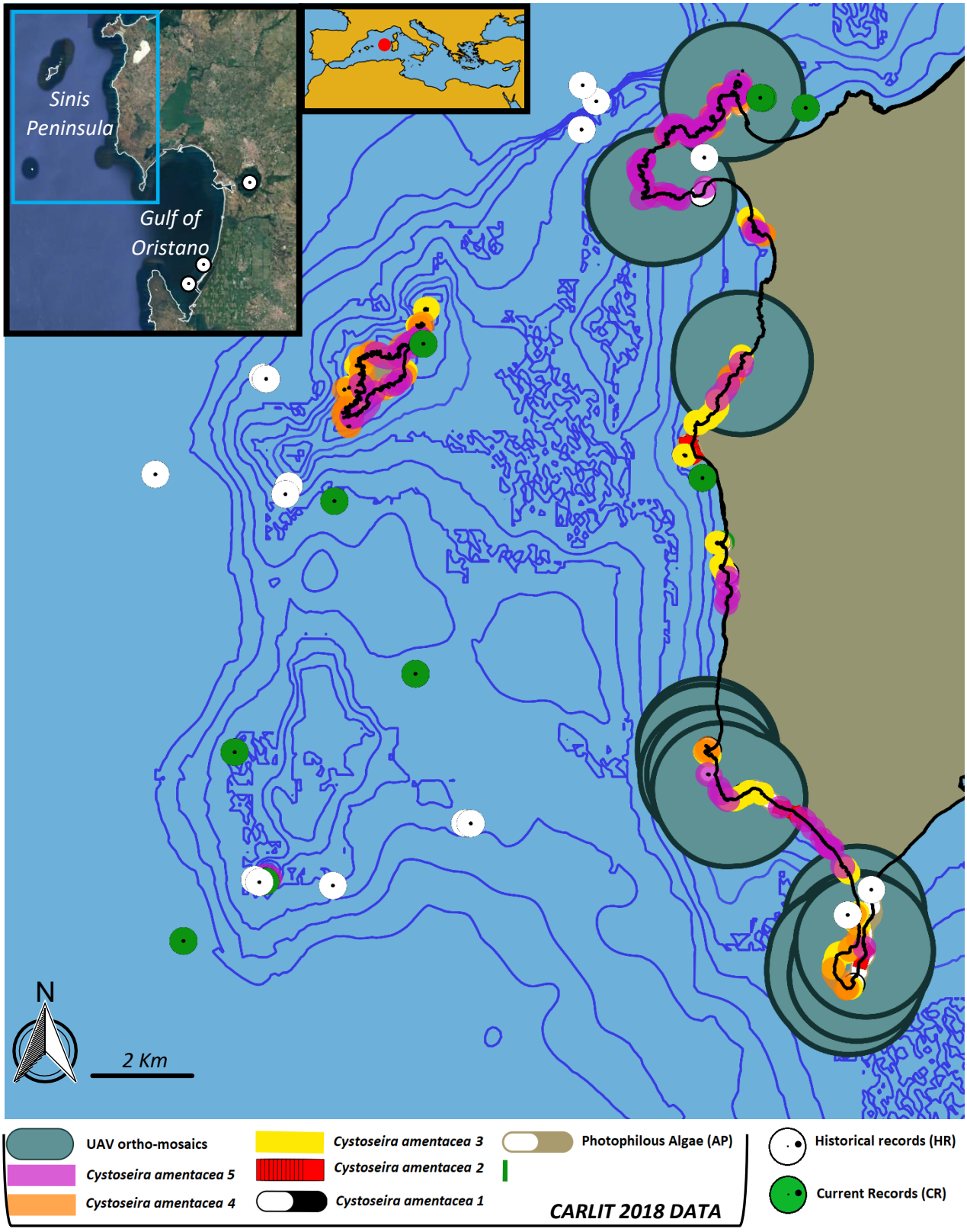

Fig. 1 Marine Forests of the study area. Bathymetry up to a depth of 45 m is represented on the map, with a step of 5 meters (Brambilla et al., 2019). Methodological CARLIT communities (e.g. *C. amentacea* 5 to 1) are based on Guala et al., (2010).

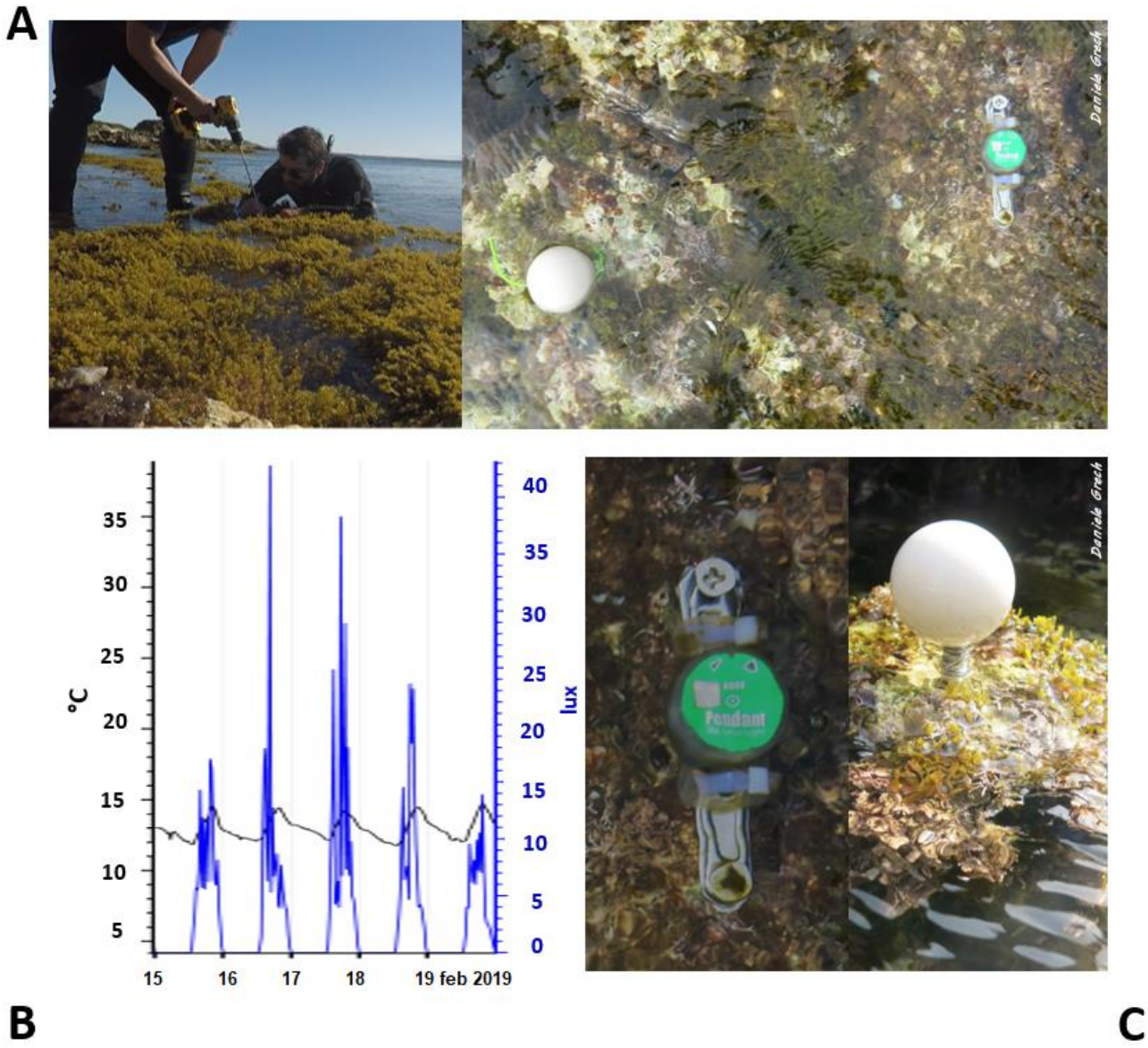

Fig. 2. Amelioration by Benthic habitat-formers under Climate Change (ABC2) set-up (A), Temperature/Light logging data (B) detail of Hobo data logger and plaster clods for water motion assessment (C).

2.4

Fallati, L., Polidori, A., Salvatore, C., Saponari, L., Savini, A., & Galli, P. (2019). Anthropogenic Marine Debris assessment with Unmanned Aerial Vehicle imagery and deep learning: A case study along the beaches of the Republic of Maldives. Science of The Total Environment, 133581. https://doi.org/10.1016/j.scitotenv.2019.133581

Anthropogenic Marine Debris assessment with Unmanned Aerial Vehicle imagery and deep learning: A case study along the beaches of the Republic of Maldives

Luca FALLATI [a,b], Annalisa POLIDORI [c], Christian SALVATORE [c], Luca SAPONARI [a,b], Alessandra SAVINI [a,b,*], Paolo GALLI [a,b]

[a] Department ofEarth and Environmental Sciences, University ofMilan-Bicocca, Milan, Italy

[b] MaRHE Center (Marine Research and High Education Center), Magoodhoo Island Faafu Atoll, Maldives

[c] DeepTrace Technologies S.R.L., Milan, Italy

Abstract

Anthropogenic Marine Debris (AMD) is one of the major environmental issues of our planet to date, and plastic accounts for 80% of total AMD. Beaches represent one of the main marine compartment where AMD accumulates, but few and scattered regional assessments are available from literature reporting quantitative estimation of AMD distributed on the shorelines. However, accessing information on the AMD accumulation rate on beaches, and the associated spatiotemporal oscillations, would be crucial to refining global estimation on the dispersal mechanisms. In our work, we address this issue by proposing an ad-hoc methodology for monitoring and automatically quantifying AMD, based on the combined use of a commercial Unmanned Aerial Vehicle (UAV) (equipped with an RGB high-resolution camera) and a deep-learning based software (i.e.: Plastic Finder). Remote areas were monitored by UAV and were inspected by operators on the ground to check and to categorise all AMD dispersed on the beach. The high-resolution images obtained from UAV allowed to visually detect a percentage of the objects on the shores higher than 87.8%, thus providing suitable images to populate training and testing datasets, as well as gold standards to evaluate the software performance. Plastic Finder reached a Sensitivity of 67%,with a Positive Predictive

Value of 94%, in the automatic detection of AMD, but a limitation was found, due to reduced sunlight.

Introduction

Environmental contamination generated by Anthropogenic Marine-Debris (AMD) represents one of the most ubiquitous and long-lasting environmental change of our planet (Laist, 1987; Ryan, 2015). AMD is responsible of several ecological, ecotoxicological, economic and social impacts. However, the extent to which it is harming wildlife and plants, endangering human health and reducing the availability of ecosystem good and services (Laist, 1987; Rochman et al., 2013; Hengstmann et al., 2017) is still to be properly understood and quantified (Eriksen et al., 2014; Thompson et al., 2009). It has been estimated that from 5 to 13 million tonnes of litter enter the oceans each year (Jambeck et al., 2015; Geyer et al., 2017) and that plastic accounts for over 80% of the total AMD (UNEP 2005; Laist, 2011; Thiel et al., 2013; Penca, 2018).

Plastic is persistent and for the most part (roughly 60%) less dense than seawater (Andrady, 2011; Ryan et al., 2009). Once introduced into the marine environment from multiple sources (both sea- and land-based), buoyant plastic can be transported by surface currents and winds (Kako et al., 2010), recaptured by shorelines (Kako et al., 2014) or degraded into microplastic (Barnes et al., 2009; Cinner et al., 2018). Distribution and accumulation of plastic into the marine environment are indeed controlled by circulation patterns and prevailing winds, coastal and seafloor geomorphology (Barnes et al., 2009; Galgani et al., 2000; Savini et al., 2014) and anthropogenic activities (Ramirez-Llodra et al., 2013). Well known hotspots of accumulation include the sea surface, where aggregations of a large amount of persistent and light plastic take place at ocean gyres, creating giant “garbage-patches” (Eriksen et al., 2014; Law et al., 2010, 2014), but also submarine canyons, where litter originating from land accumulates in large quantities (Pierdomenico et al., 2019) and the shores, particularly beaches (Corcoran et al., 2009). Although data documenting the occurrence of plastic everywhere in the oceans (from the surface to the deep seafloor - Thompson et al., 2004 and Van Cauwenberghe at al., 2013) are quite exhaustive, a consistent quantification of the total amount accumulated within the diverse marine compartments, has not been accurately outlined. While reliable estimations have been provided for the giant surface garbage-patches (Lebreton et al., 2018; Eriksen et al., 2014), scarce information is available from the deep and poorly unexplored seafloor, but nonetheless for the shorelines, where only a few and scattered regional assessments were provided (Martin et al., 2018; Vlachogianni et al., 2018; Andrades et al., 2016; Ebbesmeyer et al., 2012). Plastic accumulation on beaches may represent the terminal phase of oceanic

transport or a transient stage with a successive washed to the sea following storms or tides movements (e.g. Shimizu et al., 2008). Knowing the accumulation rate on beaches and associated spatiotemporal oscillations would be a crucial information to refine global estimation on the dispersal mechanisms of plastic in the marine environment and its amount in each compartment. Most of our knowledge on the quantity of plastic accumulated on beaches, at different temporal scales, is based on sparse and regional monitoring activities, performed following different protocols and without standardized procedures, making difficult data integration and comparisons among regions (e.g. Galgani et al., 2015; Watts et al., 2017). Beach litter estimation, at places performed within the framework of dedicated monitoring activities (among others the Marine Strategy Framework Directive - Directive 2008/56/EC – Galgani et al., 2014), is also commonly subjective and time-labor consuming, since it relies on visual census where items are recorded along transects (Lavers et al., 2016; Lavers and Bond, 2017). Only recently the use of aerial imagery has been proved to be an appropriate and efficient method to monitor beach litter (Kako et al., 2012; Kataoka et al., 2018; Sha et al., 2018; Deidun et al., 2018). In particular, the use of Unmanned Aerial Vehicles (UAVs) equipped with RGB cameras, beside the advantage of the low-cost, allows the collection of high resolution imagery data (i.e.: at centimetre level - Casella et al., 2016; Flynn and Chapra, 2014) over quite large areas (e.g. hundreds of hectares), also not easily accessible, with great flexibility in terms of time and frequency of data collection (i.e. decades of hectares per day), and under conditions where satellites would be of limited use (i.e.: high cloud cover, limited image resolution). Nevertheless, estimation of beach litter from RGB imagery of various sources (UAVs included), over large and even remote areas, still requires standardization of sampling techniques and data processing. Also, objective identification of plastic items on aerial imagery, based on automatic image classification is a novel field of investigation. To the best of our knowledge, only one work has been recently published on the use of UAV Remote Sensing combined to Artificial Intelligence (AI) for beach-litter monitoring by Martin et al. (2018). They proved the ability of machine learning (ML) in performing less time-labour consuming (40 times faster than humans) and subjective methodologies to detect AMD, but the best sensitivity reported in Martin et al. (2018) for AMD automatic quantification was low (i.e.: 44%).

In our study, we therefore focused on the improvement of the sensitivity of the AI algorithm and the associated positive predicted values, which account for the false positive AMD. For this purpose, we provided a deep learning, rather than a random-forest, machine-learning approach, as previously implemented by Martin et al. (2018), being deep learning more

beneficial for object detection (LeCun at al., 2015; Chollet 2017; Guest at al., 2018). An essential output of our work is, in addition, the formulation of a combination of protocols to automatically detect and quantify beach litter along the shores of selected remote islands in the Republic of Maldives, defined by the 2010 UNPD's Assessment of Development Results a vulnerable "Small Island Developing State (SIDS)". The protection of the environment from pollution is indeed extremely important for SIDS as, aside from other reasons that are common to all countries, two important industries (tourism and fisheries) depend on a pristine environment (UNEP, 1999).

Our study proposes an ad-hoc combination of protocols to: 1) collect UAV-images suitable for the training of a deep-learning algorithm, 2) provide smart gold standards to estimate the algorithm performances, 3) train and test the deep-learning algorithm in near real-time conditions. We believe that our work could be useful to propose new best-practices for applying deep learning to automate the procedure of litter detection and quantification by UAV systems on beaches, which in turn could offer an instrumental tool for sustainable solid waste management.

Materials and Methods

Study Area

The case-study area consists of different islands of the Republic of Maldives (Fig. 1a), an archipelago composed of 1192 atoll islands stretched for 860 km, in North-South direction, located in the middle of the Indian Ocean. The islands are grouped in 20 administrative atolls and divided under three distinct categories: inhabited, uninhabited and resort islands (Fallati et al., 2017). The archipelago, with its peculiar geographical location and its 644 km of coastline, represents the perfect place for the deposition of plastic debris that are drifted from the surface currents of the Indian Ocean (Barnes, 2004). In addition, local sources of littering are represented by the waste production on the inhabited islands and those discharged into the sea from the numerous boats that daily cross the atolls. In the Maldives, the high dispersion of land mass and population, both of them spread over a distance of 860 km, creates a negative effect on solid waste management issue. With the exception of resort islands, which represent the 6% of the total archipelago surface and where beach clean-up is a daily routine operated by resort employees, most part of the coastline of each Maldivian island, is indeed covered, to an undefined extent, by AMD coming from different sources (Fig. 2)

As testing regions for our study, we selected three different coastal areas. Two of these islands (Adangau and Jinnathuga) are in Faafu Atoll, one (En'Boodhoo) is in Alif Dhaalu Atoll (Fig. 1b, c). The three islands were chosen as representatives of small-size uninhabited islands of the archipelago, where beach-cleaning cannot be guaranteed by resort employees or government personnel. En'Boodhoo is an island of 1.8 ha, located in the western lagoon of Alif Dhaalu Atoll. The island is desert, and the human presence is mainly related to the safari boats that stop nearby, and to touristic picnic and barbeques on the beach. Adangau (1.1 ha) and Jinnathuga (1.9 ha) are two islands of Faafu Atoll located in the Atoll's eastern lagoon. These two are similarly used as picnic island from the inhabitants of the Atoll. The primary sources of litter on these islands are both the direct release of waste and oceanic transport. The target testing area within the islands was selected as a portion of the beach with direct access to the sea, different exposition to the winds and currents, with the presence of psammophytes plants and natural debris (leaves, roots and twigs) as well as litter.

Aerial Surveys

UAV

In order to achieve large-scale reproducibility of a protocol to collect UAV images, we propose to use a consumer-grade UAV, equipped with a high-resolution RGB camera, to survey the study area. For this purpose, we used the DJI Phantom 4 drone, a quadcopter with high sensing qualities, equipped with a 1/2.3" CMOS camera sensor (12.4 MP) that can collect images with a resolution (R) of 4000x3000 pixels and an integrated GPS/GLONASS system. Compared to fixed-wing UAVs, that can cover with a single flight a larger area and can handle a higher quality camera, Phantom 4 is lightweight, easy to carry, and can smoothly fly at low altitude to obtain good ground-resolution images. Moreover, easy take off and landing procedures make this drone an outstanding, cost-effective solution for low altitude and short-range studies. All the metadata are recorded in an EXIF (Exchangeable Image File Format) file, which includes information on the pictures such as shutter speed, apertures, ISO and GPS coordinates (latitude, longitude and altitude). Flight time with a single battery is roughly 25 min.

UAV Survey Protocols

Three different altitudes, namely 10, 15 and 35m were considered to define the optimal protocol in terms of image quality and number of images required to cover the area of interest (AOI):

1) ground sample distance (GSD) being defined as:

$$GSD\ mm/pix = \frac{SW \times FH}{FL \times IW}$$

where SW is the sensor width, FH is the flight high, FL is the focal length of the camera, and IW is the image width (Ventura et al., 2018), and

2) number of images of interest (IOI) being defined as:

$$IOI = \frac{AOI\ [m^2]}{D\ [m^2]} = \frac{AOI\ [m^2]}{R\ [pixels^2]\ \ GSD^2[m^2/pixels^2]}$$

where D is the dimension of the area covered by a single image at a specific GSD, and R is the resolution in terms of pixel of the images, as defined in paragraph 2.2.1.

The surveys were planned using DJI GS PRO (www.dji.com/it/ground-station-pro) a free Ipad application released by DJI. This app allows designing all the aspects of the drone mission: generate optimal flight paths, set camera parameters and directly monitor data acquisition on the Ipad screen. For all the surveys we set a fix flight altitude with a frontal and lateral overlap of 80 % and 70 %, respectively, a -90° gimbal angle (nadir orientation), a shooting interval of 2 seconds (equal time interval mode) and a constant velocity of 1.3 m/s. Before starting the UAV overflight weather condition (wind speed, cloud coverage) and the presence of obstacles along the path was checked. A metric tape was laid on the beach (e.g. for several meters), in order to check the spatial accuracy of the orthomosaic during the postprocessing. Once all the parameters were set, the UAV automatically took off and completed the mission (e.g. trajectory in Fig. 3 a, b).

Reconstruction of the AOI

The images were processed by Agisoft PhotoScan (www.agisoft.com), a commercial Structure from Motion (SfM) software, widely used by the scientific community for its user-friendly interface, spontaneous workflow and the excellent quality of the point cloud output (Burns at al., 2017; Cook, 2017; Bonali et al., 2019). The process is dived in three main steps (Fig. 3 c): drone photos alignment using high accuracy setting; high-quality dense 3D point cloud generation; creation of a Digital Terrain Model (DTM) from the dense could. As final outputs we obtained, from the DTM, orthomosaics with a GSD of 4.4 mm/px, 8.2 mm/pix and 14 mm/pix respectively for the three flights altitude (10, 15 and 35 m). The models are geo-referenced thanks to the coordinates stored into the EXIF files of each image. For more extensive information on the process, see Verhoeven (2011) and Ventura et al., (2016). The orthomosaics generated from images collected at 10 m altitude, were considered as our AOI and used for data assessment.

Gold Standards

In-Situ Ground Assesment

We performed an in-situ ground assessment (GA) of the AOI, aimed at quantifying the AMD on the studied shorelines in order to calculate the efficiency of the UAV survey-protocols. This quantity represents our first Gold Standard (GA-GS). As a first step, a recognition of the investigated shorelines was conducted to detect AMD. The items found during the inspection

were counted and classified by the operators into different subtypes (Table 1). The category named “other” refers to objects and fragments that were smaller than 5 cm, which is the minimum size of the target objects that we decided when defining the optimal protocol described in terms of the image quality. Then, these objects were re-arranged in the specific AOI to be monitored by UAV overflights.

Image Screening

In order to evaluate the quality of the images, a comparison was made between the number and type of items counted by the operators during the in-situ GA on the beach, and the number and type of items counted by an operator during an image screening (IS) of the orthomosaic on a PC. The AMD recognised via IS represents our second GS (IS-GS), and a smart best-estimate of the actual GA-GS. Indeed, proving the feasibility of identifying and estimating the AMD by screening images collected by UAVs, rather than by operators on the ground, is crucial to choose the optimal UAV survey-protocol for the collection of images suitable for deep learning, and to establish procedures that allow avoiding the time-consuming GA of the operators.

The Deep-Learning Algorithm

In order to allow easy access to AI non-expert users, we used a commercial software – PlasticFinder (Italian software license 012677 D011755, DeepTrace Technologies, www.deeptracetech.com/) – to detect and quantify AMD. The core algorithm of the software is a deep-learning convolutional neural network (CNN). CNNs are a class of multilayer architecture suitable for processing RGB images for classification and object detection tasks, where the stack of convolutional layers allows for translation invariance - i.e. the net is trained to recognize an object independently of its position within the image.

The adoption of a deep learning approach has one main motivation. In order to provide a tool that could favour a scalable approach, i.e. adaptable to different scenarios, a large image-database was needed to provide a general training set, i.e. a set of images to let the algorithm learn the classes of interest. The main advantage of deep learning is that it automates the most critical part of a ML workflow: the feature extraction. In contrast to conventional ML methods (e.g. Random Forest, Support Vector Machine, Gradient Boosting Machines), that require hand-design features as input, a neural network is made of trainable multilayers that learn automatically the features through geometric transformations and gradual adjustments of

learning weights with respect to a feedback signal, thus being more suitable than conventional ML for large dataset training (LeCun 2015, Chollet 2017). The PlasticFinder CNN has been tailored for 5 classes of images, namely: “vegetation”, “sea”, “sand”, “AMD” and “other” (i.e. sand with small pieces of wood, stones, algae). UAV images obtained from the survey of Jinnathuga island were used for the collection of the training set (Fig. 4)

The island was chosen on the basis of the fact that all the classes of interest were present. Therefore, we selected training images, within the AOI, representing the classes of interest. For each class, a balanced number - of the order of thousands – of different samples was collected, in order to tailor the algorithm on the specific experimental settings. A subsample of UAV images (N=3) collected on the other two islands, Adangau and En’Boodhoo, were used for the testing set. The surveys of the testing-set islands were finalised at different experimental conditions (Table 1) which allowed to investigate the influence of climate, light and shadow on the efficacy of the algorithm. When a tested image is input in the software, it returns pixel-wise classification heatmaps, representing a pixel probability-map for each class, and a bounding-boxes map with the detected AMD.

The performance of the automatic detection, classification and quantification were measured by comparing the results with the two GS. The metric is expressed in terms of true positive (TP), false negative (FN) and the false positive (FP) items, rather than in terms of pixels, for an easier interpretation. The statistical measure of the performances is expressed through the *Sensitivity = TP / (TP+FN)*, the Positive Predictive Value *PPV = TP/(TP+FP)*, and the harmonized mean of Sensitivity and PPV, given by the *F-score = 2TP/(2TP+FP+FN)*.

Results

Optimization of UAV Survey Protocols

The optimal protocol for the UAV survey, as a compromise between image resolution and number of IOI to cover the AOI, was found at a UAV altitude of 10 m, corresponding to a GSD of 4.4 mm/pixels. The know dimension of the objects (metric tape) in the orthomosaics strongly matches the true dimensions measured on the beaches with an average accuracy of ≈1mm. Table 1 reports the different AOI covered following the optimal protocol for three selected islands, namely Jinnathuga, Adangau and En'Boodhoo islands, and the corresponding number of minimum IOI.

Gold Standards

Table 1 reports the experimental results of the in-situ GA and of the IS of the AOI. The matching scores express the ratio of the AMD found via IS to the AMD found during the GA. This score accounts for the estimated error in the use of the GS produced via IS.

The Deep-Learning Algorithm

Training, testing and performance

The training of the tailored CNN, performed on images from Jinnantuga-island (Fig. 4), achieved a validation accuracy higher than 95%. Adangau and En'Boodhoo-islands images (Fig. 5-a. – Fig 6-a.) were used to test the algorithm. A pixel-wise probability heat-map of each input image has been obtained by the software, as well as a bounding-boxes map for the detected AMD (Fig. 5-a. – 6-a.). In particular, for each pixel, a probability is given to be classified as AMD, thus allowing a visual understanding of the specific areas that might be subjected – with a different probability of risk exposure – to the presence of plastic debris.

Figure 5-c. and 6-c., shows bounding-boxes maps with all AMD detected. Table 2 reports the numerical results obtained by comparing the software output and the IS-GS for each image. The results highlight the average software-performance for En'Boodhoo drops of a factor of about 3 with respect to the Adangau case.

Therefore, these results give the evidence that the collection of UAV- images suitable for the training and testing of the deep-learning algorithm, should rely on specific recommendations regarding the optimization of the UAV survey, the collection of the GS, and the development of the algorithm itself

Discussion

The UAV survey and the AMD detection

The low cost, the high resolution and the high flexibility of UAVs quickly turned out to make them extremely versatile and useful tools for the investigation and analysis of a number of environmental issues. Small UAVs are used indeed with increasing frequency, in many research activities with applications in different fields: structural geology (Bonali et al., 2019), forestry sciences (Baron et al., 2018; Mlambo et al., 2017), mapping of sensitive marine habitats (Ventura et al., 2018), marine megafauna surveys (Colefax et al., 2018; Kiszka et al., 2016), coral bleaching detection (Levy et al., 2018). These platforms, especially the commercial drones, are proving to be useful tools for high-resolution remote sensing data collection, especially because of their small size, the increased lifetime of the batteries and the possibility to plan autonomous flights with user-friendly ground station software. Moreover, SfM algorithms allow obtaining accurate Digital Terrain Models (DTMs) and orthomosaics over large areas.

AMD was monitored worldwide through aerial surveys, along the beaches, since 2012 (Kako et al., 2012; Deidun et al., 2018; Kataoka et al., 2018; Martin et al., 2018; Sha et al., 2018) but explored locations are still limited (Fig. 7). Besides, more significant, it is the absence of a standardized protocol for data acquisition and elaboration. Previous studies, performed using a balloon equipped with a digital camera (Kako et al., 2012) and aerial photographs (Kataoka et al., 2018), faced problems related to the orthorectification and to the pixel-size of the images: a GSD of 10 cm/pix allowed identifying only groups of debris and not the single objects. The recent adoption of UAVs for AMD monitoring overcome a number of limitations mainly related to the flight altitude and to the GSD, to the orthorectification of the images, and to the repeatability of the surveys in a short time. However, the data-processing procedures are not uniform, ranging from visual interpretation of the images (Deidun et al., 2018) and spectral profile analysis of litter (Sha et al., 2018), to the use of machine learning methods (Martin et al., 2018). The use of AI classifiers (Martin et al., 2018) is more complex for different reasons, among which the lack of publicly available large databases (providing adequate images to train algorithms) is notable. The difficulty of developing scalable approaches, i.e. procedures that do not depend on local environmental constrains, is also a major issue for the use of AI clasisfiers.

The advantages in using UAVs, in terms both of resolution and monitoring repeatability, match perfectly with the need of understanding the pattern of aggregation in a remote area such as the Republic of Maldives. Here, a considerable amount of marine litter has been reported, despite the

remoteness of the location (Imhof et al., 2017). However, Imhof et al. (2017) highlighted the need for a robust protocol, allowing extensive sampling in space and time to collect scientifically sound data (Imhof et al., 2017). Remote-sensing studies, related to the accumulation and transportation of AMD, were not conducted before this work in the Republic of Maldives (Fig. 7). The lack of such monitoring studies for this area is significant, considering that plastic debris from the rivers of South Asia contributes to 67% of the global annual input (Lebreton et al., 2017) and that countries on the Indian Ocean are among the principal producer of mismanaged plastic waste (Jambeck et al., 2015). Besides, it is not clear where all this plastic, that should accumulate in the Indian Pacific, gyre is going (Mheen et al., 2019). Thus, the proposed methodology will improve and standardise the data collection of marine-litter accumulation on beaches and shorelines, gathering valuable and comparable data, even in remote and isolated areas.

The results of our study confirm most of the advantages of using a consumer-grade drone to carry out environmental monitoring. In particular, the use of a DJI Phantom 4 drone allowed to speed up considerably the standard walking beach survey and to access remote areas such as Maldives.
On the surveyed islands, anthropogenic debris were found everywhere: on the water's edge, just left there from waves and tides; on the upper part of the beaches and in the bushy coastal vegetation, likely carried there from storm tides and winds, or left by local tourists. The selected GSD allowed the identification and categorization of debris for each single detected item, making our remote observations comparable to the ones performed by operators on the ground. In fact, the matching between the ground-assessment and the visual screening of the images is higher than 87% (Tab. 1). In addition, the results of our survey protocol shows that the majority of the detected objects (Tab. 1) were plastics bottles and aluminium cans. Particularly abundant were also flip flops on En'Boodhoo and Adangau. These three categories of debris were observed with different degradation level: from brand new, with labels and the colours still intact, to partially disrupted. This can indicate the heterogeneity of the sources: some of them can be just washed up on the shore from the closest inhabited island or discharged from boats that passed nearby; others may have float in the ocean for thousands of kilometres before reaching the shore. Instead, the higher presence of plastic bags (foods wraps and plastic bags) on Adangau island is most probably due to the use of the island as a picnic and barbeque location from the inhabitants of the atoll.
The graphical outputs and the numerical results for Adangau Island show good performances (Figure 5, Table 2) and, in particular, in the face of an average sensitivity of 67%, the average PPV reaches 94%. This means that the deep-learning algorithm performance is affected by a non-negligible number of FN items – impacting on the sensitivity – but also that, on the other hand, the software is

highly specific in the ability to recognize AMD with respect to FP items. In addition, it should be noted that, for Adangau island, the software performance is quite stable, even when the number of real AMD-items on the beach increases (Table 2). The pixel-wise classification heatmaps for En'Boodhoo-island, shown in Figure 6-b, qualitatively confirm the good ability of deep learning algorithm, in recognizing the presence or absence of elements belonging to the "sea" class. Also, the software correctly reports on a low-probability with respect to the presence of vegetation (below 30%). On the contrary, the heatmaps for the other classes draw attention to issues that become evident when looking at the zoomed bounding-boxes maps in Figure 8, and to the quantitative results shown in Table 2. In this case, the average software-performance for En'Boodhoo drops of a factor of about 3 with respect to the Adangau case. This limitation can be explained by considering the different lighting conditions. In particular, Adangau-island images were collected at 12 am of a sunny day, therefore with similar sunlight-conditions of the testing set of Jinnathuga island. On the contrary, En'Boodhoo images were collected at 5 pm, and the shadows in the proximity of footprints (Fig.8) or of real AMD, represent pitfalls for the algorithm, as clarified by the high number of FP items in Table 2. As a matter of facts, the software was not trained to recognize footprints or shadows, and therefore such a limitation restricts the use of PlasticFinder, in its present version, to specific sunlight-conditions. For these reasons, we suggest conducting the survey with the sun high on the horizon, in order to avoid excessive shadows on the surveyed areas. However, to date, and to the best of our knowledge, there is only another algorithm presented to the scientific community, that has been developed for the specific purpose of automatically detect and quantify AMD along the shores by using a combination of UAV images and AI. In their pioneering work, Martin et al. (2018), focused their efforts in the Saudi-Arabian shorelines. They faced the highly-challenging task of both detecting and classifying the AMD typology with a series of multi-class random-forest classifiers, based on the extraction of HoG features. The authors validated the feasibility of using AI for AMD detection, but pointed out that the use of deep learning would have been more beneficial with respect to their approach that achieved a maximum sensitivity of only 44%. Therefore, our work represents the first implementation to automatically detect and accurately quantify AMD, based on a deep-learning approach. Results in Table 3 point out that PlasticFinder performances give better results, with respect to all the metrics, especially if used in the appropriate sunlight conditions. In particular, PlasticFinder PPV is much higher than the one obtained by Martin et al. (2018), allowing for a more specific tool to alarm on and quantify the presence of AMD.

In fact, it is important to highlight that, in order to monitor the presence of AMD and to know which are the areas that require an urgent intervention (i.e. those where AMD accumulate the most), it is essential to have a tool that is able to detect only AMD, without mistaken false positives. To this

extent, reaching a high PPV is more crucial than a high Sensitivity. Also, the fact that the reached Sensitivity is constant, despite the different loads of litter on the beach, is also a good result because it shows that the more is the AMD, the higher is the litter detected by PlasticFinder, i.e. this technology is able to detect accumulation zones.

These results reflect the major advantage of deep learning, with respect to conventional ML methods, which is the fact that it is not necessary to pre-transform data (e.g. an image) into selected features to feed models, but data can be input into neural-network models to let them automatically identify the best representations that allows tasks such as detection or classification (LeCun et al., 2015).

Best-practices optimization and future improvements

In order to optimize and enhance best practices for AMD remote-sensing monitoring, further improvements should be applied to the adopted protocols and methods.

In terms of the UAV survey, we reckon that once all the flight parameters have been set, the monitoring can be carried out from a small boat, in the proximity of the shores, without the need of reaching the beach, often inaccessible for the presence of coral reefs all around the islands. Therefore, this methodology can be particularly useful in geographical sites, such as the Maldives, where the presence of many small remote uninhabited islands, and the need to optimise the AMD beach-monitoring, represents a pressing matter.

In terms of the ground assessment protocol, such assessment is used to validate the reliability of the methodology, but, in implementing the protocol, it is not supposed to happen every time (otherwise the protocol would lose its time-efficiency). For this reason it has been not included in the Protocol recommendations (Table 4). In general, the beach should be left untouched before the UAV survey to avoid footprints or other environment manipulations that could affect the methodology performance, especially in remote places.

Another important remark is that, for a relevant fraction of the AMD, the deposition on the beach is only a transitory phase before being taken up by the currents to resume the floating travel in the ocean. Instead, other AMD can be trapped on the upper part of the beach, where environmental factors and the erosive action of the sand can accelerate the plastic degradation processes. The microplastics particles (< 5mm) produced by the degradation of the AMD trapped on the upper part of the shore can enter in the sediments or can be released as contaminants in the water of the lagoon (Saliu et al., 2018; Saliu et al., 2019). Therefore, fast and efficient data collection and image analysis of the distribution of AMD on the shore, as well as specific AI tools for its automatic and objective assessment are necessary, but not sufficient, since microplastic is lost from this detection and quantification. However, the distribution and quantitation of AMD, as obtained from our protocol,

could be used to understand which are the most impacted areas, and the AMD depositional seasonal trends connected to the Indian Ocean currents patterns (Mheen et al., 2019). The creation of an integrated model could allow stakeholders (e.g. governments, NGO) using this information in order to promote mitigation actions, such as specific citizenship awareness initiatives, beach–clean up events, but also addressing – with a data-driven approach - the interception of the floating AMD, before reaching the shorelines.

Finally, we would suggest some improvement for PlasticFinder, for example, by a more in-depth training, with the aim of avoiding sunlight-conditions dependence for its use, which represents, to date, one of its major limitations. Also, optimization should be implemented to scale up the algorithm speed and ability to process full orthomosaic images, overcoming time-scale limitations due to processing of a large amount of data. In Table 4, we summarize and suggest an optimal protocol, with key recommendations.

Conclusion

Our work was aimed at proposing an efficient and reliable monitoring protocol, to address a pressing worldwide environmental issue such as AMD deposition along the shores. Low altitude remote-sensing data are essential for obtaining a synoptic overview of extended areas, and UAVs are powerful tools to acquire them. Our study, confirmed the use of a commercial drone for AMD monitoring as a fast and reliable surveys methodology. The use of UAV is instrumental to survey remote areas and the spatial resolution achieved in the collected images allowed to detect a percentage of the objects on the shores higher than 87.8%. A deep-learning based software, PlasticFinder, has been used for the automatic detection and quantification of AMD, providing analysis of the UAV collected images. In the Maldivian case study, the overall performances were good, reaching a PPV of 94% with the better sunlight conditions, much greater than the only state-of-the-art AI algorithm so far published in literature. The only critical limitations, observed in our study, are determined by environmental circumstances encountered during the survey, and especially sunlight conditions and the associated terrain shading effects: restrictions are given for the images that can be analysed with the deep-learning algorithm in its present version, where the PPV is reduced to 54%.

References

Andrades, R., Martins, A. S., Fardim, L. M., Ferreira, J. S., & Santos, R. G. (2016). Origin of marine debris is related to disposable packs of ultra-processed food. Marine Pollution Bulletin, 109(1), 192–195. https://doi.org/10.1016/J.MARPOLBUL.2016.05.083

Andrady, A. L. (2011). Microplastics in the marine environment. Marine Pollution Bulletin, 62(8), 1596–1605. https://doi.org/10.1016/J.MARPOLBUL.2011.05.030

Barnes, D. K. A. (2004.). Surveys from Negombo in West Sri Lanka, Ari Atoll in the Maldives. Retrieved from http://www.cordell.org/HD/HD_documents/HE_Library/Debris/RIA.pdf

Barnes, D. K. A., Galgani, F., Thompson, R. C., & Barlaz, M. (2009). Accumulation and fragmentation of plastic debris in global environments. Philosophical Transactions of the Royal Society B: Biological Sciences, 364(1526), 1985–1998. https://doi.org/10.1098/rstb.2008.0205

Baron, J., Hill, D. J., & Elmiligi, H. (2018). International Journal of Remote Sensing Combining image processing and machine learning to identify invasive plants in high-resolution images Combining image processing and machine learning to identify invasive plants in high-resolution images. Remote Sensing, 39, 5099–5118. https://doi.org/10.1080/01431161.2017.1420940

Bonali, F. L., Tibaldi, A., Marchese, F., Fallati, L., Russo, E., Corselli, C., & Savini, A. (2019). UAV-based surveying in volcano-tectonics: An example from the Iceland rift. Journal of Structural Geology. https://doi.org/10.1016/j.jsg.2019.02.004

Burns, J. H. R., & Delparte, D. (2017). Comparison of commercial structure-from-motion photogrammety software used for underwater three-dimensional modeling of coral reef environments. In International Archives of the Photogrammetry, Remote Sensing and Spatial Information Sciences - ISPRS Archives (Vol. 42, pp. 127–131). https://doi.org/10.5194/isprs-archives-XLII-2-W3-127-2017

Casella, E., Collin, A., Harris, D., Ferse, S., Bejarano, S., Parravicini, V., … Rovere, A. (2016). Mapping coral reefs using consumer-grade drones and structure from motion photogrammetry techniques. Coral Reefs. https://doi.org/10.1007/s00338-016-1522-0

Cinner, J. E., Maire, E., Huchery, C., MacNeil, M. A., Graham, N. A. J., Mora, C., … Mouillot, D. (2018). Gravity of human impacts mediates coral reef conservation gains. Proceedings of the National Academy of Sciences. Retrieved from http://www.pnas.org/content/early/2018/06/12/1708001115

Colefax, A. P., Butcher, P. A., & Kelaher, B. P. (2018). The potential for unmanned aerial vehicles (UAVs) to conduct marine fauna surveys in place of manned aircraft. ICES Journal of Marine Science. Oxford University Press. https://doi.org/10.1093/icesjms/fsx100

Cook, K. L. (2017). An evaluation of the effectiveness of low-cost UAVs and structure from motion for geomorphic change detection. Geomorphology, 278, 195–208. https://doi.org/10.1016/j.geomorph.2016.11.009

Corcoran, P. L., Biesinger, M. C., & Grifi, M. (2009). Plastics and beaches: A degrading relationship. Marine Pollution Bulletin. https://doi.org/10.1016/j.marpolbul.2008.08.022

Deidun, A., Gauci, A., Lagorio, S., & Galgani, F. (2018). Optimising beached litter monitoring protocols through aerial imagery. Marine Pollution Bulletin, 131, 212–217. https://doi.org/10.1016/J.MARPOLBUL.2018.04.033

Department of Economic and Social Affairs Division for Sustainable Development TRENDS IN SUSTAINABLE DEVELOPMENT Small Island Developing States (SIDS). (2011). Retrieved from https://sustainabledevelopment.un.org/content/documents/313Trends_in_Sustainable_Development_SIDS.pd

Ebbesmeyer, C. C., Ingraham, W. J., Jones, J. A., & Donohue, M. J. (2012). Marine debris from the oregon dungeness crab fishery recovered in the Northwestern Hawaiian Islands: Identification and oceanic drift paths. Marine Pollution Bulletin. https://doi.org/10.1016/j.marpolbul.2011.09.037

Eriksen, M., Lebreton, L. C. M., Carson, H. S., Thiel, M., Moore, C. J., Borerro, J. C., … Reisser, J. (2014). Plastic Pollution in the World's Oceans: More than 5 Trillion Plastic Pieces Weighing over 250,000 Tons Afloat at Sea. PLoS ONE. https://doi.org/10.1371/journal.pone.0111913

Fallati, L., Savini, A., Sterlacchini, S., & Galli, P. (2017). Land use and land cover (LULC) of the Republic of the Maldives: first national map and LULC change analysis using remote-sensing data. Environmental Monitoring and Assessment, 189(8), 417. https://doi.org/10.1007/s10661-017-6120-2

Flynn, K. F., & Chapra, S. C. (2014). Remote sensing of submerged aquatic vegetation in a shallow non-turbid river using an unmanned aerial vehicle. Remote Sensing, 6(12), 12815–12836. https://doi.org/10.3390/rs61212815

Chollet F., Deep learning with Python. Mannig Publications Co., Greenwich, CT, USA, 1st edition, 2017

Galgani, F., Leaute, J. P., Moguedet, P., Souplet, A., Verin, Y., Carpentier, A., … Nerisson, P. (2000). Litter on the sea floor along European coasts. Marine Pollution Bulletin. https://doi.org/10.1016/S0025-326X(99)00234-9

Galgani, François, Hanke, G., & Maes, T. (2015). Global distribution, composition and abundance of marine litter. In Marine Anthropogenic Litter (pp. 29–56). Cham: Springer International Publishing. https://doi.org/10.1007/978-3-319-16510-3_2

Galgani, Francois, Ryan, P. G., Moore, C. J., Eriksen, M., Borerro, J. C., Carson, H. S., … Thiel, M. (2014). Plastic Pollution in the World's Oceans: More than 5 Trillion Plastic Pieces Weighing over 250,000 Tons Afloat at Sea. PLoS ONE, 9(12), e111913. https://doi.org/10.1371/journal.pone.0111913

Geyer, R., Jambeck, J. R., & Law, K. L. (2017). Production, use, and fate of all plastics ever made. Science Advances. https://doi.org/10.1126/sciadv.1700782

Guest, D., Cranmer, K., & Whiteson, D. (2018). Deep Learning and its Application to LHC Physics. Annual Review of Nuclear and Particle Science, 68(1), 161–181. https://doi.org/10.1146/annurev-nucl-101917-021019

Hengstmann, E., Gräwe, D., Tamminga, M., & Fischer, E. K. (2017). Marine litter abundance and distribution on beaches on the Isle of Rügen considering the influence of exposition, morphology and recreational activities. Marine Pollution Bulletin, 115(1–2), 297–306. https://doi.org/10.1016/J.MARPOLBUL.2016.12.026

Imhof, H. K., Sigl, R., Brauer, E., Feyl, S., Giesemann, P., Klink, S., … Laforsch, C. (2017). Spatial and temporal variation of macro-, meso- and microplastic abundance on a remote coral island of the Maldives, Indian Ocean. Marine Pollution Bulletin, 116(1–2), 340–347. https://doi.org/10.1016/j.marpolbul.2017.01.010

Jambeck, J. R., Geyer, R., Wilcox, C., Siegler, T. R., Perryman, M., Andrady, A., … Law, K. L. (2015). Marine pollution. Plastic waste inputs from land into the ocean. Science (New York, N.Y.), 347(6223), 768–771. https://doi.org/10.1126/science.1260352

Kako, S., Isobe, A., Kataoka, T., & Hinata, H. (2014). A decadal prediction of the quantity of plastic marine debris littered on beaches of the East Asian marginal seas. Marine Pollution Bulletin. https://doi.org/10.1016/j.marpolbul.2014.01.057

Kako, S., Isobe, A., & Magome, S. (2012). Low altitude remote-sensing method to monitor marine and beach litter of various colors using a balloon equipped with a digital camera. Marine Pollution Bulletin, 64(6), 1156–1162. https://doi.org/10.1016/j.marpolbul.2012.03.024

Kako, S., Isobe, A., Seino, S., & Kojima, A. (2010). Inverse estimation of drifting-object outflows using actual observation data. Journal of Oceanography. https://doi.org/10.1007/s10872-010-0025-9

Kataoka, T., Murray, C. C., & Isobe, A. (2018). Quantification of marine macro-debris abundance around Vancouver Island, Canada, based on archived aerial photographs processed by projective transformation. Marine Pollution Bulletin, 132(September 2017), 44–51. https://doi.org/10.1016/j.marpolbul.2017.08.060

Kiszka, J. J., Mourier, J., Gastrich, K., & Heithaus, M. R. (2016). Using unmanned aerial vehicles (UAVs) to investigate shark and ray densities in a shallow coral lagoon. Marine Ecology Progress Series, 560, 237–242. https://doi.org/10.3354/meps11945

Laist, D. W. (1987). Overview of the biological effects of lost and discarded plastic debris in the marine environment. Marine Pollution Bulletin. https://doi.org/10.1016/S0025-326X(87)80019-X

Laist, D. W. (2011). Impacts of Marine Debris: Entanglement of Marine Life in Marine Debris Including a Comprehensive List of Species with Entanglement and Ingestion Records. https://doi.org/10.1007/978-1-4613-8486-1_10

Lavers, J. L., Oppel, S., & Bond, A. L. (2016). Factors influencing the detection of beach plastic debris. Marine Environmental Research. https://doi.org/10.1016/j.marenvres.2016.06.009

Lavers, J. L., & Bond, A. L. (2017). Exceptional and rapid accumulation of anthropogenic debris on one of the world's most remote and pristine islands. Proceedings of the National Academy of Sciences, 114(23), 6052–6055. https://doi.org/10.1073/pnas.1619818114

Law, K. L., Morét-Ferguson, S. E., Goodwin, D. S., Zettler, E. R., Deforce, E., Kukulka, T., & Proskurowski, G. (2014). Distribution of surface plastic debris in the eastern pacific ocean from an 11-year data set. Environmental Science and Technology. https://doi.org/10.1021/es4053076

Law, K. L., Morét-Ferguson, S., Maximenko, N. A., Proskurowski, G., Peacock, E. E., Hafner, J., & Reddy, C. M. (2010). Plastic accumulation in the North Atlantic subtropical gyre. Science. https://doi.org/10.1126/science.1192321

Lebreton, L. C. M., Van Der Zwet, J., Damsteeg, J. W., Slat, B., Andrady, A., & Reisser, J. (2017). River plastic emissions to the world's oceans. Nature Communications, 8, 1–10. https://doi.org/10.1038/ncomms15611

Lebreton, L., Slat, B., Ferrari, F., Sainte-Rose, B., Aitken, J., Marthouse, R., … Reisser, J. (2018). Evidence that the Great Pacific Garbage Patch is rapidly accumulating plastic. Scientific Reports, 8(1), 1–15. https://doi.org/10.1038/s41598-018-22939-w

LeCun, Y., Bengio, Y., & Hinton, G. (2015). Deep learning. Nature, 521(7553), 436–444. https://doi.org/10.1038/nature14539

Levy, J., Hunter, C., Lukacazyk, T., & Franklin, E. C. (2018). Assessing the spatial distribution of coral bleaching using small unmanned aerial systems. Coral Reefs, pp. 1–15. https://doi.org/10.1007/s00338-018-1662-5

Martin, C., Parkes, S., Zhang, Q., Zhang, X., McCabe, M. F., & Duarte, C. M. (2018). Use of unmanned aerial vehicles for efficient beach litter monitoring. Marine Pollution Bulletin, 131, 662–673. https://doi.org/10.1016/j.marpolbul.2018.04.045

Mheen, M., Pattiaratchi, C., & Sebille, E. (2019). Role of Indian Ocean Dynamics on Accumulation of Buoyant Debris. Journal of Geophysical Research: Oceans, 2018JC014806. https://doi.org/10.1029/2018JC014806

Mlambo, R., Woodhouse, I. H., Gerard, F., & Anderson, K. (2017). Structure from motion (SfM) photogrammetry with drone data: A low cost method for monitoring greenhouse gas emissions from forests in developing countries. Forests, 8(3), 68. https://doi.org/10.3390/f8030068

Penca, J. (2018). European Plastics Strategy: What promise for global marine litter? Marine Policy, 97, 197–201. https://doi.org/10.1016/J.MARPOL.2018.06.004

Pierdomenico, M., Casalbore, D., & Chiocci, F. L. (2019). Massive benthic litter funnelled to deep sea by flash-flood generated hyperpycnal flows. Scientific Reports, 9(1), 5330. https://doi.org/10.1038/s41598-019-41816-8

Programme, U. N. E. (2005). Marine Litter An analytical overview www.unep.org. Retrieved from http://wedocs.unep.org/handle/20.500.11822/8348

Ramirez-Llodra, E., De Mol, B., Company, J. B., Coll, M., & Sardà, F. (2013). Effects of natural and anthropogenic processes in the distribution of marine litter in the deep Mediterranean Sea. Progress in Oceanography. https://doi.org/10.1016/j.pocean.2013.07.027

Rochman, C. M., Browne, M. A., Halpern, B. S., Hentschel, B. T., Hoh, E., Karapanagioti, H. K., … Thompson, R. C. (2013). Policy: Classify plastic waste as hazardous. Nature. https://doi.org/10.1038/494169a

Ryan, P. G. (2015). A brief history of marine litter research. In Marine Anthropogenic Litter. https://doi.org/10.1007/978-3-319-16510-3_1

Ryan, P. G., Moore, C. J., Van Franeker, J. A., & Moloney, C. L. (2009). Monitoring the abundance of plastic debris in the marine environment. Philosophical Transactions of the Royal Society B: Biological Sciences, 364(1526), 1999–2012. https://doi.org/10.1098/rstb.2008.0207

Saliu, F., Montano, S., Garavaglia, M. G., Lasagni, M., Seveso, D., & Galli, P. (2018). Microplastic and charred microplastic in the Faafu Atoll, Maldives. Marine Pollution Bulletin, 136, 464–471. https://doi.org/10.1016/j.marpolbul.2018.09.023

Saliu, F., Montano, S., Leoni, B., Lasagni, M., & Galli, P. (2019). Microplastics as a threat to coral reef environments: Detection of phthalate esters in neuston and scleractinian corals from the Faafu Atoll, Maldives. Marine Pollution Bulletin, 142, 234–241. https://doi.org/10.1016/j.marpolbul.2019.03.043

Savini, A., Vertino, A., Marchese, F., Beuck, L., & Freiwald, A. (2014). Mapping cold-water coral habitats at different scales within the Northern Ionian Sea (Central Mediterranean): an assessment of coral coverage and associated vulnerability. PLoS One, 9(1), e87108. https://doi.org/10.1371/journal.pone.0087108

Sha, J., Shifaw, E., Bao, Z., Li, X., & Hanchiso, T. (2018). Monitoring of beach litter by automatic interpretation of unmanned aerial vehicle images using the segmentation threshold method. Marine Pollution Bulletin, 137, 388–398. https://doi.org/10.1016/j.marpolbul.2018.08.009

Shimizu, T., Nakai, J., Nakajima, K., Kozai, N., Takahashi, G., Matsumoto, M., & Kikui, J. (2008). Seasonal variations in coastal debris on Awaji Island, Japan. Marine Pollution Bulletin. https://doi.org/10.1016/j.marpolbul.2007.10.005

Thiel, M., Hinojosa, I. A., Miranda, L., Pantoja, J. F., Rivadeneira, M. M., & Vásquez, N. (2013). Anthropogenic marine debris in the coastal environment: A multi-year comparison between coastal waters and local shores. Marine Pollution Bulletin, 71(1–2), 307–316. https://doi.org/10.1016/J.MARPOLBUL.2013.01.005

Thompson, Richard C ; Olsen, Ylva ; Mitchell, Richard P ; Davis, Anthony ; Rowland, Steven J ; John, Anthony W G ; Mcgonigle, Daniel ; Russell, A. E., Thompson, R. C., Olsen, Y., Mitchell, R. P., Davis, A., Rowland, S. J., … Russell, A. E. (2004). Lost at sea: Where is all the plastic? Science. https://doi.org/doi:10.1126/science.1094559

Thompson, R. C., Moore, C. J., Saal, F. S. V., & Swan, S. H. (2009). Plastics, the environment and human health: Current consensus and future trends. Philosophical Transactions of the Royal Society B: Biological Sciences. https://doi.org/10.1098/rstb.2009.0053

UNEP: 1999b, Western Indian Ocean Environment Outlook-1999, Nairobi, UNEP.

Van Cauwenberghe, L., Vanreusel, A., Mees, J., & Janssen, C. R. (2013). Microplastic pollution in deep-sea sediments. Environmental Pollution. https://doi.org/10.1016/j.envpol.2013.08.013

Ventura, D., Bruno, M., Jona Lasinio, G., Belluscio, A., & Ardizzone, G. (2016). A low-cost drone based application for identifying and mapping of coastal fish nursery grounds. Estuarine, Coastal and Shelf Science, 171, 85–98. https://doi.org/10.1016/j.ecss.2016.01.030

Ventura, D., Bonifazi, A., Gravina, M. F., Belluscio, A., & Ardizzone, G. (2018). Mapping and classification of ecologically sensitive marine habitats using unmanned aerial vehicle (UAV) imagery and Object-Based Image Analysis (OBIA). Remote Sensing, 10(9), 1331. https://doi.org/10.3390/rs10091331

Verhoeven, G. (2011). Taking computer vision aloft - archaeological three-dimensional reconstructions from aerial photographs with photoscan. Archaeological Prospection, 18(1), 67–73. https://doi.org/10.1002/arp.399

Vlachogianni, T., Fortibuoni, T., Ronchi, F., Zeri, C., Mazziotti, C., Tutman, P., … Scoullos, M. (2018). Marine litter on the beaches of the Adriatic and Ionian Seas: An assessment of their abundance, composition and sources. Marine Pollution Bulletin, 131, 745–756. https://doi.org/10.1016/J.MARPOLBUL.2018.05.006

Watts, A. J. R., Porter, A., Hembrow, N., Sharpe, J., Galloway, T. S., & Lewis, C. (2017). Through the sands of time: Beach litter trends from nine cleaned north cornish beaches. Environmental Pollution. https://doi.org/10.1016/j.envpol.2017.05.016

Tables and Figures

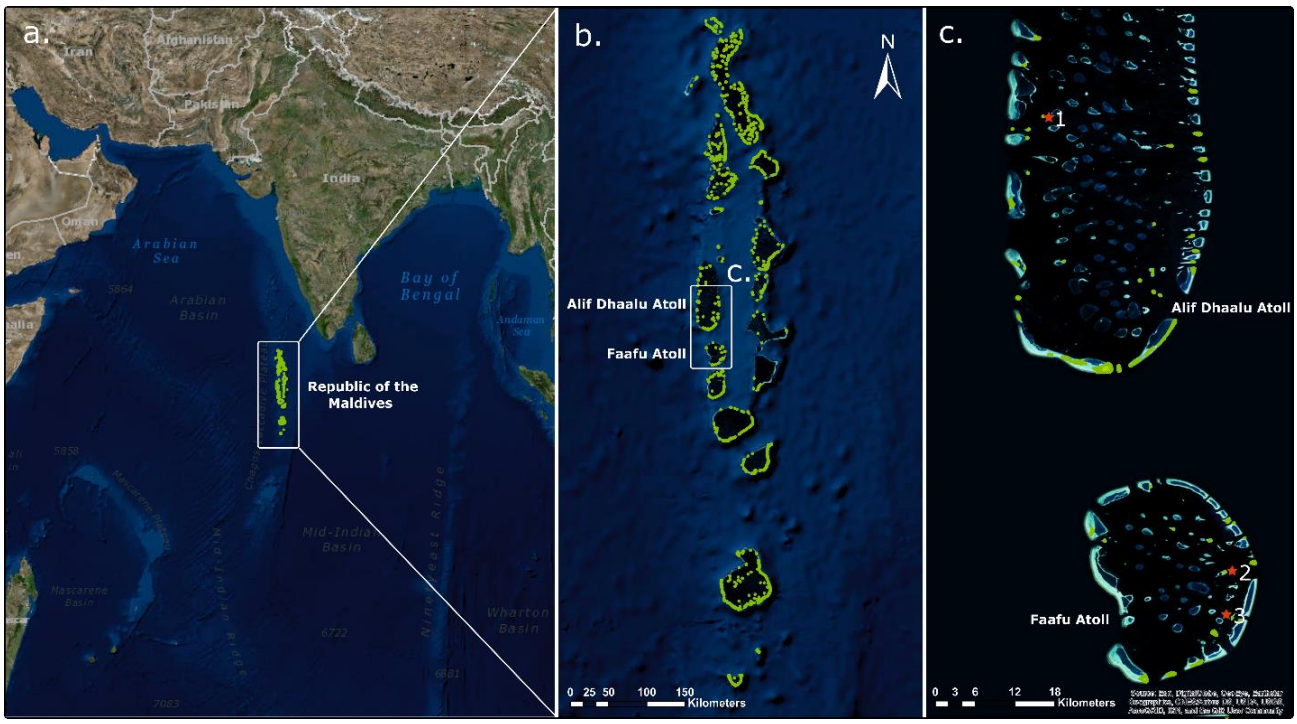

Fig. 1. Geographic location of the study area, Republic of Maldives (a.), Alif Dhaalu and Faafu Atolls (b.), and islands selected as testing sites (c.): 1 En'Boodhoo, 2 Jinnathuga, 3 Adangau.

Fig. 2. Debris accumulation in the Maldives: (a) one of the ferries port in Malè (capital city) with evident accumulation ofplastic bottles released in the ocean from the boats or from the streets of the city; (b) Litter and plastic debris accumulated near the shore of Thilafushi, the only landfill island of the archipelago; (c, d) plastic waste deposited by the high tide on the beach of Adangau; (e, f) plastic waste deposited in the bushes and on the shores of En'Boodhoo.

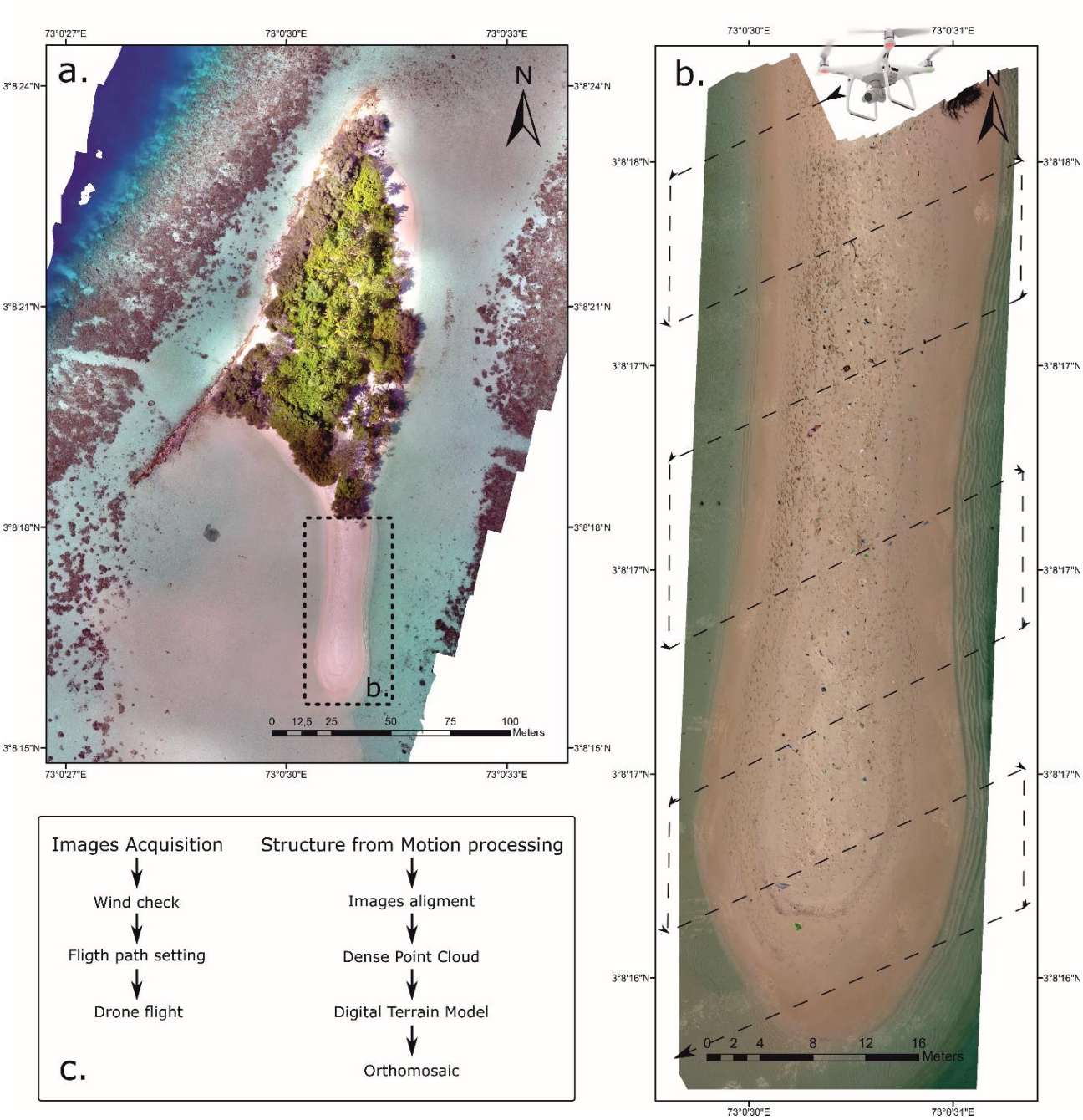

Fig. 3. Drone survey over Adangau (a.) sandy long beach. The path followed by the drone (b.) is overlayed on the high-resolution orthomosaic that was generated applying the SfM workflow (c.) to RGB images.

v

Table 1. AOI, number of minimum IOI, climate, light and weather conditions of each investigated Maldivian island during the UAV survey and the in-situ ground assessment (GA). The number of items collected during the GA on each beach is listed per each class, and the items identified via image screening (IS) via PC are also reported.

	Jinnathuga		**Adangau**		**En'Boodhoo**	
AOI (m^2)	216		1056		225	
IOI	1		5		1	
Climate (Month)	April		November		October	
Light (Time)	12 pm		12 pm		5 pm	
Weather (Conditions)	Sunny		Sunny		Cloudy	
Use	Training Set		Testing Set		Testing Set	
AMD Class	**GA**	**IS**	**GA**	**IS**	**GA**	**IS**
Lighter	4	1	1	1	4	4
Bottle	21	21	50	54	47	43
Straw	1	0	1	0	0	0
Net	11	8	3	3	2	3
Plastic Bag	7	7	43	50	3	2
Aluminum Can	8	6	11	13	21	14
Plastic containers	3	3	1	1	12	7
Plastic utensils	0	0	20	8	1	0
Flip Flop	1	1	13	8	32	29
Other	26	25	4	3	13	19
TOTAL	**82**	**72**	**147**	**141**	**135**	**120**
Matching Score (%)	**87.8**		**95.9**		**88.8**	

Fig. 4. Examples ofJinnathuga island images (a., b. and c.), used as training set for the deep-learning algorithm. Note the presence ofthe different classes in the images, in particular "AMD" in (a), "sand" in (a), (b) and (c), "sea" in (b), "vegetation" and "other" in images (a) and (c).

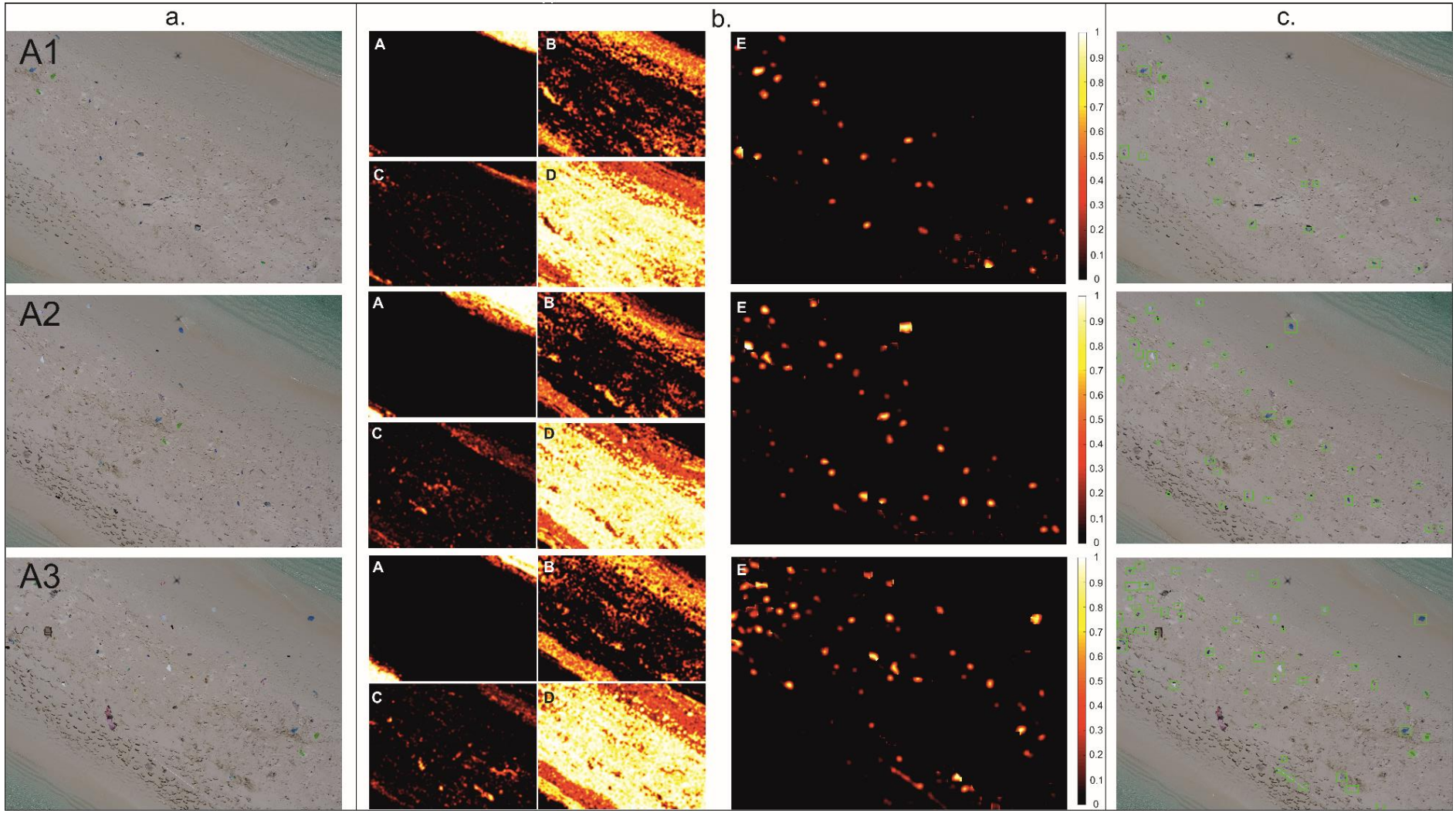

Fig. 5. Canvas on the left (a.), fromtop to bottom: testing-set images A1, A2 and A3 for Adangau-island. Central canvas (b.), from top to bottom: PlasticFinder pixel-wise classification heatmaps for Adangau-island images A1, A2 and A3 representing, respectively, the classes sea (A), sand (B), vegetation (C) other/AMD (D), and AMD(E)with the probability scale ranging from 0 to 1. Canvas on the right (c.), fromtop to bottom: PlasticFinder bounding-boxesmaps for the Adangau island images A1, A2 and A3. Each green bounding box is identified as an item of AMD by the software.

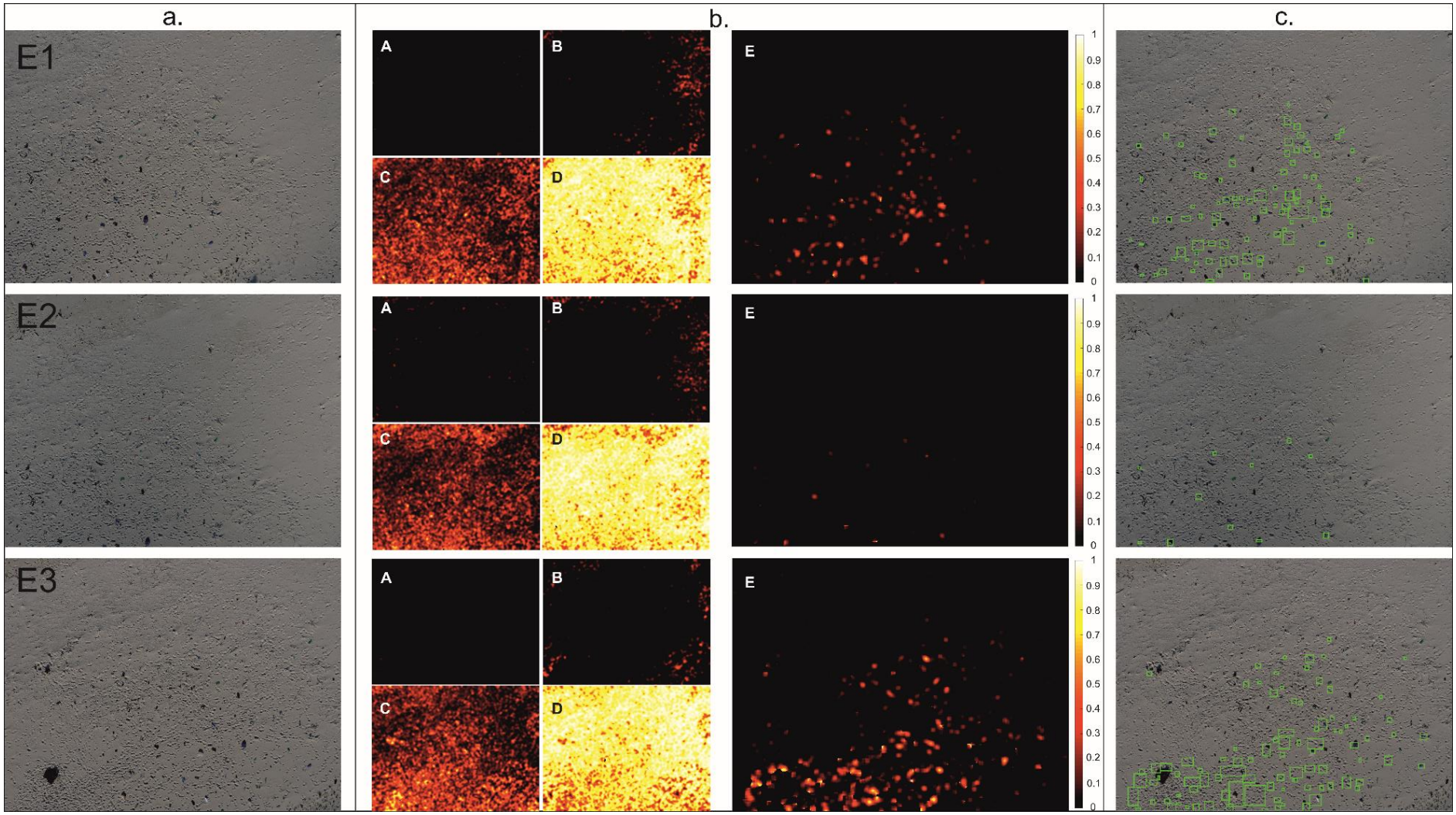

Fig. 6. Canvas on the left (a.), from top to bottom: testing-set images E1, E2, E3 for En'Boodhoo island. Central canvas (b.), from top to bottom: PlasticFinder pixel-wise classification heatmaps for En'Boodhoo-island images E1, E2, E3 representing, respectively, the classes sea (A), sand (B), vegetation (C), other/AMD (D), and AMD (E) with the probability scale ranging from 0 to 1. Canvas on the right (c.), fromtop to bottom: PlasticFinder bounding-boxesmaps for the

Table 2. Results for the Adangau and En'Boodhoo testing-set images A1, A2, A3 and E1, E2, E3, respectively. Average scores (AVG) are also given for each set. AMD accounts for the total real items in each image, as identified by the gold standard. True positive (TP), false negative (FN) and false positive (FP) items are combined to express the software performance in terms of sensitivity, PPV and F-score.

IMG	**AMD**	**TP**	**FN**	**FP**	***Sensitivity (%)***	***PPV (%)***	***F-score (%)***
Adangau							
A1	37	25	12	0	0.68	1.00	0.81
A2	58	40	18	4	0.69	0.91	0.78
A3	89	56	33	6	0.66	0.90	0.74
AVG	61.3	40.3	21	3.3	0.67	0.94	0.78
En'Boodhoo							
E1	71	23	48	66	0.32	0.26	0.29
E2	43	5	38	6	0.12	0.45	0.19
E3	98	25	73	65	0.26	0.28	0.27
AVG	70.6	17.6	53	45.6	0.23	0.25	0.33

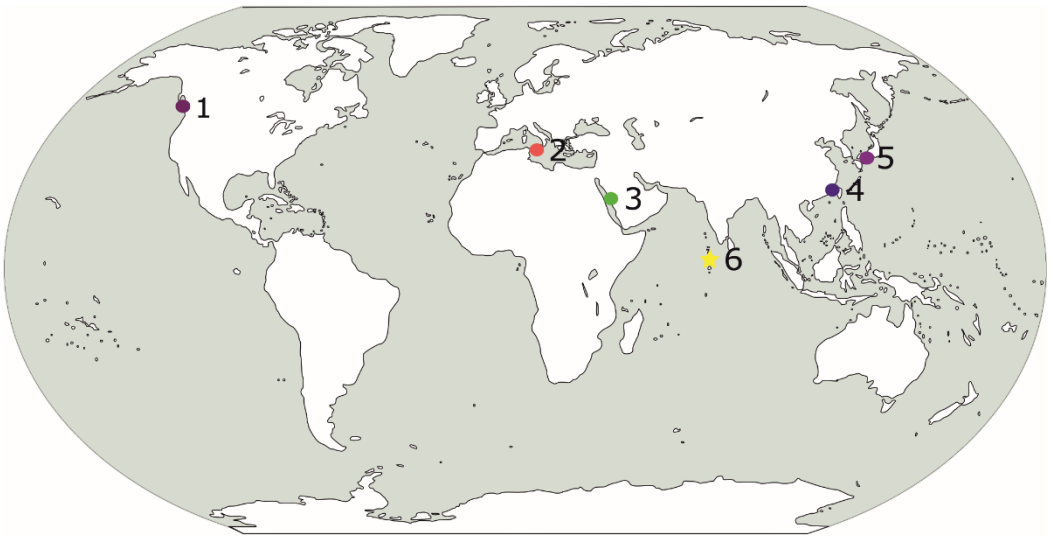

Fig. 7. Geographic distribution ofstudies that used remote sensing techniques tomonitor anddetect beachdebris: 1Vancouver Island, Canada (Kataoka et al., 2018); 2Malta (Deidun et al., 2018); 3 Saudi Arabia (Martin et al., 2018); 4 Fuzhou, Fujian, China (Sha et al., 2018); 5 Seto Inland Sea, Japan (Kako et al., 2012); 6 Republic ofMaldives, present study area

Table 3. Comparison between results from Martin et al. (2018) (average on the overall results), PlasticFinder results for Adangau island and averaged results for Adangau and En'Boodhoo island

Algorithm	TOT	TP	FN	FP	Sens (%)	PPV (%)	F-score (%)
Martin et al.	415	164	251	1941	0.40	0.08	0.13
PlasticFinder (Adangau)	61.3	40.3	21	3.3	0.67	0.94	0.78
PlasticFinder (AVG A/E)	131.9	57.9	74	48.9	0.44	0.54	0.49

Fig. 8. Examples ofshadows in the proximity offootprints (left image) and ofitems ofAMD (right image), that aremistaken as AMD by the software, representing pitfalls for the algorithm in its present version.

Table 4. Optimal protocol and key recommendations for the optimization of the UAV survey, the collection of gold standards and of UAV images suitable for the training and testing of a deep-learning algorithm.

UAV Survey	
Flight Altitude	10 m
GSD	4.36 mm/pix
Camer Gimbal Orientation	-90° (nadir orientation)
Images acquisition along fixed paths	80% frontal overlap
	70% lateral overlap
	2 seconds of shooting interval
	1,3 m/s costant velocity
Gold Standard	
Ground Assessment	AMD inspection and subtype classification (to be limited to few representative areas for the validation of methodology)
	AMD Size > 5 cm
Image Screening	AMD counting and subtype classification
	Matching Score > 80%
Deep Learning	
Training	# of images per class ~ 10^3
	Validation accuracy for tailored CNN > 95%
Testing	# of images ~ # IOI
	Use IS-GS to test performances with metrics
	Use GA-GS to estimate error on the IS-quantified performance

Chapter 3

Moving below the surface: underwater photogrammetry and acoustic remote sensing

3.1

Anelli, M., Julitta, T., Fallati, L., Galli, P., Rossini, M., & Colombo, R. (2017). Towards new applications of underwater photogrammetry for investigating coral reef morphology and habitat complexity in the Myeik Archipelago, Myanmar. Geocarto International, 6049(December), 1–14. https://doi.org/10.1080/10106049.2017.1408703

Towards new applications of underwater photogrammetry for investigating coral reef morphology and habitat complexity in the Myeik Archipelago, Myanmar

Martina ANELLI [a], Tommaso JULITTA [a], Luca FALLATI [b], Paolo GALLI [c], Micol ROSSINI [a], Roberto COLOMBO [a]

[a] Remote Sensing of Environmental Dynamics Lab, Department of Earth and Environmental Sciences, University of Milano-Bicocca, Milano, Italy

[b] Department of Earth and Environmental Sciences, University of Milano-Bicocca, Milano, Italy

[c] Department of Biotechnology and Biosciences, University of Milano-Bicocca, Milano, Italy

Abstract

Photogrammetry represents a non-destructive, cost-effective tool for coral reef monitoring, able to integrate traditional remote sensing techniques and support researchers' work. However, its application to submerged habitats is still in early stage. We present new ways to employ Structure from Motion techniques to infer properties of reef habitats. In particular, we propose the use of Digital Surface Models and Digital Terrain Models for assessing coral colonies extension and height and discriminating between seabed and coral cover. Such information can be coupled with digital rugosity estimates to improve habitat characterisation. DTM, DSM and orthophotos were derived and used to compute a series of metrics like coral morphologies, reef topography, coral cover and structural complexity. We show the potentialities offered by underwater photogrammetry and derived products to provide useful basic information for marine habitat mapping, opening the possibility to extend these methods for large-scale assessment and monitoring of coral reefs.

Introduction

Coral reefs are often called the 'tropical rainforests of the sea' for their astounding richness of life. Indeed, they are unique habitats in terms of productivity and biodiversity: they sustain the food chain, provide shelter for a wide variety of marine life, act as a buffer for shorelines and contribute to the creation of sand for beaches (Moberg and Folke 1999). They also support the subsistence of local communities, commercial fisheries and are home to organisms able to be potential source of medicines (Moberg and Folke 1999). According to data from the Food and Agriculture Organization of the United Nations (FAO), which have been reported by the CBI Market Information Database, more than 2 million tonnes of marine fish is captured each year in the Burmese coastal areas. As regards tourism, coral reefs attract foreign and domestic visitors and generate revenues, including foreign exchange earnings, in over 100 countries and territories. Some 30% of the world's reefs are of value in the tourism sector, with a total value estimated at nearly US$36 billion per year (Spalding et al. 2017).

Moreover, corals embody a relevant source of recreation and tourism. Climate change and anthropic stress represent the main threat for the integrity of such habitats and the setting-up of management plans is becoming ever more urgent (Rogers et al. 2014).

A detailed characterization of reef areas is essential and coral mapping can provide many useful information for planning conservation strategies. For example, coral cover, coral biodiversity and morphology, reef health status and topographic complexity (rugosity) can be considered key factors related to coral reef resilience (Ferrari et al. 2016).

Remote sensing techniques represent a powerful tool for characterizing morphology and habitat complexity in coral reefs. Indeed, several studies demonstrated the successful use of spectral information for mapping coral cover at medium–large scale (from tens to hundreds of square kilometres), by exploiting traditional remote sensing techniques like airborne or satellite systems, multispectral or hyperspectral devices (Hochberg et al. 2003; Joyce and Phinn 2013; Joyce et al. 2013; Hedley et al. 2016). However, there are some limitations concerning these techniques, primarily imposed by the spectral variability of benthic types and sub-pixel mixing at large scales (Knudby et al. 2007; Hedley et al. 2012).

Photogrammetric analysis and Structure from Motion (SfM) techniques can integrate traditional remote sensing techniques, providing high-resolution models (pixel size of few millimetres) able to reproduce small areas at a significant scale. The application of photogrammetric techniques is increasing due to technological evolution and is becoming more relevant for underwater remote sensing studies, as it represents a cost-effective method for the monitoring of coral reefs (Burns et al.

2015) and a valid support to human interpretation (Williams et al. 2012), especially on large areas. In addition, photogrammetry is a non-destructive technique allowing the acquisition of information without coral removal and is less time-consuming than visual estimation, so larger areas can be covered (Bythell et al. 2001; Cocito et al. 2003; Gutierrez-Heredia et al. 2016) and repeatedly mapped to obtain time series.

Although SfM techniques are well introduced for terrestrial surveys (Fonstad et al. 2013; Colomina and Molina 2014; Javernick et al. 2014; Gonçalves and Henriques 2015), they are still at an early stage for underwater studies. In relation to coral reefs, close-range photogrammetry was first used by Bythell et al. (2001) to compute structural complexity metrics from coral colonies. Since then, only few studies on underwater 3D photogrammetry have been published and they are mainly focused on colony-scale (Bythell et al. 2001; Cocito et al. 2003; Courtney et al. 2007; McKinnon et al. 2011; Burns et al. 2015; Lavy et al. 2015; Gutierrez-Heredia et al. 2016). Only recently, the application of this technique at reef scale received wider attention, being a still open and challenging issue (Friedman et al. 2012; Williams et al. 2012; Figueira et al. 2015; Leon et al. 2015; Ferrari et al. 2016; Guo et al. 2016).

When talking about conservation and monitoring, the analyses of topographic features are needed to investigate structural complexity, which can fill the gap in understanding the dynamics driving biodiversity, function and resilience of coral reefs (Ferrari et al. 2016). So, three-dimensionality is essential to realistically describe the reef structure (Fisher et al. 2007; Burns et al. 2015). Rugosity can be considered one of the best descriptor of structural complexity (Knudby and LeDrew 2007). Currently, on-field methods are widely applied in marine ecological studies. The most common one is the 'chain-and-tape' method (Knudby and LeDrew 2007), where the ratio between the linear distance and the contour of the benthos under the chain is calculated as a measure of structural complexity. However, such sampling technique is time consuming and requires multiple chains of different size to be efficient at different spatial scales. Moreover, chains can easily tangle with reef organisms and damage them (Dustan et al. 2013). Technology comes to help, allowing the digital estimation of such parameter. Digital Surface Models (DSM) and Digital Terrain Models (DTM) provide the basic three-dimensional products and recent studies demonstrated their efficacy (Figueira et al. 2015; Leon et al. 2015; Ferrari et al. 2016; Storlazzi et al. 2016). A DSM is an elevation model that includes the tops of any objects, while the DTM is a bare-earth elevation model.

In addition to rugosity, taxonomical identification (Done 1982) and estimate of live coral cover (Jokiel et al. 2015) concur in integrating the assessment of reef biodiversity and structural complexity. Although the taxonomical details are not retrievable from SfM, digital modelling offers different

approaches that may provide feasible alternatives, able to improve the set of information for assessing reef health status.

The generation of orthophotos provides a wide overview of the study area, which could be used as a preliminary instrument for the visual analysis of the seabed coverage.

From an accurate photointerpretation, a trained observer can retrieve information on the abundance of the different coral morphologies. Such morphological classification can then be coupled with an ecological approach, aimed to the evaluation of the conservation status of the reef: each morphology corresponds to one of three different adaptive strategies, corresponding to the vertices of a ternary diagram in which the abundances can be plotted (Edinger and Risk 2000). So, products derived from SfM analysis can provide information of ecological relevance with two main advantages: on one hand, the critical issues of taxonomic identification are avoided; on the other hand, there is integration between coral biodiversity and the estimate of live coral cover.

The main aim of this study is to explore how underwater photogrammetric techniques and derived products (i.e. DTMs, DSMs and orthomosaics) can show the complexity and heterogeneity of the underwater marine habitat. In particular, the novelty of this study is to integrate DTMs and DSMs for assessing the height of coral colonies and for discriminating between seabed and coral cover, in order to compute their areal extent. This approach leads to the generation of meaningful data, which may support marine biologists' in characterizing and monitoring marine habitat.

For the first time, these techniques were applied to coral reefs belonging to an extremely relevant but still unexplored area: the Myeik Archipelago, Myanmar. More in detail, we focused on two representative bays located in Lampi Marine National Park (LMNP) (Figure 1), which differ in coral status, and we demonstrated the use of underwater photogrammetry as an innovative tool for characterizing coral reef.

Materials and methods

Study Area

LMNP was designated in 1996 and includes a group of islands belonging to the Myeik Archipelago in the Tanintharyi region of southern Myanmar (Figure 1). The park protects evergreen and mangrove forests, beaches and dunes, coral reefs, seagrass and a rich biodiversity, with over 1000 recorded species. It also supports the living of about 3000 people in 5 settlements. Despite coral reefs in Rakhine and Tanintharyi Regions, in particular offshore islands of Myeik Archipelago, are the most extensive and diverse in Myanmar, the species diversity and health of this ecosystem were largely unexplored and thus poorly known until recently (Wongthong et al. 2015). The prolonged isolation of north Andaman reefs is conducive to speciation, therefore, the likelihood of endemism amongst corals is high (Brown 2007). In addition, Myanmar, and particularly the Myeik Archipelago, is threatened by the increasing illegal human activities (Wongthong et al. 2015). Population growth in the adjacent areas causes corresponding increase in the use of natural resources to satisfy the growing human needs. Unfortunately, such exploitation takes the form of illegal hunting, illegal fishing, overharvesting of marine flora and fauna (including sea cucumbers, sea shells, etc.) and illegal logging for house and boat construction. Marine habitats in the archipelago are particularly damaged by blast fishing and trawlers, which are dramatically damaging the coral reefs inside and outside the Park.

Lampi (N 10°50′, E 98°12′) is the largest island (205 km2) and represents the core of the park. It is 48 km long and hilly (150–270 m asl), with both rocky coastline and sandy beaches. The sea depth between LMNP and the mainland is on average 12 m and nowhere deeper than 24 m (Oikos 2014).

Due to anthropogenic impact, the reef conservation status is highly heterogeneous across Lampi island. In particular, healthier reefs can be found in the north more than in the southern part: the combination of the 2010 bleaching event and relentless destructive fishing have seriously affected the southern reefs (BOBLME 2015), so we chose two areas capable of outlining such opposite conditions. On one hand, ‘Site 1’ represents a well-preserved area, with a high coral biodiversity. The complexity of the reef increases with depth. The first part of the transect, the shallowest, is dominated by branching corals and small massive colonies. The increase in depth and the reduction of sediment deposition leads to the dominance of a variety of growth forms. In the deepest part of the transect huge Porites colonies, small branching, tabular and mushroom corals are inserted in a complex and extensive framework of living corals. On the other hand, ‘Site 2’ represents a highly degraded area, where habitat complexity is lost and almost all corals are dead and covered by algae. This site is poorly populated with few growth forms. The corals biodiversity is low, just some Porites sp. and

Heliopora coeruela are alive. The seabed is covered by coral rubbles and algae turf. Algae cover the surface of recently dead massive corals too.

Underwater filming

Images of the two different bays (Figure 1) have been collected through underwater videos, which have been realized during a spring campaign in 2016 lasted from the 16th to the 26th of March.

The device used for the image collection is an Olympus Digital Camera, model TG-4, with an acquisition rate of 30 frames/second and a focal length of 4.5–18 mm (35 mm equivalent). The filmed areas consisted of transects or quadrats, whose geographic position and perimeter were defined by buoys, which served as ground control points (GCPs). The filming has been performed by snorkelling. The camera has been assembled on a floating wooden board, which permitted to maintain the device at the water surface level (Figure 2). GPS positioning with field notes and photographs/video of submerged habitats, coral health and bottom depth were also collected. For geolocation, we used a Garmin eTrex10. The device is equipped with the WAAS (Wide Area Augmentation System) system, thus providing position with an associated error of less than 3 m.

DSM, DTM and orthophoto generation

The extracted and processed with Agisoft PhotoScan (version 1.2.6), a stand-alone software product that performs photogrammetric processing of digital images and generates 3D spatial data (Agisoft LLC 2011; Leon et al. 2015).

Once photos were loaded, they were grouped in blocks (chunks) as they were too numerous. A subsequent inspection was then required for removing blurred images and photos with unrelated elements (e.g. bubbles, parts of bodies). Then, image quality was estimated and pictures with a low-quality value (<0.5) have been discarded.

The resulting 3D model was georeferenced by assigning geographic coordinates (X, Y) and elevation values (Z) to the buoys reproduced in the model, with Agisoft providing a scaling accuracy of 0.005 m. Photoscan requires at least three GCPs to perform georeferencing, so the manual insertion of extra points was performed where necessary. For extra points, X, Y values were obtained from a GIS base map and Z values from a bathymetric chart of the island. Table 1 summarizes the parameters applied for the image processing.

The processing chain led to the generation of a DSM and an orthomosaic for each area. The very high-resolution orthophoto (pixel size 1.6 mm) was subsequently used for the morphological description of coral colonies. In addition, the DTM was also obtained by editing and interpolating the dense point cloud: points corresponding to the seabed were classified as ‘Ground’, in order to

distinguish them from the rest of the cloud. Unlike the DSM, which does not discern between the seabed and the top of coral colonies, the DTM represented the elevation of the seabed.

Computation of coral metrics

Basing on both the DSM and DTM models, three different coral metrics related to habitat complexity were retrieved using digital image processing and GIS techniques:

(i) Coral morphologies
(ii) Reef properties: topography and coral cover
(iii) Structural complexity

These metrics were selected because they can be accurately derived from DSM and DTM models and provide useful information about reef conservation status (Edinger and Risk 2000; Burns et al. 2015; Figueira et al. 2015).

Characterization of coral morphologies

A visual classification of coral morphologies (massive, branching, plate like/tabular, foliaceous/laminar, free living, columnar) was initially performed on the whole area: each coral colony reproduced in the orthophoto was assigned to a specific growing morphology.

Then, based on the assumption that coral morphologies can be associated with adaptive strategies, each colony was assigned to one of the three groups defined according to the r-K-S ternary diagram proposed by Edinger and Risk (2000) and firstly proposed by Grime for land plant (Grime 1977):

(i) Ruderals (R): pioneer organisms with high grow and mortality rates, which rapidly colonize the environment.
(ii) Competitors (K): Competitors are species that thrive in areas of low intensity stress and disturbance and excel in biological competition. Competitors do this through a combination of favourable characteristics, including rapid growth rate.
(iii) Stress tolerators (S): slow-growing organisms that are able to survive the environmental stresses. They generally respond to environmental stresses through physiological variability.

The percentage cover of each morphological category was calculated and summed to the other percentages belonging to the same adaptive strategy, in order to calculate X and Y values for plotting the bays into the diagram.

Inferring reef properties

The DSM and the DTM contain useful information about the three-dimensionality of the reproduced areas, which allowed exploring other descriptors of habitat heterogeneity such as topography and coral extension. For both the reference sites, the two raster layers were compared along arbitrary transects in order to describe the seabed topography.

Slope is one of the main metrics related to the seabed topography and average values for the two sites were computed from slope maps derived from the DTM.

The DSM and DTM were also used to detect coral colonies and map their areal extent, based on their height on the seabed. We produced a raster layer describing the height of coral colonies, by subtracting the values of the DSM (elevation of the top of the coral colonies) to the ones of the DTM (elevation of the seabed, alias the base of the colonies). The resulting raster was classified in 'seabed' and 'coral colonies' by defining an elevation threshold of 0.05 m: pixels with elevation values smaller than 0.05 m were assigned to the 'seabed' class, otherwise to the class 'coral colonies'. A threshold of 0.05 m was selected to include sand, small bumps of the seabed and coral rubbles.

Mapping reef structural complexity

Reef structural complexity was computed as the ratio between 3D and 2D areas, in accordance with previous studies (Burns et al. 2015; Figueira et al. 2015). For both the reference sites, we estimated an average rugosity for the whole extent and a 'local' rugosity, in order to detect variations across the reef. In the second case, the DSM of the areas was split into three sectors from shallow waters close to the shore to the deeper areas: shallow, intermediate and deep, then an area of 25 m2 was considered for each sector.

Results and discussion

Bays overview and processed data

Given the large number of pictures, frames were grouped in blocks (chunks) and the models (DSM and DTM) were obtained by merging the partial reconstructions. Where edges were clearly unrepresentative because of errors in the projection or insufficient overlapping between cameras, they were cut. Tables 2 and 3 sum up details from the processing report generated with Photoscan.

Site 1 (health bay) resulted in a straight transect of about 50 m in length and 375 m2 in extent, spreading from the near-shore to the reef top. Site 2 (degraded bay) consisted of an area of about 352 m2 delimitated by four buoys. The gap in the reef status is well shown in the derived orthophotos: in site 1 coral reefs show large biodiversity, high structural complexity and coral colonies occupy all the available spaces; rugosity is high, especially in the deepest area, and the presence of algae and coral rubble is marginal. Conversely, site 2 showed a significant reduction in biodiversity and structural complexity, with coral colonies in a visible state of sufferance or dead and coral rubble covering the seabed. Columnar and ruderal corals are dominant and the algal turf is abundant.

A three-dimensional representation of the DSMs is shown in Figure 3. We used the same colour ramp with fixed intervals to make the topography represented in the two digital models comparable. For site 1, minimum and maximum depth was, respectively, −0.19 and −6.23 m; for site 2 was −2.5 and −5.3 m. The comparison between the two models highlighted a difference in the average depth: –2.64 m in site 1 and −3.95 m in site 2. Such difference in depth increases if considering the modal values shown in the histograms in Figure 3; in particular, for site 2, we noticed that modal values exceed the average depth, setting a gap of almost 2 m in depth with site 1.

During the survey, we noticed a different structure of the seabed in the two bays and the Digital Models are in line with such observation: in site 1 there is a wide back-reef area with remarkably shallow waters (which is visible from satellite images too), beyond which waters get deep fast and denote a net, rapid change in the slope of the seabed; in site 2 the backreef area is not well delimited and depth values are more homogeneous across the site.

Although an assessment of the absolute accuracy of the two models was not possible due to the lack of true reference model against which to compare those generated from photogrammetry approaches, there is a general accordance between the digital products and the on-field observations, demonstrating the reliability of the approach. Recent studies also demonstrated that a good relative accuracy (few millimetres) is achievable in 3D models reconstructed in both air and water using a

camera similar to the one employed in this study. Although accuracy in air resulted higher than in water, both results were acceptable (Guo et al. 2016).

It is reasonable to think that the accuracy of the model could have been affected by four main critical issues which emerged during the filming:

(i) oscillation of the camera because of waves, leading to sudden changes in the shot and, consequently, blurred frames;
(ii) the maintenance of the swimming trajectory in order to allow a partial overlapping while filming on the way to and the way back;
(iii) the formation of condensation and bubbles in front of the lenses, which hide part of the scene, lower the frame quality and affect the correct alignment of the frames;
(iv) low visibility because of water turbidity. In case of abundant resuspension of sediments, the seabed is not clearly visible.

Morphological analysis

The visual classification brought to the quantification of the abundance of both coral morphologies (Table 4) and rKS groups (Table 5). Massive morphologies, considered as stress tolerators, were dominant in site 1, representing more than 40% of coral cover. At a larger scale, the same dominance was noticed by Fauna and Flora International during a fast reef check survey of the Myeik archipelago (Wongthong et al. 2015). The abundance of rKS groups represents the data-set used to plot the sites in the ternary diagram (Figure 4). As a result, the estimated conservation quality for site 1 is good (CC = 4), while it's lower for site 2 (CC = 3). The quantification of dead coral cover would have improved the analysis, widening the difference in the conservation quality between the two bays.

Topography and coral cover

The use of transects concurs in providing a general overview of the reference areas. In particular, the degradation of the seabed, the increase in depth and the progressive increase in height and size of coral colonies (the latter for site 1) can be appreciated by shifting from point A to point B (Figure 5). Regarding slope, average values of 22 and 16 degrees, were computed, respectively, for site 1 and site 2.

Figure 6 shows the classification in 'seabed' and 'coral colonies' of the two sites, based on the difference between DSM and DTM. For site 1, coral colonies occupy an area of 183.7 m2, corresponding to about the 49% of the whole area. For site 2, coral extends for 199 m2 and covers an area of about 53%. The estimate for site 1 results in accordance with the estimation of hard coral

cover in Lampi Island provided by Fauna and Flora International, which indicated a percentage of 40–60%.

Such result provides a preliminary mapping of coral cover and could be used as basic information for fieldworks. Then, it can be integrated by trained biologists able to assess whether a colony is dead or alive. It is clear that the latter step is essential for the assessment of the conservation status: the coral cover is almost the same, but site 2 is highly impacted and most of the colonies are dead, so there is a huge gap in the quality of the two habitats.

Reef structural complexity evaluation

The ratio between the 3D and 2D areas allowed to quantify an abstract concept like the one of complexity and provided a common numerical attribute for making a comparison between the two reference sites. Figure 7 shows the DSMs with the selected areas of 25 m2, which have been highlighted with a different colour ramp.

As expected, for Site 1 local rugosity was higher in correspondence of the deepest area of the reef, where coral colonies are close together, higher and more massive (Table 6); 'shallow' and 'intermediate' areas of site 1 belonged to the backreef area and showed similar values, so they were considered homogeneous.

Site 2 exhibited structural differences compared to bay 1. Coral colonies were in fact more scattered and no remarkable differences in the 'local' rugosity were appreciated among the three sectors (Table 7). In ecology, structural complexity is a key factor positively related to biodiversity and carrying capacity of habitats (Yanovski et al. 2017). The overall higher rugosity values in site 1 compared to site 2 thus confirmed its better health status and degree of conservation.

Such observations were supported by the visual analysis of the orthophotos, which depicted habitats with substantial structural differences: while in site 1 there was a clear gradient from the shallowest part of the reef to the reef top (e.g. increase in colony size, coral colonies density), site 2 appeared more homogeneous. Such gap between the two bays may be related to hydrodynamics: in site 1, coral colonies are shallower and may undergo a greater hydrodynamism, especially on the top of the reef where waves break, while in site 2 coral colonies are deeper and grow in a lower energy environment. Indeed, the overall estimated rugosity was very similar to the estimated rugosity in the backreef area of site 1, which represents a low-energy environment too. This consideration is supported by other studies, which demonstrated the fact that corals can benefit from increased currents: high densities of living corals were found in areas of enhanced currents, with living colonies abundant at the summit where current speed were highest also in other study areas (Dorschel et al. 2007; Lenihan et al. 2014).

Conclusions

The underwater world represents a present-day topic, especially when talking about delicate ecosystems like coral reefs, which are terribly suffering the effects of climate change and anthropic stress. For this reason, it is also a fascinating challenge for scientific research and remote sensing techniques represent a source of solutions, continuously in progress, for supporting the efforts of marine biologists.

In this study, we demonstrated the potential of Structure from Motion techniques and GIS tools for retrieving basic information and coral metrics for the support of marine conservation plans in two bays characterized by different health conditions. In particular, we introduced the use of three-dimensional products like DSM and DTM not only for describing the seabed topography and structural complexity but also for assessing coral colony extent and heights.

The relatively simplicity of this workflow encourages its repeatability and permits non-specialists to learn photogrammetry for coral monitoring, opening the possibility for local inhabitants to perform their own surveys and make their datasets accessible for coral researchers (Gutierrez-Heredia et al. 2016).

From a remote sensing perspective, these data will help to monitor coral processes by combining bathymetric maps and spectral information from satellite data, to generate time series and a useful tool for pursuing management strategies in the context of sustainable development and produce a satellite derived nautical chart of the area using physics-based model inversion.

Some future desirable developments are the setting up of a method of validation with ground data and the improvement of coral extension assessment as regards the discrimination of dead colonies and the digital classification of corals genera based on their morphology.

While ecological and biological knowledges can be still integrated and supported by technology, computer vision sciences may widen the frontiers of image classification (Varma and Zisserman 2005), improving the chances for technology to permeate and support the world of habitat mapping.

References

Agisoft LLC. 2011. Agisoft PhotoScan User Manual – Professional Edition, Version 1.0.0.

BOBLME. 2015. Report of the national technical workshop on the conservation strategy for the Myeik Archipelago. Dawei, Myanmar, February 27, 2015. BOBLME-2015-Ecology-41.

Brown BE. 2007. Coral reefs of the andaman sea – an integrated perspective. Oceanogr Mar Biol an Annu Rev. 45:173–194.

Burns JHR, Delparte D, Gates RD, Takabayashi M. 2015. Utilizing underwater three-dimensional modeling to enhance ecological and biological studies of coral reefs. ISPRS – International Archives of the Photogrammetry, Remote Sensing and Spatial Information Sciences. 40:61–66.

Bythell J, Pan P, Lee J. 2001. Three-dimensional morphometric measurements of reef corals using underwater photogrammetry techniques. Coral Reefs. 20:193–199.

Cocito S, Sgorbini S, Peirano A, Valle M. 2003. 3-D reconstruction of biological objects using underwater video technique and image processing. J Exp Mar Bio Ecol. 297:57–70.

Colomina I, Molina P. 2014. Unmanned aerial systems for photogrammetry and remote sensing: a review. ISPRS J Photogramm Remote Sens. 92:79–97.

Courtney LA, Fisher WS, Raimondo S, Oliver LM, Davis WP. 2007. Estimating 3-dimensional colony surface area of field corals. J Exp Mar Bio Ecol. 351:234–242.

Done TJ. 1982. Patterns in the distribution of coral communities across the central Great Barrier Reef. Coral Reefs. 1:95–107.

Dorschel B, Hebbeln D, Foubert A, White M, Wheeler AJ. 2007. Hydrodynamics and cold-water coral facies distribution related to recent sedimentary processes at Galway Mound west of Ireland. Mar Geol. 244:184–195.

Dustan P, Doherty O, Pardede S. 2013. Digital reef rugosity estimates coral reef habitat complexity. PLoS One. 8:1–10.

Edinger EN, Risk MJ. 2000. Reef classification by coral morphology predicts coral reef conservation value. Biol Conserv. 92:1–13.

Ferrari R, McKinnon D, He H, Smith RN, Corke P, González-Rivero M, Mumby PJ, Upcroft B. 2016. Quantifying multiscale habitat structural complexity: a cost-effective framework for underwater 3D modelling. Remote Sens. 8:113.

Figueira W, Ferrari R, Weatherby E, Porter A, Hawes S, Byrne M. 2015. Accuracy and precision of habitat structural complexity metrics derived from underwater photogrammetry. Remote Sens. 7:16883–16900.

Fisher WS, Davis WP, Quarles RL, Patrick J, Campbell JG, Harris PS, Hemmer BL, Parsons M. 2007. Characterizing coral condition using estimates of three-dimensional colony surface area. Environ Monit Assess. 125:347–360.

Fonstad MA, Dietrich JT, Courville BC, Jensen JL, Carbonneau PE. 2013. Topographic structure from motion: a new development in photogrammetric measurement. Earth Surf Process Landforms. 38:421–430.

Friedman A, Pizarro O, Williams SB, Johnson-Roberson M. 2012. Multi-scale measures of rugosity, slope and aspect from benthic stereo image reconstructions. PLoS One. 7(12).

Gonçalves JA, Henriques R. 2015. UAV photogrammetry for topographic monitoring of coastal areas. ISPRS J Photogramm Remote Sens. 104:101–111.

Grime JP. 1977. Evidence for the existence of three primary strategies in plants and its relevance to ecological and evolutionary theory. Am Nat. 111:1169–1194.

Guo T, Capra A, Troyer M, Gruen A, Brooks AJ, Hench JL, Schmitt RJ, Holbrook SJ, Dubbini M. 2016. Accuracy assessment of underwater photogrammetric three dimensional modelling for coral reefs. Int Arch Photogramm Remote Sens Spat Inf Sci. 41:821–828.

Gutierrez-Heredia L, Benzoni F, Murphy E, Reynaud EG. 2016. End to end digitisation and analysis of three-dimensional coral models, from communities to corallites. PLoS One. 11(12).

Hedley JD, Roelfsema CM, Phinn SR, Mumby PJ. 2012. Environmental and sensor limitations in optical remote sensing of coral reefs: Implications for monitoring and sensor design. Remote Sens. 4:271–302.

Hedley JD, Roelfsema CM, Chollett I, Harborne AR, Heron SF, Weeks SJ, Skirving WJ, Strong AE, Mark Eakin C, Christensen TRL, et al. 2016. Remote sensing of coral reefs for monitoring and management: a review. Remote Sens. 8:118.

Hochberg EJ, Atkinson MJ, Andréfouët S. 2003. Spectral reflectance of coral reef bottom-types worldwide and implications for coral reef remote sensing. Remote Sens Environ. 85:159–173.

Javernick L, Brasington J, Caruso B. 2014. Modeling the topography of shallow braided rivers using Structure-from-Motion photogrammetry. Geomorphology. 213:166–182.

Jokiel PL, Rodgers KS, Brown EK, Kenyon JC, Aeby GS, Smith WR, Farrell F. 2015. Comparison of methods used to estimate coral cover in the Hawaiian Islands. Program. 3:1–22.

Joyce KE, Phinn SR. 2013. Spectral index development for mapping live coral cover. J Appl Remote Sens. 7(073590):1–20.

Joyce KE, Phinn SR, Roelfsema CM. 2013. Live coral cover index testing and application with hyperspectral airborne image data. Remote Sens. 5:6116–6137.

Knudby A, LeDrew E. 2007. Measuring Structural Complexity on Coral Reefs. Proc Am Acadamy Underw Sci 26th Symp. 181–188.

Knudby A, LeDrew E, Newman C. 2007. Progress in the use of remote sensing for coral reef biodiversity studies. Prog Phys Geogr. 31:421–434.

Tables and Figures

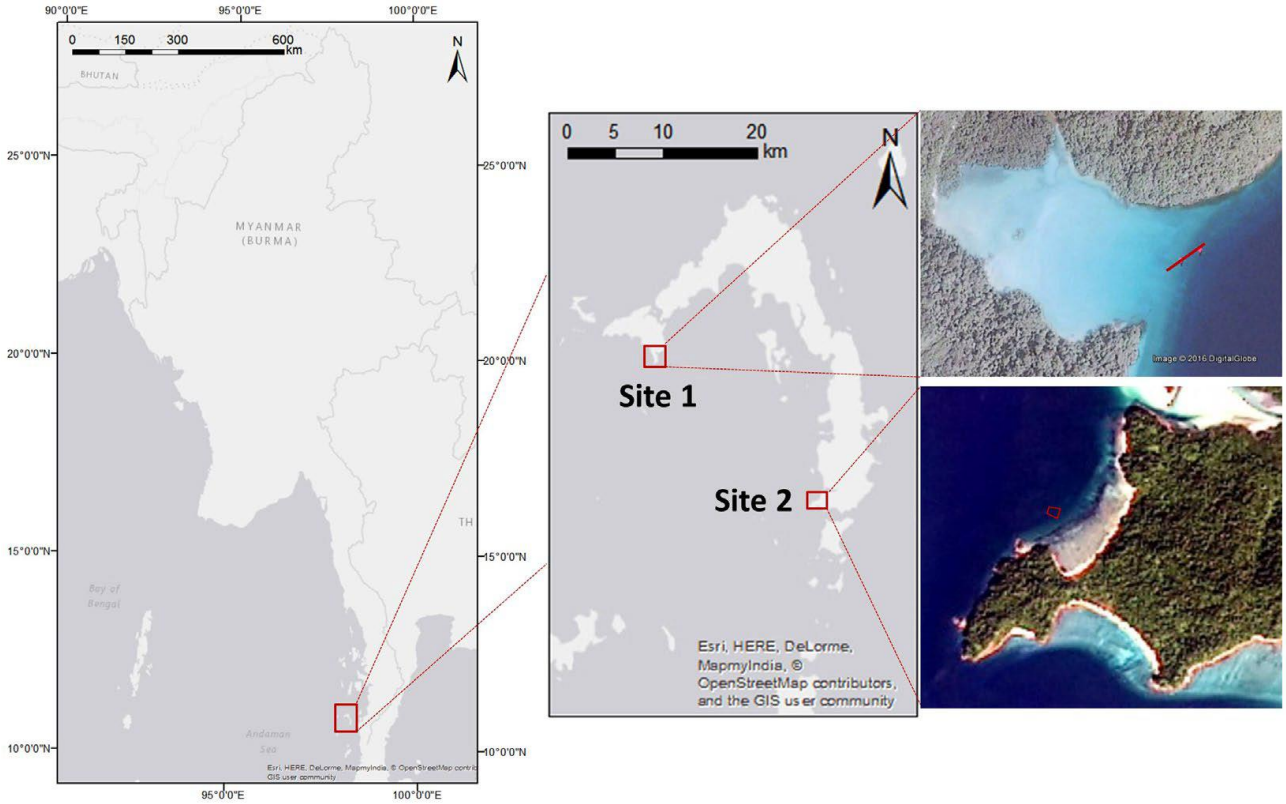

Figure 1. location of the study area: from a general view of Myanmar to Lampi Island, with a focus on the two bays used as case study.

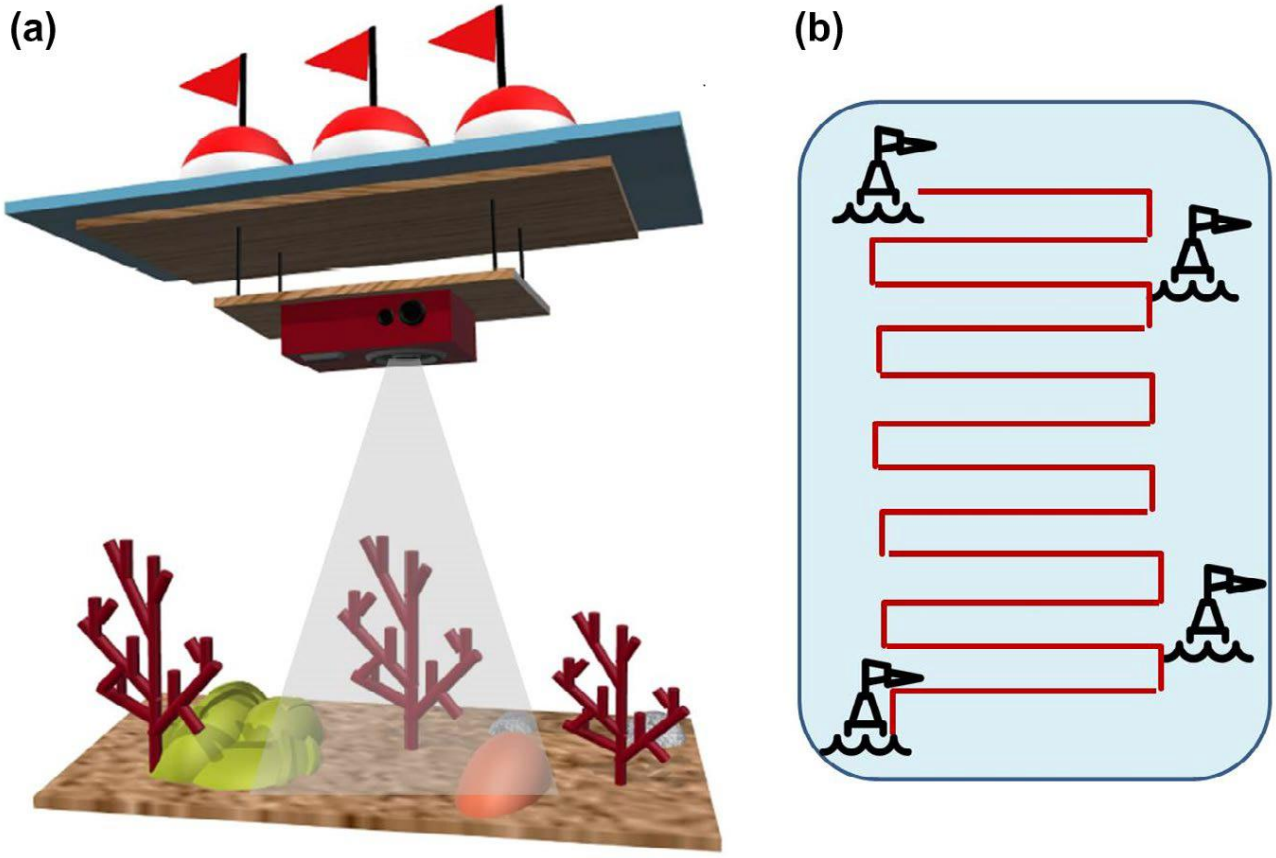

Figure 2. Illustration of the assembled filming device (a) and sampling scheme (b).

Table 1. Processing parameters for Site 1 and Site 2.

Alignment	Quality: medium-highest
Dense point cloud	Quality: medium
	Depth filtering: aggressive
Mesh	Surface type: arbitrary
	Interpolation: enabled
	Geometry type: point cloud
Texturing	Mapping mode: generic
	Blending mode: mosaic
DSM	Coordinate system: WGS84/UTM zone 47 N
	Source data: point cloud
	Interpolation: enabled
Orthomosaic	Coordinate system: WGS84/UTM zone 47 N
	Surface: mesh

Table 2. Image processing output data

	Site 1	Site 2
Aligned cameras	1,243	1,742
Tie points	346,408	402,296
Markers	71	65
Projections	1,221,514	1,455,583
Reprojection error	1.72 pix	1.65 pix

Table 3. Digital Surface Model data

	Site 1	Site 2
Resolution	6.61 mm/pix	8.6 mm/pix
Point density	2.29 points/cm^2	1.35 points/cm^2
Coverage area	378 m^2	357 m^2

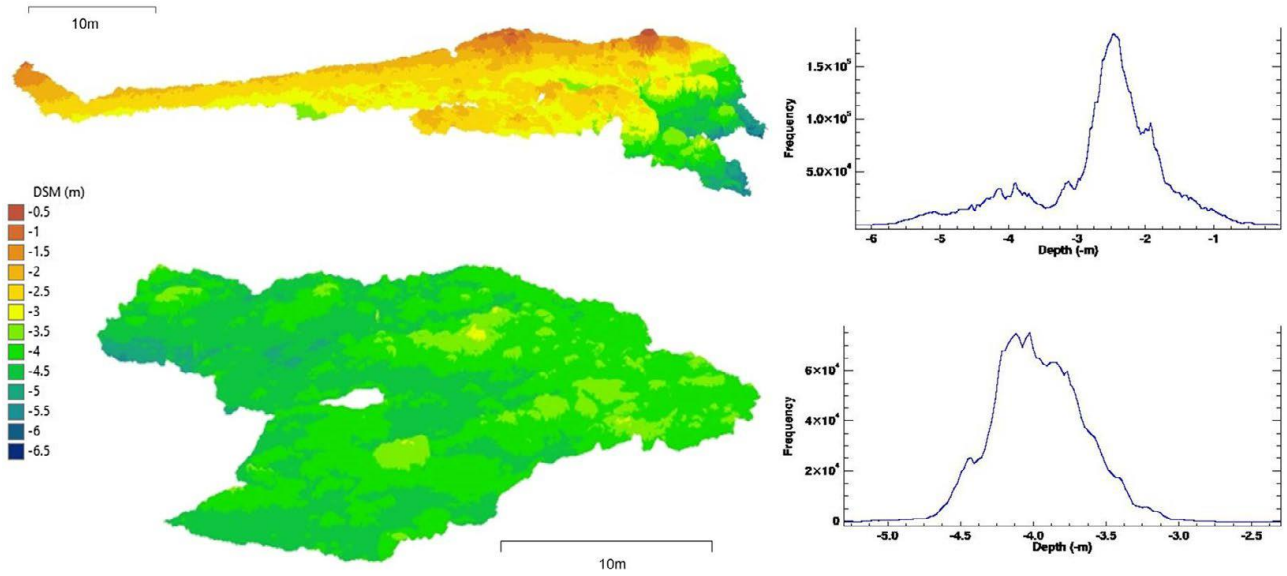

Figure 3. DSMs of sites 1 (above) and 2 (below), with related histograms showing the frequency of depth values. note: the three-dimensional representation enhances the topography of the seabed.

Table 4. Abundance of coral morphologies for sites 1 and 2.

Morphology	rKS group	Site 1 q.ty (%)	Site 2 q.ty (%)
Massive	S	67 (44.4%)	8 (19.1%)
Branching	r	19 (12.6%)	–
Plate like/tabular	r	18 (11.9%)	–
Foliaceous/laminar	r	28 (18.5%)	1 (2.4%)
Free living	K	16 (10.6%)	9 (21.4%)
Columnar	r	3 (2%)	24 (57.1%)
TOT		151	42

Note: Quantities are expressed as the number of counted coral colonies.

Table 5. Abundance of rKS groups for sites 1 and 2.

	Site 1	%	Site 2	%
r	68	45.03	25	59.52
K	16	10.60	9	21.43
S	67	44.37	8	19.05

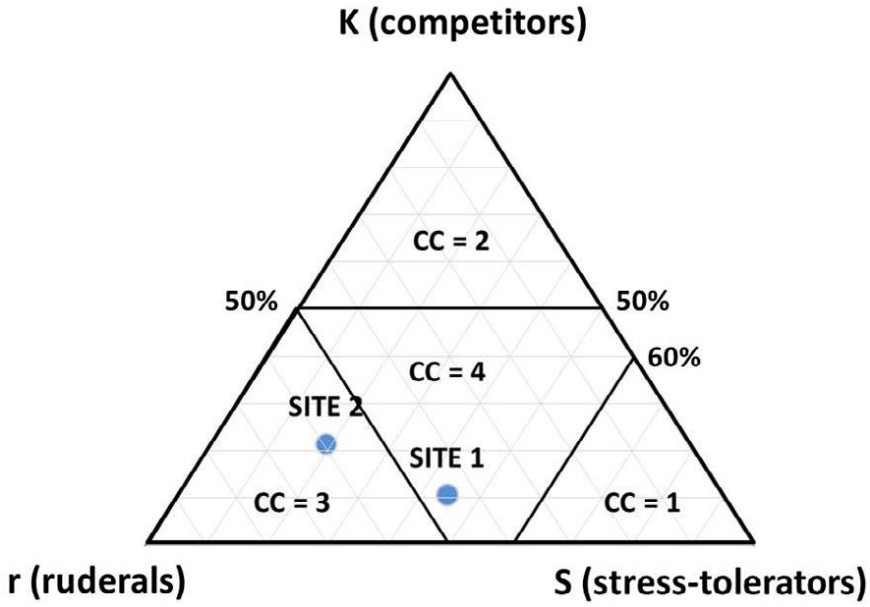

Figure 4 ternary diagram defining the conservation value (cc) for both the reference sites.

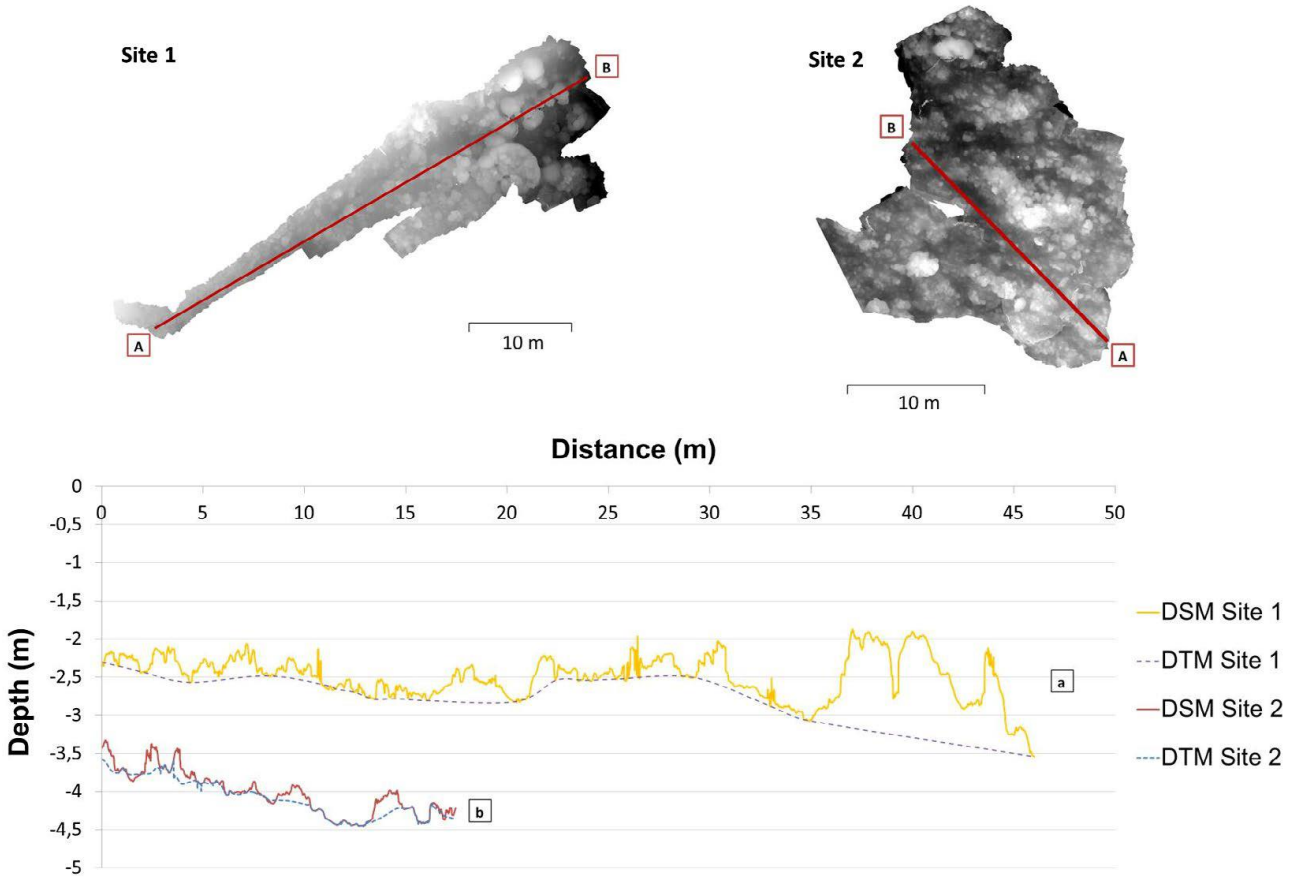

Figure 5. Transects for sites 1 and 2 and corresponding profiles (a and b, respectively).

Notes: the solid lines display the profiles of the top of the coral colonies (DSM), while the dashed blue lines delineate the depth of the bottom (DTM). the greater the distance from the shore, the deeper the seabed.

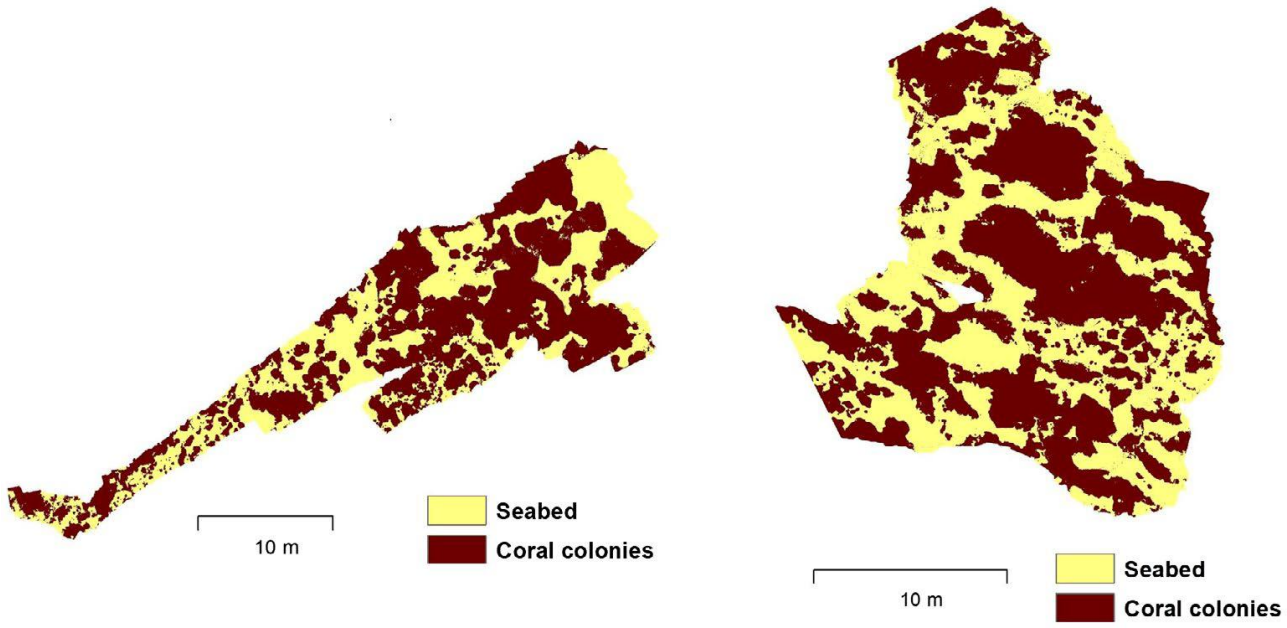

Figure 6. Seabed classification

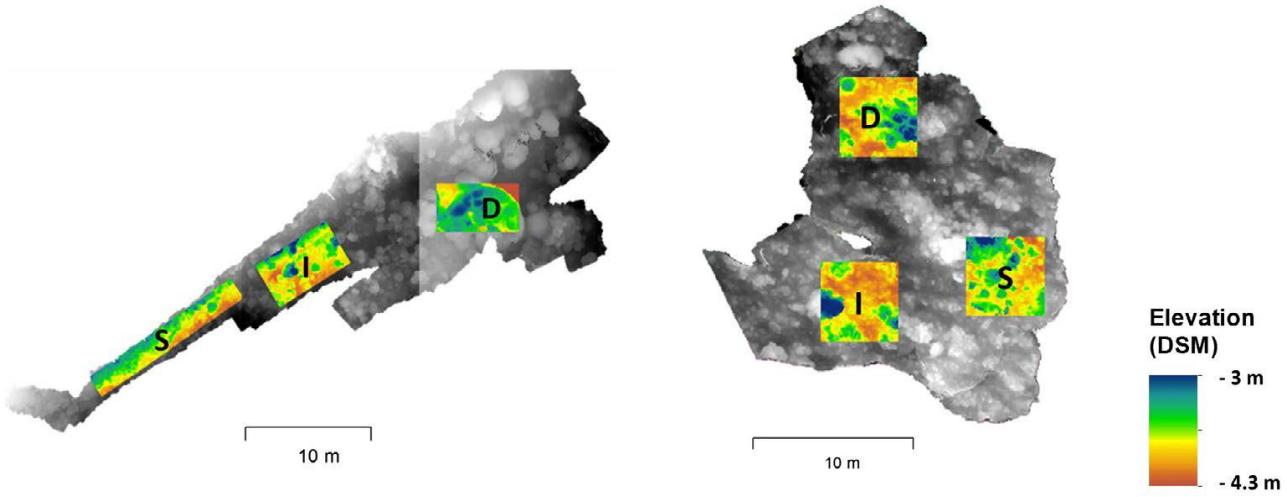

Figure 7. Sectors of 25 m2 defined on the DSM and used for measuring local rugosity in site 1 and 2. note: S = shallow; I = intermediate; D = deep.

Table 6. Estimated rugosity for site 1

Site 1	2D area (m^2)	3D area (m^2)	3D/2D
Whole area	375.058	731.198	1.95
Shallow	25	44.32	1.77
Intermediate	25	39.3	1.57
Deep	25	58.42	2.33

Notes: The average rugosity is 1.95, if considering the sectors the highest rugosity (so the highest habitat complexity) corresponds to the reef crest.

Table 7.Estimated rugosity for site 2

Site 2	2D area (m^2)	3D area (m^2)	3D/2D
Whole area	352.1	641.16	1.82
Shallow	25	45.45	1.81
Intermediate	25	40.12	1.60
Deep	25	41.23	1.64

Notes: The average rugosity is 1.82, the absence of remarkable differences among sectors suggested a more homogenous area compared to site 1.

3.2

Marchese F., Savini A., **Fallati L.**, Corselli C., Galli P. (2019). Integrating acoustic depth measurements and photogrammetry-based 3D point clouds for the generation of a continuous digital terrain model in coral reef environments. IMEKO International Workshop on Metrology for the Sea (MetroSea 2019), Genova 3-5 October 2019 (*Conference Paper*)

Integrating acoustic depth measurements and photogrammetry-based 3D point clouds for the generation of a continuous digital terrain model in coral reef environments

Fabio Marchese[1], Alessandra Savini[1,2], Luca Fallati[1,2], Cesare Corselli[1], Paolo Galli[1,2]

1 Department of Earth and Environmental Sciences (DISAT), University of Milano-Bicocca, P.za della Scienza 1, Milano, Italy

2 MaRHE center, Magoodhoo, Faafu Atoll, Republic of Maldives

Abstract

Our work presents a tested methodological protocol for the generation of a fine-scale digital terrain model (DTM) in coral reef environments. A portion of an atoll reef (namely the Magoodhoo reef located in the Maldivian archipelago, the southern part of Faafu atoll) has been remotely mapped from the reef flat area to the connected and deeper lagoon environment, collecting elevation data by different sources according to the surveyed depths. In particular we acquired acoustic depth measurements using a multibeam echosounder (MBES) and 3D point clouds applying the Structure from Motion (SfM) technique to RGB images, collected using an Unmanned Aerial Vehicle (UAV). All obtained data were calibrated and validated with RTK-GNSS measurements and successfully integrated in order to generate a harmonized DTM for the surveyed sector of the Magoodhoo reef.

Introduction

Until no more than a decade ago, geomorphological mapping in coral reef environments was carried out using satellite data ground-truthed by field studies, and focused on the investigation of the recent evolution of basically the shallow or emerged coral-reef associated landforms. Mainly because of their complex topography and the considerable extension of very shallow areas (i.e. reef flat areas), traditional mapping methods lacked, in most of the cases a continuous 3-dimensional representation of coral reef landforms at high resolution, across all their extension, with the deeper lagoon regions included. Nevertheless, as for all coastal landforms, the knowledge of the fine-scale submerged topography (and derived terrain parameters) is instrumental for a better understanding of geomorphological changes and for proposing in turn informed management measures.

The present-day most advanced techniques used to collect high resolution elevation data and multi-spectral imagery – both for land surface and the seafloor – in coral reef environments, span from traditional acoustic mapping (multibeam echosounder bathymetry and backscatter) to the use of satellite-derived bathymetry, LIDAR technology, Unmanned Aerial Vehicles (UAV - equipped with RGB cameras and additional innovative sensors) coupled with photogrammetry and traditional topographic surveys (which although they provide only point data, are instrumental for remote data calibration and validation). Data processing represents in all the cases a fundamental step for ensuring accuracy and reliability of obtained measurements, especially for allowing a precise integration of all data sources into a continuous digital terrain model (DTM).

In our work a harmonised DTM is generated for the Magoodhoo reef (southern Faafu Atoll, Republic of Maldives) from multibeam echosounder-based depth measurements, 3D point clouds (obtained applying SfM technique to UAV imagery) and topographic surveys. All employed techniques are presented, and limits in their use are briefly discussed.

Study Area

The surveyed area is a part of an atoll reef of the Republic of Maldives, an archipelago, stretched for 860 km in a North-South direction and formed by a double chain of atolls separated by an Inner Sea (<500 m deep), in the middle of the Indian Ocean. The atolls of the Maldives are very complex structures in form of annular mid-ocean reefs. The reef rim is broad and flat and contains islands in some instances (composed of unlithified or poorly consolidated sand or gravel), or can be a broad reef flat in others. It encloses a central lagoon and is interrupted by major passages that enable

significant water exchange between ocean and lagoon. Maldivian atolls can be formed by heavily dissected atoll reef rim and moderate lagoon depths (40-60 m), with numerous lagoonal patch reefs (with or without islands) and faros (i.e.: central/northern atolls), or by a more continuous atoll reef rim containing extended islands, but deeper lagoons (70-80 m) and few lagoonal patch reefs (i.e.: southern atolls).

Faafu atoll has a sub-circular shape, with a convex side toward west, and is 29 kilometres long from North to South and separated from the northern Ari atoll by the channel known as Ariadhoo Kandu. Few, slightly straight, broad and elongated reefs typify the western side, while more abundant and smaller reefs mark the eastern rim. It forms a perfect semicircle on the east, but its western side is rather indented. There are not many islands. In the interior of its lagoon, there are four islands and several large farus, dry at low tide.

Materials and Methods

Elevation data for the emerged and very shallow areas are derived from SfM techniques application to UAV imagery.

UAV data were collected using a DJI Phantom 4 quadcopter equipped with a 12.4 megapixels camera integrated with a high precision 3-axis gimbal and, with a global navigation satellite system (GPS/GLONASS). Survey routes were planned using DJI Ground Station Pro Software and photos were collected every 2 seconds at 30m fixed altitude with an overlap of 90% along the path and 80% between adjacent routes, at 2 m/s horizontal speed. Data were collected during low tide and dawn daytime to avoid excessive sun glint and with calm wind conditions, to avoid distortions caused by water motion. UAV photos were processed using Agisoft Metashape Pro, following the common workflow for SfM techniques.

In order to reach the maximum accuracy, SfM model was calibrated using 10 Ground Control Points (GPCs) collected with a high-resolution GNSS. Due to the lack of an official GNSS base station network in the Maldivian Archipelago, a local RTK system was prepared using a couple of Emlid Reach RS© in Base-Rover configuration. Emlid Reach RS© single frequency receiver runs with the open-source RTK processing software RTKLIB [1], and they can reach centimetre-level accuracy with the ambiguity parameters resolved. The base station was fixed in the same location every day, collecting satellite data continuously, and it was used as caster on rtk2go service. Rover received our local base correction using NTRIP (Networked Transport of RTCM via Internet Protocol) as client on the same service. Baseline was always less than 10 km.

Bathymetric data were collected using a Teledyne Reson 8125 (455kHz) multibeam echosounder system (MBES). Speed of sound in the water was measured using a Valeport miniSVS for the correction at the sonar head and a Teledyne Reson SVP15 as sound velocity profiler for the water column. Positioning data coming from the Emlid Reach RS rover in RTK mode, NTRIP corrected by rtk2go from our local base station. MBES sonar head was pole-mounted on the dhoni side (typical Maldivian boat) in horizontal and 45-degree inclination configuration, in order to reach the very shallow reef flat zone and to allow the overlap between the UAV SfM point clouds and the MBES model. Bathymetric survey was performed using QPS Qinsy and acoustic data were processed with QPS Qimera software.

After MBES data processing and the generation of 3D point clouds, the work focused on the generation of a unique DTM integrating the two datasets, using the overlapping MBES data as GCPs for the SfM model. SfM technique by itself produce a model of a surface without any measurements, consequently, resulting models are more subjected to deformation called "dome effect" [2, 3, 4]. To reduce this effect and to give a correct spatial location, GCPs and referencing scale were introduced to the model. Since the processing of MBES data includes corrections of tide variations, speed of sound measurements, correct patch test calibration, wobble analysis and TU Delf sound speed inversion, the generated DTM is not affected by deformations and accuracy is high.

Selected depth values obtained from the MBES-based DTM was then used as GCPs to calibrate the UAV-based DTM. The overlap between the two datasets allowed in particular to recognize common and well-defined morphological features, used as a second generation of GCPs for SfM processing. Therefore, we obtained, as a final output of SfM processing, a DTM with a significant reduction of the "dome effect" (thanks to to the additional GCPs), with a calibrated spatial reference.

Results and Discussions

The overall workflow for the generation of a continuous DTM in coral reef environments is shown in Figure 1, further details are given hereunder.

The most accurate data set acquired, in term of elevation measurements, is represented by the bathymetric multibeam surveys, where minimum standards for hydrographic surveys were employed, as reported by the International Hydrographic Organization (IHO 2008). 3D point clouds data obtained by the UAV survey still do not have international standard as reference for defining data accuracy. Nevertheless, our methodology included the selection of calibrated multibeam bathymetric data values as additional GCPs used to calibrate the DTM obtained from the generated UAV-based 3D point clouds. The proposed methodology leads thus to the generation of a continuous DTM

(Figure 2), based on the integration of two datasets, where the more accurate data at lower resolution (i.e.: bathymetric data with a 0.50m grid cell size) drove the calibration of high-resolution photogrammetry-based 3D point clouds.

Conclusions

The workflow proposed for integrating different elevation data sets acquired in coral reef environments appears to be effective insofar as the resulting product is continuous and has a high spatial resolution.

The critical point is represented by the need to develop an effective and standardised technique for improving the accuracy of bathymetric data derived from the UAV-based 3D point clouds. Nevertheless, results proved to be efficient in producing a continuous DTM for coral reef environments, where the main constraint for the final model is related to the resolution. SfM model reaches a cell resolution less than 5cm compared to the 50 cm cell of the MBES model. In order to merge both the model we downgraded the SfM model to 50cm, that in any case still represents a high-resolution DTM for studying geomorphological changes in coral reef environments.

References

[1] T. Takasu RTKLIB: Open Source Program Package for RTK-GPS FOSS4G 2009, Tokyo, Japan (2009)

[2] James, M.R., Robson, S., 2012. Straightforward reconstruction of 3D surfaces and topography with a camera: accuracy and geoscience application. J. Geophys. Res. 117,F03017.

[3] Turner, D., Lucieer, A., Watson, C., 2012. An automated technique for generating georectified mosaics from ultra-high resolution unmanned aerial vehicle (UAV) imagery, based on structure from motion (SfM) Point clouds. Rem. Sens. 4, 1392–1410.

[4] Westoby, M.J., Brasington, J., Glasser, N.F., Hambrey, M.J., Reynolds, J.M., 2012. "Structure-from-Motion" photogrammetry: a low-cost, effective tool for geoscience applications. Geomorphology 179, 300–314.

Figures and Tables

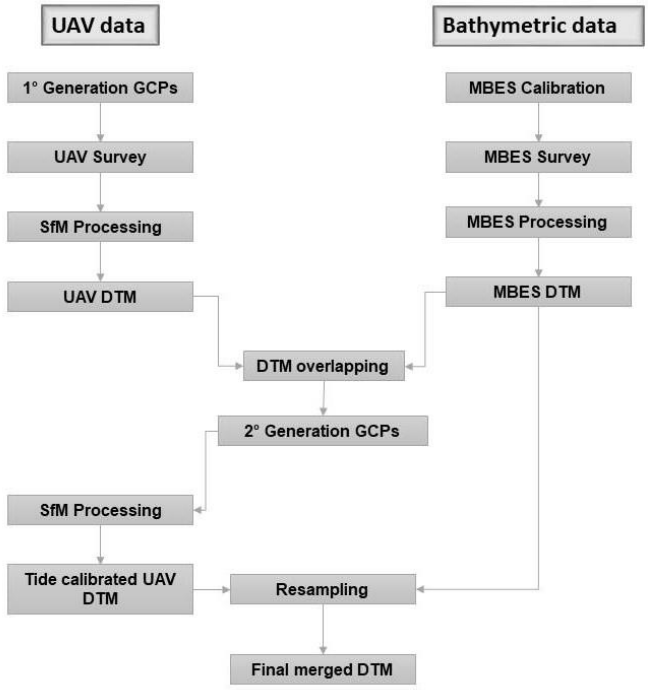

Fig. 1. Workflow for the generation of a continuous DTM, integrating 3D point clouds data acquired by UAV and MBES bathymetric data.

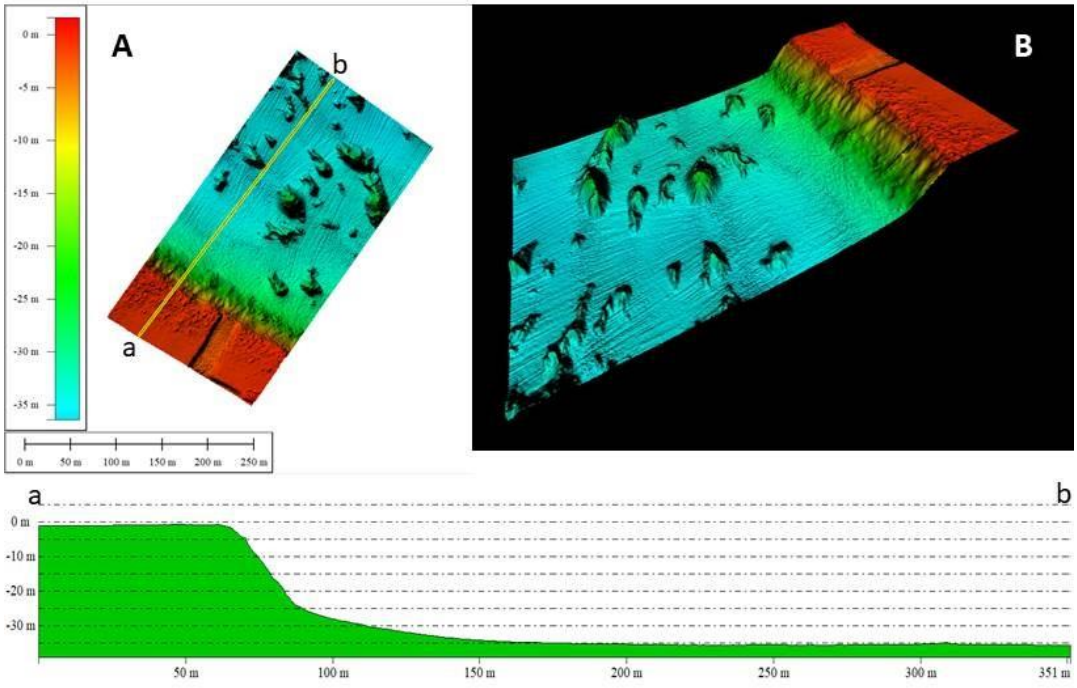

Fig. 2. A: Plot view (A) and 3D view (B) of the continuous DTM, generated from the integration of 3D point clouds data acquired by UAV and MBES bathymetric data.

General Discussion and Conclusion

Climate change and anthropogenic activities are profoundly modifying coastal environments worldwide (Baker et al., 2008; Dolan & Walker, 2006; Fine et al., 2019; Hughes et al., 2019; Pergent et al., 2014). These impacts are affecting some of the most productive ecosystems on Earth, causing habitat loss, fragmentation, contamination and communities shifts (Hughes et al., 2007). The reduction of the recurrence time between these impacts is limiting the recovery and can eliminate the resilience capacity of the habitats (Adger et al., 2005; Jordà et al., 2012; Mcleod et al., 2019). The direct consequences of these degradations process on the population in low-lying and developing countries are concrete and will vary between and within regions (Wong et al., 2014). In fact, coastal and marine ecosystems provide a wide variety of benefits to humans in the form of goods and services, and the relative loss of income is difficult to estimate (Hicks, 2017; Moberg & Folke, 1999; Moberg & Rönnbäck, 2003). Under these prospects for the future, monitoring activities are crucial to identify and quantify anthropogenic or climatic stresses and their effects on coastal environments, highlighting the occurrence of community shift and tracking subsequent recovery or decline over time and space (Malthus & Mumby, 2003; Manfreda et al., 2018).
This doctoral project was focused on proposing efficient and reliable monitoring protocols for collecting and analysing remote sensing data suitable for all coastal regions around the world.

Satellite remote sensing data allowed to collect information on extended areas and the presence of longterm databases facilitate temporal analysis (Ampou et al., 2018; El-Askary, Abd El-Mawla et al., 2014; Were et al., 2013). In **Chapter 1** these imageries were found useful for monitoring processes on large-scale like Land Use and Land Cover Change (LULCC) that, in coastal regions can have a direct impact on marine environments. The land-use and land-cover map produced in this study, together with change analysis, can help to understand the effects of LULCC on coral reefs and the increase in erosion. It can also contribute to the development of sustainable land-use policies for forecasting the impacts of climate change on the islands of the archipelago.
In **Chapter 2** was highlighted the potential of consumer-grade Unmanned Aerial Vehicles (UAV) as powerful low altitude remote-sensing platforms for obtaining synoptic overviews of selected key areas. Above all, the use of UAV allowed to collect data in inaccessible coastal zones. The processing of the images with Structure from Motion (SfM) algorithms allowed obtaining high-resolution orthomosaics, with a centimetric resolution, and Digital Terrain Model (DTM). Innovative processing techniques as Machine Learning (ML) and Object Base Image Analysis (OBIA) were used to elaborate data with several purposes. The UAV data were acquired under different climatic conditions

and geographic regions both over tropical and temperate coastal sea. All the studies collected in this chapter confirmed the potential of the use of a commercial UAV as a fast and reliable survey methodology. Therefore, the protocols developed have proved their worth regardless locations of the tested area.

The article in ***Paragraph 2.1*** described, for the first time, the use of UAV images coupled with SfM and OBIA algorithms to monitor and map changes in coral reefs benthic assemblages following a mass bleaching event (2016). The spatial resolution achieved from the orthomosaics allowed us to classify benthic community types with reasonable accuracy, and the comparison of the maps through time has shown clearly the deterioration of the fore reef environments. Moreover, the maps generated with the described protocols can be used as a starting point for a long term monitoring program to check the dynamics of shallow water assemblages in this new *human-dominated* era.

In ***Paragraphs 2.2*** and ***2.3,*** the same procedures were applied to create a new mapping method for the cartography and the monitoring of littoral assemblages of the Mediterranean, including the key coastal community of Cystorseira forest. The innovative technique of post-processing images from UAV proposed in this study allowed us to compute coastal surfaces covered by the most abundant community assemblages with centimetric accuracy through a relatively low sampling effort, also considering the increased amount of information acquired. Besides, the information coming from orthomosaics and terrain attributes allow detailing characterise the forests and open new scenarios of studies and analysis such as the Index of Cystoseirety (IoC) and the computation of spatial patterns through a seascape ecology approach.

In this research project was considered not only the potential of UAV for mapping and quantify natural impacts on coastal communities, but also to asses one of the most significant environmental issues of our planet to date: Anthropogenic Marine Debris (AMD) and their accumulation on the beaches (Cozar et al., 2015; Jambeck et al., 2015). Access information on the AMD accumulation rate on beaches and the associated spatio-temporal oscillations would be crucial to refining global estimation on the dispersal mechanisms. In ***Paragraph 2.4*** was described a novel and an ad-hoc methodology for monitoring and automatically quantifying AMD, based on the combined use of UAV and a deep-learning based software. The results proved that the use of UAV is instrumental in surveying remote areas and the spatial resolution achieved in the collected images allowed detecting a percentage of the objects on the shores higher than 87.8%. The deep-learning based software, PlasticFinder, has been tested for the automatic detection and quantification of AMD, providing analysis of the UAV collected images. In the Maldivian case study, the overall performances were excellent, much higher than the only state-of-the-art AI algorithm so far published in the literature. Furthermore, although the methodology was tested in the Maldives its applicability is global.

Satellite and drone allowed to map and monitor coastal environments in optimal condition to a maximum of 20/30 meters (J. D. Hedley et al., 2018; Traganos et al., 2018) but to go deeper are necessary different sensing techniques with submerged platforms (Micallef et al., 2017; Goodman et al., 2013).. **Chapter 3** described two methodologies used to collect data in near coast environments where the condition are not suitable (water not enough transparent or benthic communities to deep) for the use of satellite or UAV. In ***Paragraph 3.1*** was defined the potential of underwater photogrammetry and SfM to infer properties of reef habitats. In particular, was proposed the use of Digital Surface Models and Digital Terrain Models, obtained from underwater photos processing, for assessing coral colonies extension and height and discriminating between seabed and coral cover. Such information can be coupled with digital rugosity estimates to improve habitat characterisation. The relative simplicity of the proposed workflow encourages its repeatability and permits non-specialists to learn photogrammetry for coral monitoring, opening the possibility for local inhabitants to perform their surveys and make their datasets accessible for coral researchers.
In ***Paragraph 3.2*** we acquired acoustic depth measurements using a multibeam echosounder (MBES) and 3D point clouds applying the SfM technique to RGB images, collected using an UAV over the shallow areas. All obtained data were calibrated and validated with RTK-GNSS measurements and successfully integrated in order to generate a harmonized DTM that describe, with high-resolution, coral reef environment from the shallow to the deepest part of the lagoon.

Technological advantages are actively supporting the diffusion of new monitoring platforms useful to track the effect of climate change and anthropogenic pressure on coastal environments. The development of automatic methods for image capture and processing combined with more accessible platforms and sensors, in term of cost and dimension, will increase our capability of capturing fine-ecological processes and communities changes. In this regard, the importance to harmonise the different approaches to impacts assessment is crucial to generate useful tools for pursuing management strategies in the context of sustainable development. This thesis described the potential of different platforms, combined with innovative data processing techniques, to address pressing global coastal environmental issues. The publications produced during the PhD project confirmed the high potential of the integration of different platforms and processing methodologies. Therefore, the innovative protocols described are efficient and reliable for collecting and analysing data in coastal regions all around the world in order to asses anthropogenic and climatic impacts.

References

Adger, W. N., Hughes, T. P., Folke, C., Carpenter, S. R., & Rockström, J. (2005). Social-ecological resilience to coastal disasters. *Science (New York, N.Y.)*, *309*(5737), 1036–1039. https://doi.org/10.1126/science.1112122

Ampou, E. E., Ouillon, S., Iovan, C., & Andréfouët, S. (2018). Change detection of Bunaken Island coral reefs using 15 years of very high resolution satellite images: A kaleidoscope of habitat trajectories. *Marine Pollution Bulletin*, *131*, 83–95. https://doi.org/10.1016/j.marpolbul.2017.10.067

Baker, A. C., Glynn, P. W., & Riegl, B. (2008). Climate change and coral reef bleaching: An ecological assessment of long-term impacts, recovery trends and future outlook. *Estuarine, Coastal and Shelf Science*. https://doi.org/10.1016/j.ecss.2008.09.003

Coral Reef Remote Sensing. (2013). *Coral Reef Remote Sensing*. https://doi.org/10.1007/978-90-481-9292-2

Cozar, A., Sanz-Martin, M., Marti, E., Gonzalez-Gordillo, J. I., Ubeda, B., Galvez, J. A., … Duarte, C. M. (2015). Plastic accumulation in the Mediterranean sea. *PLoS One*, *10*(4), e0121762. https://doi.org/10.1371/journal.pone.0121762

Dolan, A. H., & Walker, I. J. (2006). *Understanding Vulnerability of Coastal Communities to Climate Change Related Risks*. *Source: Journal of Coastal Research* (Vol. III). Retrieved from https://www.jstor.org/stable/pdf/25742967.pdf?refreqid=excelsior%3A29132cd7149feda67cb1ec4e8737ae1a

El-Askary, H., Abd El-Mawla, S. H., Li, J., El-Hattab, M. M., & El-Raey, M. (2014). Change detection of coral reef habitat using Landsat-5 TM, Landsat 7 ETM+ and Landsat 8 OLI data in the Red Sea (Hurghada, Egypt). *International Journal of Remote Sensing*, *35*(6). https://doi.org/10.1080/01431161.2014.894656

Fine, M., Hoegh-Guldberg, O., Meroz-Fine, E., & Dove, S. (2019). Ecological changes over 90 years at Low Isles on the Great Barrier Reef. *Nature Communications*, *10*(1), 4409. https://doi.org/10.1038/s41467-019-12431-y

Hedley, J. D., Roelfsema, C., Brando, V., Giardino, C., Kutser, T., Phinn, S., … Koetz, B. (2018). Coral reef applications of Sentinel-2: Coverage, characteristics, bathymetry and benthic mapping with comparison to Landsat 8. *Remote Sensing of Environment*, *216*, 598–614. https://doi.org/10.1016/j.rse.2018.07.014

Hicks, F. (2017). *Ecosystem Services Assessment of North Ari Atoll Ecosystem Services Assessment of North Ari Atoll Tundi Agardy*. IUCN. Retrieved from https://portals.iucn.org/library/sites/library/files/documents/2017-003_0.pdf#targetText=The key habitats that contribute,offshore pelagic areas and seamounts.

Hughes, Terence P., Rodrigues, M. J., Bellwood, D. R., Ceccarelli, D., Hoegh-Guldberg, O., McCook, L., … Willis, B. (2007). Phase Shifts, Herbivory, and the Resilience of Coral Reefs to Climate Change. *Current Biology*. https://doi.org/10.1016/j.cub.2006.12.049

Hughes, Terry P., Kerry, J. T., Baird, A. H., Connolly, S. R., Chase, T. J., Dietzel, A., … Woods, R. M. (2019). Global warming impairs stock–recruitment dynamics of corals. *Nature*, *568*(7752), 387–390. https://doi.org/10.1038/s41586-019-1081-y

Jambeck, J. R., Geyer, R., Wilcox, C., Siegler, T. R., Perryman, M., Andrady, A., … Law, K. L. (2015). Marine pollution. Plastic waste inputs from land into the ocean. *Science (New York, N.Y.)*, *347*(6223), 768–771. https://doi.org/10.1126/science.1260352

Jordà, G., Marbà, N., & Duarte, C. M. (2012). Mediterranean seagrass vulnerable to regional climate warming. *Nature Climate Change*, *2*(11), 821–824. https://doi.org/10.1038/nclimate1533

Malthus, T. J., & Mumby, P. J. (2003). Remote sensing of the coastal zone: An overview and priorities for future research. *International Journal of Remote Sensing*, *24*(13), 2805–2815. https://doi.org/10.1080/0143116031000066954

Manfreda, S., McCabe, M. F., Miller, P. E., Lucas, R., Madrigal, V. P., Mallinis, G., … Toth, B. (2018, April 20). On the use of unmanned aerial systems for environmental monitoring. *Remote Sensing*. Multidisciplinary Digital Publishing Institute. https://doi.org/10.3390/rs10040641

Mcleod, E., Anthony, K. R. N., Mumby, P. J., Maynard, J., Beeden, R., Graham, N. A. J., … Tamelander, J. (2019, March 1). The future of resilience-based management in coral reef ecosystems. *Journal of Environmental Management*. Academic Press. https://doi.org/10.1016/j.jenvman.2018.11.034

Moberg, F., & Folke, C. (1999). Ecological goods and services of coral reef ecosystems. *Ecological Economics*, *29*(2), 215–233. https://doi.org/10.1016/S0921-8009(99)00009-9

Moberg, F., & Rönnbäck, P. (2003). Ecosystem services of the tropical seascape: interactions, substitutions and restoration. *Ocean & Coastal Management*, *46*(1–2), 27–46. https://doi.org/10.1016/S0964-5691(02)00119-9

Pergent, G., Bazairi, H., Bianchi, C. N., Boudouresque, C. F., Buia, M. C., Calvo, S., … Verlaque, M. (2014, February 28). Climate change and Mediterranean seagrass meadows: A synopsis for environmental managers. *Mediterranean Marine Science*. https://doi.org/10.12681/mms.621

Traganos, D., Aggarwal, B., Poursanidis, D., Topouzelis, K., Chrysoulakis, N., & Reinartz, P. (2018). Towards global-scale seagrass mapping and monitoring using Sentinel-2 on Google Earth Engine: The case study of the Aegean and Ionian Seas. *Remote Sensing*, *10*(8), 1227. https://doi.org/10.3390/rs10081227

Were, K. O., Dick, T. B., & Singh, B. R. (2013). Remotely sensing the spatial and temporal land cover changes in Eastern Mau forest reserve and Lake Nakuru drainage basin, Kenya. *Applied Geography*, *41*, 75–86. https://doi.org/10.1016/j.apgeog.2013.03.017

Wong, P. P., Losada, I., Gattuso, J., Hinkel, J., Khattabi, A., McInnes, K., … Sallenger, A. (2014). Climate Change 2014: Coastal systems and low-lying areas. *Climate Change 2014: Impacts, Adaptation, and Vulnerability. Part A: Global and Sectoral Aspects. Contribution of Working Group II to the Fifth Assessment Report of the Intergovernmental Panel on Climate Change*, 361–409. Retrieved from https://www.ipcc.ch/site/assets/uploads/2018/02/WGIIAR5-Chap5_FINAL.pdf

Appendix

In this paragraph are collected the abstract of the articles produced during the PhD but not closely linked to the project.

Appendix 1

Gerloni, I. G., Carchiolo, V., Vitello, F. R., Sciacca, E., Becciani, U., Costa, A., … Tibaldi, A. (2018). Immersive Virtual Reality for Earth Sciences. 2018 Federated Conference on Computer Science and Information Systems (FedCSIS), 15, 527–534. https://doi.org/10.15439/2018F139

Immersive Virtual Reality for Earth Sciences

Ilario Gabriele Gerloni, Vincenza Carchiolo
Department of Electrical, Electronic and Computer Engineering, University of Catania, Italy Email: ilario.gerloni@gmail.com
Fabio Roberto Vitello, Eva Sciacca, Ugo Becciani, Alessandro Costa, Simone Riggi
Astrophysical Observatory of Catania, Italian National Institute for Astrophysics (INAF), Italy Email: fabio.vitello@inaf.it
Fabio Luca Bonali, Elena Russo, **Luca Fallati**, Fabio Marchese, Alessandro Tibaldi
Department of Earth and Environmental Sciences, University of Milan Bicocca Email: alessandro.tibaldi@unimib.it

Abstract

This paper presents a novel immersive Virtual Reality platform, named ARGO3D, tailored for improving research and teaching activities in Earth Sciences. The platform facilitates the exploration of geological environments and the assessment of geo-hazards, allowing reaching key sites of interest (some of them impossible to be reached in person) and thus to take measurements and collect data as it can be done in the real field. The target audience of ARGO3D encompasses students, teachers and early career scientists, as well as civil planning organisations and non-academics. The overall workflow for real ambient reconstruction, processing and rendering of the virtual ambient is presented, as well as a detailed description of the VR software tools and hardware devices employed.

Appendix 2

Mel, K., Luca, B. F., Fabio, V., Varvara, A., Ugo, B., Elena, R., … Whitworth, M. (n.d.). Workflows for Virtual Reality Visualisation and Navigation Scenarios in Earth Sciences. https://doi.org/10.5220/0007765302970304

Workflows for Virtual Reality Visualisation and Navigation Scenarios in Earth Sciences

Krokos Mel[1,3], Bonali Fabio Luca[2], Vitello Fabio[3], Antoniou Varvara[4], Becciani Ugo[3], Russo Elena[2], Marchese Fabio[2], **Fallati Luca**[2], Nomikou Paraskevi[4], Kearl Martin[1], Sciacca Eva[3] and Malcolm Whitworth[5]

[1]University of Portsmouth, School of Creative Technologies, Eldon Building, Winston Churchill Ave, Portsmouth, PO1 [2]UP, U.K
[2]University of Milano-Bicocca, Department of Earth and Environmental Sciences, Piazza della Scienza 4 – Ed. U04, 20126 Milan, Italy
[3]Italian National Institute for Astrophysics (INAF), Astrophysical Observatory of Catania, Italy
[4]National and Kapodistrian University of Athens, Department of Geology and Geoenvironment, Panepistimioupoli Zografou, 15784 Athens, Greece
[5]University of Portsmouth, School of Earth and Environmental Sciences, Burnaby Road, Portsmouth, PO1 3QL, U.K

Abstract

This paper presents generic guidelines for constructing customised workflows exploiting game engine technologies aimed at allowing scientists to navigate and interact with their own virtual environments. We have deployed Unity which is a cross-platform game engine freely available for educational and research purposes. Our guidelines are applicable to both onshore and offshore areas (either separately or even merged together) reconstructed from a variety of input datasets such as digital terrains, bathymetric and structure from motion models, and starting from either freely available sources or ad-hoc produced datasets. The deployed datasets are characterised by a wide range of resolutions, ranging from a couple of hundreds of meters down to single centimetres. We outline realisations of workflows creating virtual scenes starting not only from digital elevation models, but also real 3D models as derived from structure from motion techniques e.g. in the form of OBJ or COLLADA. Our guidelines can be knowledge transferred to other scientific domains to support virtual reality exploration, e.g. 3D models in archaeology or digital elevation models in astroplanetary sciences.

Appendix 3

Bonali, F.L., Tibaldi, A., Marchese, F., Fallati, L., Russo, E., Corselli, C., Savini, A., UAV-based surveying in volcano-tectonics: An example from the Iceland rift, Journal of Structural Geology (2019), doi: https://doi.org/10.1016/j.jsg.2019.02.004

UAV-based surveying in volcano-tectonics: An example from the Iceland rift

Bonali, F. L., Tibaldi, A., Marchese, F., **Fallati, L**., Russo, E., Corselli, C., Savini, A.

Department of Earth and Environmental Sciences, University of Milan-Bicocca, Milan, Italy

Abstract

In the present work, we applied the use of an Unmanned Aerial Vehicle (UAV) - a quadcopter - and the Aerial Structure from Motion digital photogrammetry image processing technique (ASfM) to study volcano-tectonics and tectonic features in an active Icelandic rift. Data have been collected in order to evaluate the Holocene deformation in the Northern Volcanic Zone of Iceland. We mapped 397 structures, mainly related to extension fractures and subordinately normal faults in the Theistareykir Fissure Swarm, obtaining 1098 and 21 structural data, respectively. This allowed to reconstruct an overall spreading direction of N108° during Holocene times, and to calculate a stretch of 1.013 regarding 8–10 ka old lava units. Deformation in the area is related to both dyke intrusions and extensional tectonics. Furthermore, detailed geological-structural field and UAV surveys were also performed in two test areas in order to determine data accuracy and the associated reliability of this approach. In addition to the above, different flight heights were tested, suggesting that photo collection with a 12.4 MPx camera at 100 m is efficient to study fracture dilation and kinematics.

Appendix 4

Fallati, L., Castiglioni, S., Galli, P., Riva, F., Gracia-Lor, E., González-Mariño, I., … Zuccato, E. (2020). Use of legal and illegal substances in Malé (Republic of Maldives) assessed by wastewater analysis. Science of The Total Environment, 698, 134207. https://doi.org/10.1016/j.scitotenv.2019.134207

Use of legal and illegal substances in Malé (Republic of Maldives) assessed by wastewater analysis

Luca Fallati [a,b], Sara Castiglioni [c], Paolo Galli [a,b], Francesco Riva [c], Emma Gracia-Lor [c,d], Iria González-Mariño [c,e], Nikolaos I. Rousis [c], Mohamed Shifah [b], Maria Cristina Messa [f], Maria Grazia Strepparava [f], Marina Vai [g], Ettore Zuccato [c]

a Department of Earth and Environmental Sciences, University of Milan – Bicocca, Piazza della Scienza 2, 20126 Milan, Italy
b MaRHE Center (Marine Research and High Education Center), Magoodhoo Island, Faafu Atoll, Maldives
c Istituto di Ricerche Farmacologiche Mario Negri IRCCS, Via Mario Negri 2, 20156 Milan, Italy
d Department of Analytical Chemistry, Faculty ofChemistry, Complutense University of Madrid, Avenida Complutense s/n, E-28040 Madrid, Spain
e Department of Analytical Chemistry, Institute for Food Analysis and Research, Universidade de Santiago de Compostela, 15782 Santiago de Compostela, Spain
f Department of Medicine and Surgery, University of Milano-Bicocca, via Cadore 48, 20052 Monza, MB, Italy
g Department of Biotechnologies and Biosciences, University of Milan-Bicocca, Piazza della Scienza 2, 20126 Milan, Italy

Abstract

This study used wastewater-based epidemiology (WBE) to investigate the lifestyle of the inhabitants of Malé, the capital of the Republic of Maldives. Raw wastewater 12-h composite samples were collected from nine pumping stations serving the city area - thus representative of the whole Malé population. Samples were analysed by liquid chromatography coupled to mass spectrometry for estimating the profile of use of a large number of substances including illicit drugs, alcohol, caffeine, tobacco and pharmaceuticals. The illicit drugs most used were cannabis (THC) and heroin (700 and 18 g/day), with lower consumption of cocaine and amphetamines (0.1–1.2 g/day). It is important to note that the consumption of cannabis in Malé was comparable to that measured in other countries, while the consumption of heroin was higher. Among cathinones, mephedrone was detected at the highest levels similar to other countries. Consumption of alcohol, which is not allowed in Maldives, was found (1.3 L/day/ 1000 inhabitants), but at a low level compared with other countries (6–44 L/day/1000 inhabitants), while the consumption of caffeine and tobacco was generally in line with reports from other countries. Unique information on pharmaceuticals use was also provided, since no official data were available. Human life style was evaluated by applying for the first time the full set

of WBE methodologies available in our laboratory. Results provided valuable epidemiological information, which may be useful for national and international agencies to understand population lifestyles better, including illicit drug issues, and for planning and evaluation of drug prevention programs in Malé.